DOT HS-801 718

EVALUATION OF GLARE REDUCTION TECHNIQUES

Contract No. DOT-HS-4-00925
September 1975
Final Report

PREPARED FOR:

U.S. DEPARTMENT OF TRANSPORTATION

NATIONAL HIGHWAY TRAFFIC SAFETY ADMINISTRATION

WASHINGTON, D.C. 20590

Technical Report Documentation Page

1. Report No.	2. Government Accession No.	3. Recipient's Catalog No.
DOT HS-801 718		

4. Title and Subtitle	5. Report Date
Evaluation of Glare Reduction Techniques	September 1975
	6. Performing Organization Code

7. Author(s)	8. Performing Organization Report No.
W. L. Raine, N. E. Chatterton, and A. R. Dunn	EE-DOT-1905

9. Performing Organization Name and Address	10. Work Unit No. (TRAIS)
Teledyne Brown Engineering Cummings Research Park Huntsville, Alabama 35807	
	11. Contract or Grant No. DOT-HS-4-00925
	13. Type of Report and Period Covered Final Report June 14, 1974 - June 20, 1975
12. Sponsoring Agency Name and Address Department of Transportation National Highway Traffic Safety Administration 400 Seventh Street S.W. Washington D.C. 20590	14. Sponsoring Agency Code N48-30

15. Supplementary Notes

16. Abstract

Degradation of the visual capacity of a motor vehicle driver caused by luminous "sources" on the driver's own vehicle during daylight is quantified according to luminance glare theory. Effects of driver's age and daylight conditions are considered, and a means for laboratory measurement of vehicle glare production characteristics is developed. Based upon a probabalistic model of target detection, allowable glare in the field of view is determined. It is found that "spot" glare sources do not materially contribute to degradation of visual capacity (with the model), that the dash of the motor vehicle is generally the largest contributor to glare, and that suitable design changes to motor vehicles would allow them to meet the criterion established. Laboratory measurements with both collimated and diffuse sources are shown to be necessary to adequately evaluate motor vehicle performance.

17. Key Words	18. Distribution Statement
motor vehicle safety, visual capacity, glare, daylight driving, motor vehicle driver aging effects, photometric measurement	Document is available to the public through the National Technical Information Service, Springfield, Virginia 22161

19. Security Classif. (of this report)	20. Security Classif. (of this page)	21. No. of Pages	22. Price
Unclassified	Unclassified	115	

Form DOT F 1700.7 (8-72) Reproduction of completed page authorized

* U. S. GOVERNMENT PRINTING OFFICE : 1973 725-504/328

PREFACE

The authors of this report express their thanks to the following individuals and organizations who contributed to the performance of this work:

Mr. Rube Chernikoff, NHTSA, Contract Technical Manager

Dr. Robert Henderson, NHTSA, who critically discussed the theoretical model

Mr. Jim Falkenberry, TBE, Project Technician

Ford Motor Company

Chrysler Corporation

General Motors Corporation

American Motors Corporation

British-Leyland Motors

Volvo of America

International Harvester

Ward Schoolbus Body Company

and the many members of the NHTSA organization who contributed through the discussions held during the course of performance of this work.

TABLE OF CONTENTS

TABLE OF CONTENTS - Concluded

LIST OF ILLUSTRATIONS

LIST OF ILLUSTRATIONS - Continued

LIST OF ILLUSTRATIONS - Concluded

LIST OF TABLES

INTRODUCTION

The capability of a person to drive safely is degraded by a loss of a portion of his visual capacity by outside optical influences. Quantifying the degree of such degradation would involve many factors that are not now understood. The purpose of this report is to define the degree of degradation of visual capacity caused by luminous sources on the driver's own vehicle under daylight conditions. A measurement technique has been developed for such sources, and a number of vehicles have been tested to see how their response relates to some "allowable" level. The approach taken is to assume that such luminous sources constitute "glare" and that their effect on the driver may be treated by using luminance glare theory. This part of the effect on total driver visual capability appears to be an important one for which a quantitative solution may be obtained. On that basis, it is worthwhile to arrive at a standard for vehicle glare, just as it has been worthwhile to develop other standards related to driver safety.

To develop a criterion on which to base a measurement procedure for vehicle glare, one must use experimental data collected previously under laboratory conditions; attempting to develop new information on human response to glare is beyond the scope of this activity. The criterion presented in this report is based on work on the determination of the threshold contrast for targets against a luminous background, as well as less extensive but authoritative work on the effects of luminous sources off the line of sight upon that threshold contrast. In particular, the work performed for this contract relates the age of the driver to the maximum glare allowable. This maximum for an older driver is used as the criterion with which vehicle characteristics are compared.

A comprehensive program of measurement of glare from vehicles under all daylight conditions requires that two sources of illumination be used in the laboratory: one to simulate direct solar illumination and the other to simulate illumination from the sky and surrounding background. Alternatives to this approach to the measurement program were examined and discarded as not giving representative results.

Measurements made with two laboratory sources were compared with measurements made outdoors on the same vehicle and shown to agree well with these measurements. A number of vehicles including automobiles, trucks, and a school bus were then measured.

Based on the theoretical developments and experimental results reported below, it is felt that a comprehensive criterion from a driver's own vehicle may be established, straightforward test procedures may be used to ensure compliance with standards developed from the criterion, and that the criterion can be met by suitable alterations to designs of most current vehicles.

RESEARCH APPROACH

PROGRAM CONTENT

The work reported on in this document was conducted in four phases:

- Phase I - Review and reevalute criteria for allowable glare (based on results from Ref. 1).
- Phase II - Update and improve the performance of equipment developed under a previous contract for laboratory measurements of glare.
- Phase III - Test motor vehicles to determine glare introduced into a driver's eyes from his own vehicle.
- Phase IV - Analytically and experimentally determine methods for reducing glare.

PHASE I - CRITERIA ANALYSIS

Criteria developed under the previous contract for allowable glare in the driver's field of view were based on luminance glare theory. The problem of defining how glare affects a driver's visual performance was resolved by relating glare to a change in threshold contrast of a single target against a uniform background. The critieria used previously and reported in Reference 1 were developed by reducing a standard threshold contrast as a function of background luminance to a contrast level of 1.0.

Two objections of serious consequence were raised to this approach: The age of the driver had not been considered, and the choice of amount of allowable degradation to the threshold contrast was somewhat arbitrary. During the current work, the available experimental data has been reevaluated and driver age considered in developing new criteria.

PHASE II - EQUIPMENT UPDATING

Measuring the glare produced by a motor vehicle at the driver's position in a laboratory environment requires a set of measurements rather than a single one; without a set of data to analyze, the importance of glare produced from one source compared with other sources cannot be ascertained. Two separate illumination systems were available. The first was designed to simulate diffuse sources in the natural environment such as skylight and the immediate surround of the vehicle. The second simulates direct sunlight by use of a parabolic reflector mounted on a transversing system, allowing one to position the source at any desired angular relationship to the vehicle. This equipment is described in detail in the section "Experimental Environment and Procedures".

A review of the measurement requirements was performed to determine alternatives to the measurement procedures previously established. Deficiencies in the collimation efficiencies of the paraboloid had been noted, and a design study was done to establish minimum acceptability specifications on the paraboloid.

PHASE III - MOTOR VEHICLE TESTS

Based on an analysis of the equipment requirements, the test vehicles were put through a measurement procedure intended to delineate the magnitude and distribution of glare sources on the vehicles. Measurements were made of the glare perceived by looking straight forward and also the direct luminance of the brightest reflective sources on each vehicle.

A total of 20 vehicles were used: 15 of the most popular automobiles, 4 truck models, and 1 bus.

PHASE IV - GLARE REDUCTION TECHNIQUE DEVELOPMENT

The test data collected in Phase III was analyzed. Two automobiles from the previously tested group were selected on the basis of providing the most information concerning reduction of the major glare produced from vehicles. Analytic and experimental procedures were carried out to evaluate to what extent such sources could be eliminated.

METHODOLOGY

THEORETICAL STUDY

Effect of Glare on Visual Detection

Generally, glare is considered to affect the performance of visual tasks on two different levels. This distinction is expressed by the names "discomfort glare" and "disability glare". Discomfort glare is light brighter than the background which causes annoyance to the observer but does not impair his visual perception characteristics. It may result in degradation of driver performance by causing fatigue, but its presence does not, by itself, produce such degradation. Disability glare is light brighter than the background which impairs the observer's ability to detect objects.

Discomfort glare is very difficult to measure because it requires a subjective judgement. Moreover, there is no agreement among authorities as to the harmfulness of discomfort glare. The purpose of the "Evaluation of Glare Reduction Techniques" study is to set numerical levels for allowable glare and to provide a physical measurement procedure for determining whether these levels are exceeded. With existing knowledge, discomfort glare and its effects cannot be expressed in the quantitative terms necessary for the aims of the study. Therefore, only disability glare will be considered.

Defining two other terms may help to clarify the effect of glare on the eye. Scotomatous glare is glare which reduces retinal sensitivity to the extent that a blind spot is temporarily produced on the retina. Veiling glare is a general brightening of the visual field which reduces the detectability of target objects by reducing their contrast below the detection threshold. This brightening may be caused by light scattered within the optical media of the eye or by light scattered by particles outside the eye but in the field of view.

The presence of spot disability glare sources may reduce the sensitivity of the retina at the positions of the spot glare source images on the retina; also, by the action of veiling glare, it impairs the

detection of objects over a portion of the field of view which is larger in angular subtense than the glare source itself. If only diffuse glare is present, the only visual degradation effect is loss of detection ability through the general loss of contrast in the visual field.

The presence of bright spot glare sources has other complicating effects which should be mentioned although they are not explicity incorporated in the standard. Recovery from glare is not instantaneous but requires a finite time which is different for different individuals. Recovery time from an intermittent or flashing glare source is longer than from a single exposure to a continuous glare source. Other visual functions may also be affected. For example, Peterson and Simonson (Ref. 2) found that the position of the accommodation near point lengthened after exposure to glare in subjects older than about 50 years. The average amount of lengthening was small, about 2.6 centimeters, but the study does suggest that glare may affect visual performance in ways that have no direct connection with photometry. These considerations emphasize the need for regulating the presence of bright glare sources anywhere in the driver's field of view, whether or not they are attached to his own vehicle.

The remainder of this section discusses in more detail the effect of glare on visual perception, subject to three restrictions: First, only results of target detection studies will be considered, and no attempt will be made to deduce amounts of visual degradation from measures of physiological changes; second, only those glare levels will be considered which are large enough to impair perception but not large enough to cause physical damage; finally, because the glare sources of particular interest to this study are reflections from the driver's own vehicle, the glare sources will be considered to be relatively uniform in time and certainly not intermittent.

Glare affects detection through the number, intensities, placement, and colors of glare sources. The effect of glare on target detectability also depends on the complexity of the visual field and on the age of the observer.

The visual degradation produced by glare increases rapidly as the angle between the glare source and the line of sight decreases (Refs. 3, 4, and 5). The studies just referred to deal with foveal vision (generally within a field of view of ±5 degrees of the line of sight), but several workers have shown that a glare source in the peripheral field also reduces the apparent contrast of a foveally fixated test object (see, for example, Ref. 6). Therefore, glare anywhere in the field of view can affect target detection. Moreover, the angle between each glare source and the line of sight is constantly changing as the driver scans his visual field. To account for these variations, the allowable glare criterion will be expressed in terms of a general glare luminance which is not to be exceeded anywhere in the field of view. This expression will also be relevant for isolated spot glare sources, since if any such source exceeds the criterion brightness, it is automatically disallowed. The number of glare sources in the field of view need not be specified, because the effect of multiple glare sources in the field of view is determined by the sum of their luminance (Ref. 7); glare sources in combination are neither more nor less disabling than a single glare source of the same luminance.

The effect of color in determining glare sensitivity has not been fully explored. Bouma (Ref. 8) reports that sodium light produces slightly less glare than a white light source of the same intensity, and an earlier Department of Transportation-sponsored glare study (Ref. 9) reported a determination by Hartman that monochromatic blue light appears to have a stronger glare effect than monochromatic red. Color effects are not at present thought to make important contributions to glare conditions. The point is mentioned here because one of the formulations used for glare effect in this study was determined from studies made using a green background, a green target object, and a green glare source instead of the more usual white and neutral gray (Ref. 5).

Just as a target object is more difficult to detect against a complex background than against a simple one, so the degradation of detection in the presence of glare also seems to be greater for a complex

background (Ref. 5). In general, the backgrounds encountered in driving situations will be complex, although degrees of complexity will vary. Probably the typical driving situation background is far more complex than would ever be used in a laboratory vision study. In this respect, psychophysical measurements of visual degradation probably result in underestimates of degradation, and that fact should be remembered when using the measured values.

Finally, glare sensitivity has been shown to be strongly correlated with age (Refs. 5 and 10). Glare is especially troublesome to people older than about 50 years. Because many drivers are older than that, glare effects as a function of age must be considered in devising an allowable glare criterion. The experimental work of Fisher and Christie (Ref. 5) was used to describe the effect of glare on vision as a function of age. Their results are in good agreement with earlier work, and they give a formula which explicitly includes the effects of age. The test situations included both uniform and "complex" background luminance distributions; the values from Experiment II, for the complex distribution, were used here.

Fisher and Christie found that, for their complex background, the effective veiling luminance B' of a glare source can be expressed by

$$B' = \frac{(0.2\,A + 5.8) \times E}{\theta^{2.3}} \quad , \qquad (1)$$

where B' is in foot-lamberts (ft-L), A is the age of the observer in years, E is the illumination at his eye produced by the glare source (in lumens/ft^2), and θ is the angular distance of the glare source from the line of sight, in degrees. The results of this equation for A = 20 and several values of θ are plotted in Figure 1. Because Fisher and Christie's experimental work was done only for two configurations (E = 1.0 lm/ft^2 at θ = 4 degrees and E = 0.1 lm/ft^2 at θ = 1.75 degrees), most of the values in Figure 1 must be considered extrapolations.

The Fisher-Christie work is the only study which has produced a quantitative measurement of the effect of glare as a function of age.

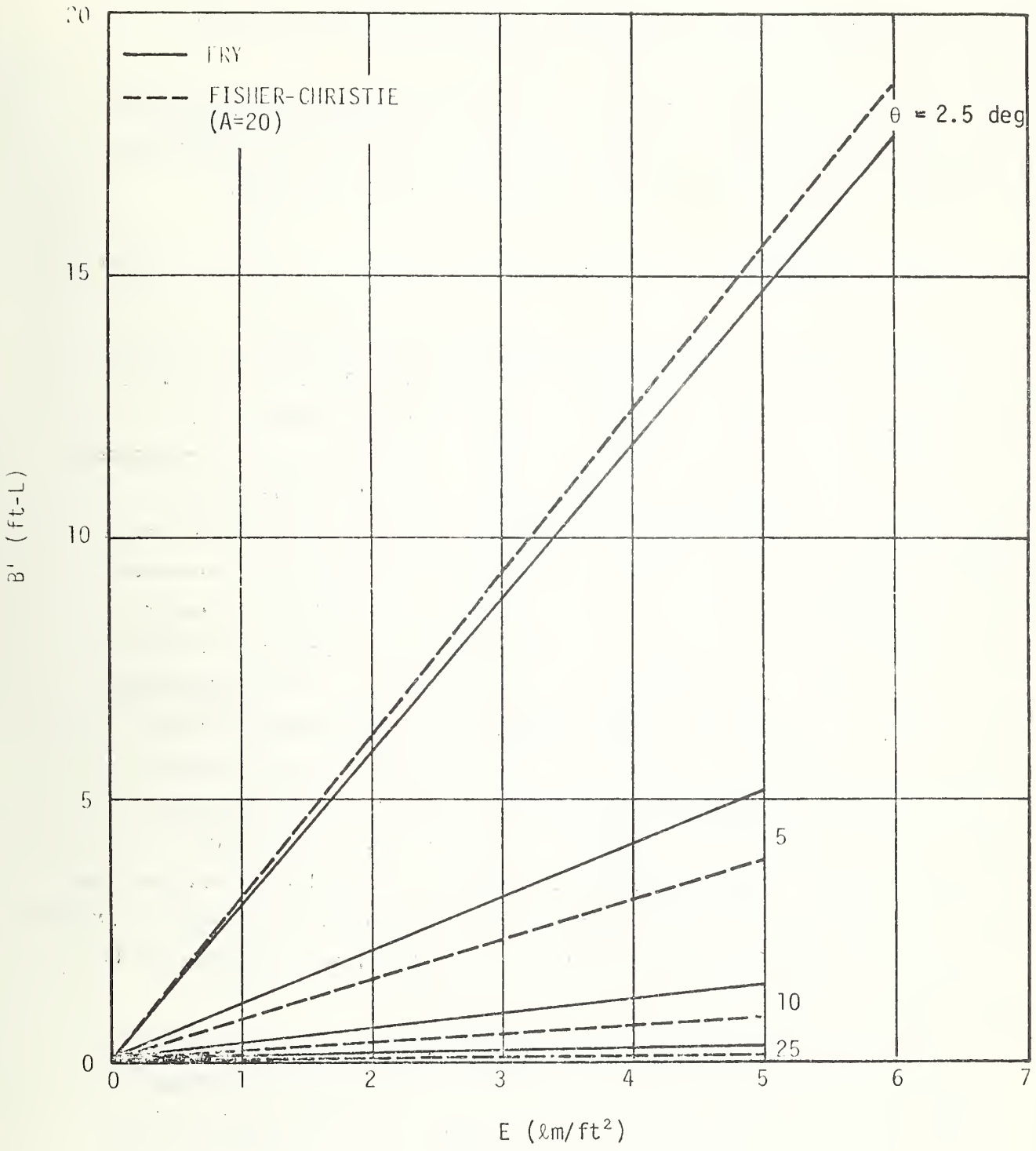

FIGURE 1. COMPARISON OF FRY AND FISHER-CHRISTIE EQUATIONS

Their expression for $k = (0.2\ A + 5.8)\ \Pi$ will therefore be used in deriving an "allowable" glare level criterion.

Although the Fisher-Christie equation, Equation 1, will be used to describe the age effect, values of glare luminances for the remainder of this study will be found from a slightly different equation,

$$B' = \frac{33.4\ E}{\theta\ (1.5 + \theta)} \quad . \tag{2}$$

This is Fry's equation (Ref. 4), re-expressed in foot-lamberts. It was derived as a compromise fit to the earlier data of Holladay and Stiles, using scattering theory to arrive at a functional form which gives a reasonable expression at small values of θ. The constant 33.4 corresponds to the value we have called $k = (0.2\ A + 5.8)\ \Pi$ in the Fisher-Christie equation; it is the value of k that Fisher and Christie would find for a 24-year-old observer. The Fry equation is used because the experimental glare measurement procedure specifies the use of a Fry lens to measure glare luminances, and the Fry lens imposes a light distribution of the form $1/\theta(\theta + 1.5)$. It will be shown later that, for glare levels which are likely to be encountered, small differences in the equation used for B' do not affect the effect of glare on detection. The B' values calculated from the Fry equation are plotted with the Fisher-Christie results for the same E and θ values in Figure 1. The Fisher-Christie form gives larger B' values for $\theta = 2.5$ degrees but smaller B' values than the Fry equation at the larger angles. However, the Fisher-Christie equation is supported by measurements only for $\theta \geq 4$ degrees, so it should not be used to predict glare luminances at large angles.

The preceding discussion has considered the determination of effective veiling glare luminance values, but the effect of the glare on visual detection ability has yet to be found. The Blackwell visual detection data will be used for that task.

The values used are the contrast threshold values published by Blackwell and Smith in 1970 (Ref. 11). Blackwell and Smith's complete table is reproduced as Table 1. The values used in this study were those

TABLE 1. TABULAR VALUES OF THE STANDARD VISUAL PERFORMANCE CURVE

BACKGROUND LUMINANCE (ft-L)	TARGET CONTRAST
10,000.	.449
3,000.	.451
1,000.	.480
300.	.540
Daylight 100.	.614
30.	.722
10.	.876
3.	1.233
1.	1.919
.3	3.373
.1	5.929
.03	12.11
.01	26.36
.003	74.47
.001	202.3
.0003	653.1
.0001	1,959.

in the background luminance range from 10 to 1,000 foot-lamberts, corresponding to the range of daylight conditions. The tabulated values are detection threshold contrasts for targets 4 minutes of arc in diameter; they contain a field factor of 6.67, which includes the "common-sense" seeing factor, correction for dynamic target presentation, and correction to 99 percent probability of seeing. These values are for young observers with good vision. To convert the contrast thresholds to values for larger portions of the normal population, another set of multipliers is required (Table 2). Table 2 is an abridgement of the more extensive table published by Blackwell and Blackwell (Ref. 12). Examination of this table shows that the contrasts of Table 1 are suitable values for 50 percent of the 20-year-old population but must be multiplied by 1.76 to include 95 percent of 20 year olds. The other multipliers in the far right-hand column are values to be applied to the threshold contracts for the five other ages shown, in order to adjust the Table 1 values to include 95 percent of the people in each are range. These 95 percent values were used as the multipliers for this study. (It will

TABLE 2. CONTRAST MULTIPLIERS FOR DIFFERENT PORTIONS OF THE NORMAL POPULATION

AVERAGE AGE (1 yr)	PERCENT OF PUPULATION INCLUDED	
	50%	95%
20	1.00	1.76
30	1.02	1.82
40	1.17	2.27
50	1.58	3.42
60	2.28	5.56
65	2.66	6.92

appear later that the "allowable glare" levels do not depend on the values of any multipliers used, but the 95 percent values were chosen to ensure generality in any case.) The table extends only to age 65 because the authors found that multipliers could not be reliably determined for older subjects.

The values in Tables 1 and 2 define the contrasts required for detection of targets at various background luminances for persons of different visual abilities; these, combined with the glare luminance values from the Fry or Fisher-Christie equations, will allow determination of the visual degradation due to glare.

Addition of a veiling luminance to a visual field decreases the apparent contrast of target objects in the field. By definition,

$$C = \frac{B_t - B}{B} \tag{3}$$

where C is target contrast, B_t is the luminance of the target, and B is the luminance of the background. If a uniform veiling luminance B' is added to the field of view, the new contrast C' is

$$C' = \frac{(B_t + B') - (B + B')}{B + B'} = \frac{B_t - B}{B + B'} \quad . \tag{4}$$

Now, let C_T represent the threshold contrast at background luminance B (C_T will be found from Tables 1 and 2).

$$C_T = \frac{B_t - B}{B} \quad . \tag{5}$$

Then, since

$$C_T = \frac{(B_t - B)}{B} \cdot \frac{(B + B')}{(B + B')}$$

and

$$C' = \frac{(B_t - B)}{(B + B')} \cdot \frac{B}{B} \quad ,$$

Equations 4 and 5 can be combined to yield

$$C_T' = \frac{B\ C_T}{B + B'} \quad , \tag{6}$$

where C_T' designates C' corresponding to C_T at a specific original background luminance. Equation 6 will be used to assess the effect of various glare luminances on perception.

The next step in finding "allowable glare" levels is specification of a "permissible" level of visual degradation. Some degradation is inevitable in any visual task performed from the driver's seat of a car, compared with performance outside the car; but, from a safety viewpoint, no degradation is justifiable. This study will make no attempt to define a level of degradation which is "safe". Instead, we will adopt a level which should be attainable in practice and probably not excessively hazardous, and we will then attempt to show the practical significance of visual degradation at that level.

The values adopted for C_T are the threshold contrasts for 99 percent probability, or virtual certainty, of detection of the target. We will assume that the maximum "permissible" degradation is from 99 percent to 90 percent probability of detection. The significance of such

a change in terms of threshold contrast values for 95 percent of the 20-year-old population is shown in Table 3. The difference in multipliers is within the range of variation among different observers in that age group (see Table 2); this can also be shown to be true for the other age groups. A degradation from 99 percent to 90 percent for an individual observer is within the range of variation of detection ability for observers in the normal population. It is therefore within the range which must be tolerated because of individual differences.

TABLE 3. THRESHOLD CONTRASTS FOR 90 PERCENT AND 99 PERCENT PROBABILITY OF DETECTION FOR 20 YEAR OLDS

BACKGROUND LUMINANCE (ft-L)	CONTRAST FOR DETECTION PROBABILITY	
	90%	99%
10	1.246	1.542
30	1.027	1.271
100	0.874	1.081
300	0.768	0.950
1,000	0.683	0.845

The change in detection time provides another indication of the effect of a decrease in detection probability from 99 percent to 90 percent. Consider the case of a driver searching for targets in a fairly simple visual field. The usual visual search technique (see Refs. 13 and 14, for example) is to scan the field with the eyes according to some pattern determined by the field background and the type of target sought. The field is sampled by eye fixations at locations which are more or less voluntarily selected; the average duration of these fixations is about 1/3 second, which seems to be a value relatively constant for all observers.

The number of samplings in this case will be assumed to be very small. The 99-percent probability target will then be detected in the first visual fixation after it appears; the maximum time required for detection is 1/3 second. Now, assume that a target which is otherwise identical to the 99-percent target appears with a contrast which gives it a 90-percent probability of detection. Define:

$P_D^{(n)}$ - probability that target is detected on at least one of n fixations

$P_F^{(n)}$ - probability that target is not detected on at least one of n fixations

$P_D^{(n)}$ - $1 - P_F^{(n)}$

$P_D^{(i)}$ - probability that target is detected on ith fixation

$P_F^{(i)}$ - probability that target is not detected on ith fixation

$P_D^{(i)}$ - $1 - P_F^{(i)}$.

Because the probabilities of detection on successive fixations are independent,

$$P_F^{(n)} = \prod_{i=1,n} P_F^{(i)}$$

$$P_D^{(n)} = 1 - \prod_{i=1,n} [1 - P_D^{(i)}] = 1 - [1 - P_D^{(i)}]^n \quad . \qquad (7)$$

The target will eventually be detected, so $P_D^{(n)} = 0.99$. However, for the 90-percent target, the probability of detection on each fixation, $P_D^{(i)}$, is 0.90. Substituting these values into Equation 7 and solving for n yields

$$0.99 = 1 - (1 - 0.90)^n$$

$$-0.01 = - (0.1)^n$$

$$n = 2.00 \quad .$$

Therefore, the target will not be detected until the second fixation after it appears, making the detection time 2/3 second. This calculation refers to an idealized case, and the detection times for both targets would probably be longer than the values given here. In any case, however, the time for the detection of the 90-percent target will be at least 1/3 second longer. If the probability of detection $P_D^{(i)}$ is reduced below 90.0 percent, n will become greater than 2.00. Because n is the number of fixations, it must be an integer; therefore, if $P_D^{(i)}$ = 89 percent, for example, n = 3. A probability of detection of 90 percent is the lowest probability which will require only one more fixation for detection than will a 99-percent probability. For this reason, the 90-percent probability level was adopted as the limit of allowable degradation.

Determination of Allowable Glare Levels

The "allowable glare" levels are defined to be the values of glare luminance for which the modified detection contrast C_T' is equal to or greater than the contrast value required for 90-percent probability of detection at the appropriate background luminance. If a uniform glare luminance acts like an increase in the general background luminance, then the new threshold contrast would be determined by the apparent background luminance value B + B', and the calculated C_T' should be compared with the 90-percent threshold contrast from the Blackwell curves for luminance level B + B'. It has not been proved that veiling glare luminance has the same effect on perception as an increase in the general background luminance. The Holladay work determined detection thresholds by increasing the target brightness until the target was detected. The later glare work has used the same experimental procedure. This research has proved that an increase in target brightness (and, by extension, in target contrast) is necessary to detect a target in the presence of glare. It has not shown whether or not the presence of glare luminance assists detection. Some preliminary work in that direction was done by Holladay (Ref. 15). He found that at very low light levels (B < 0.1 mL = 0.01 ft-L) the presence of a glare source may aid vision, but that the glare source degrades vision at higher background luminances. He also

found that a glare source may assist detection if it provides an illumination of the background which is substantially greater than its illumination at the eye. For the conditions he used, a factor of 2.7 in illumination of background over illumination of eye was required. This work suggests that it would be unwise to assume that the veiling glare iluminance will assist vision under the conditions a driver is likely to encounter.

Because it has not been established that veiling glare luminance contributed to perception, the modified threshold contrast values have been compared with the 90-percent probability threshold values corresponding to the original background luminance B which exists in the absence of glare. The contrasts for 90-percent detection probability were determined by multiplying the C_T values by 1.60/1.98 = 0.808*. A 90-percent probability value was found in this way for each age and background luminance value used; the 90-percent values are listed in Table 4. For reference, the corresponding 99-percent values are given in Table 5. The values of contrast modified by glare, C_T', were calculated for the same ages and background luminances for a number of glare source intensities and positions. The modified contrast values were then plotted as a function of glare luminance, B', for each case calculated.

TABLE 4. 90-PERCENT CONTRAST VALUES

BACKGROUND LUMINANCE (ft-L)	AGE (yr)					
	20	30	40	50	60	65
10	1.246	1.288	1.606	2.421	3.935	4.898
30	1.027	1.062	1.324	1.995	3.244	4.037
100	0.874	0.903	1.126	1.697	2.759	3.434
300	0.768	0.794	0.991	1.492	2.426	3.020
1,000	0.683	0.706	0.881	1.327	2.157	2.684

*This multiplier was determined by the method used by Blackwell and Smith (Ref. 11, p. 392). The value is that which is obtained for detection probabilities which follow the normal distribution curve obtained by Blackwell and Smith to determine the "New Standard Visual Performance Curves" which are presented in Reference 11 and which are used here as the standards for detection of targets.

TABLE 5. 99-PERCENT CONTRAST VALUES

BACKGROUND LUMINANCE (ft-L)	AGE (yr)					
	20	30	40	50	60	65
10	1.542	1.594	1.988	2.996	4.870	6.062
30	1.271	1.314	1.639	2.469	4.014	4.996
100	1.081	1.117	1.394	2.100	3.414	4.249
300	0.950	0.983	1.226	1.847	3.002	3.737
1,000	0.845	0.874	1.090	1.642	2.669	3.322

To avoid combining the Fisher-Christie age factors with the Fry angular dependence, the calculations were actually done with the Fisher-Caristie equation for B' (Equation 1). The results are the same for both the Fry and the Fisher-Christie equations, however, as can be seen from Figure 2, which shows plots of C_T' as a function of B' for various background luminances for a 20-year-old observer. The reason for the lack of dependence on the form of the equation for B' is that the quantity considered, C_T', is given by

$$C_T' = \frac{B\ C_T}{B + B'} \quad .$$

For B > 10 ft-L, the two equations yield essentially identical solutions to Equation 6. They can be used interchangeably to describe glare luminances at background luminance levels which are characteristic of daytime driving conditions.

The results of the calculations are the series of plots shown in Figures 3 through 7. In each of these figures, C_T' is plotted as a function of B' for a different background luminance. The B' values were calculated from Equation 1 using the same range of values of E and 0 that were used to calculate the values shown in Figure 1. The B' values obtained were constrained by the values of E and 0, so the range of B' values shown on the plots does not exceed about 35 ft-L. The choice

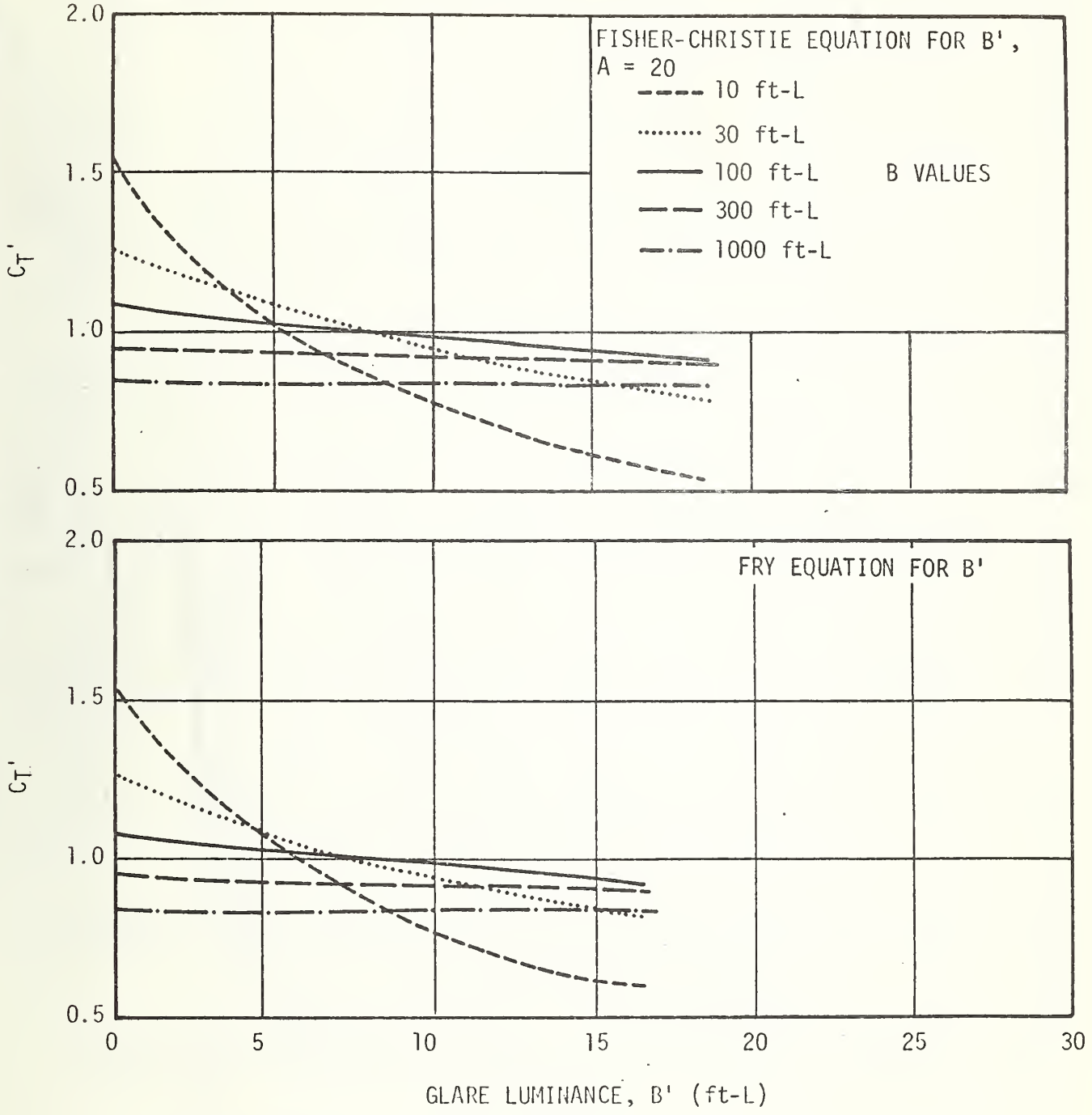

FIGURE 2. COMPARISON OF C_T' VALUES FOUND FROM FRY AND FISHER-CHRISTIE VALUES

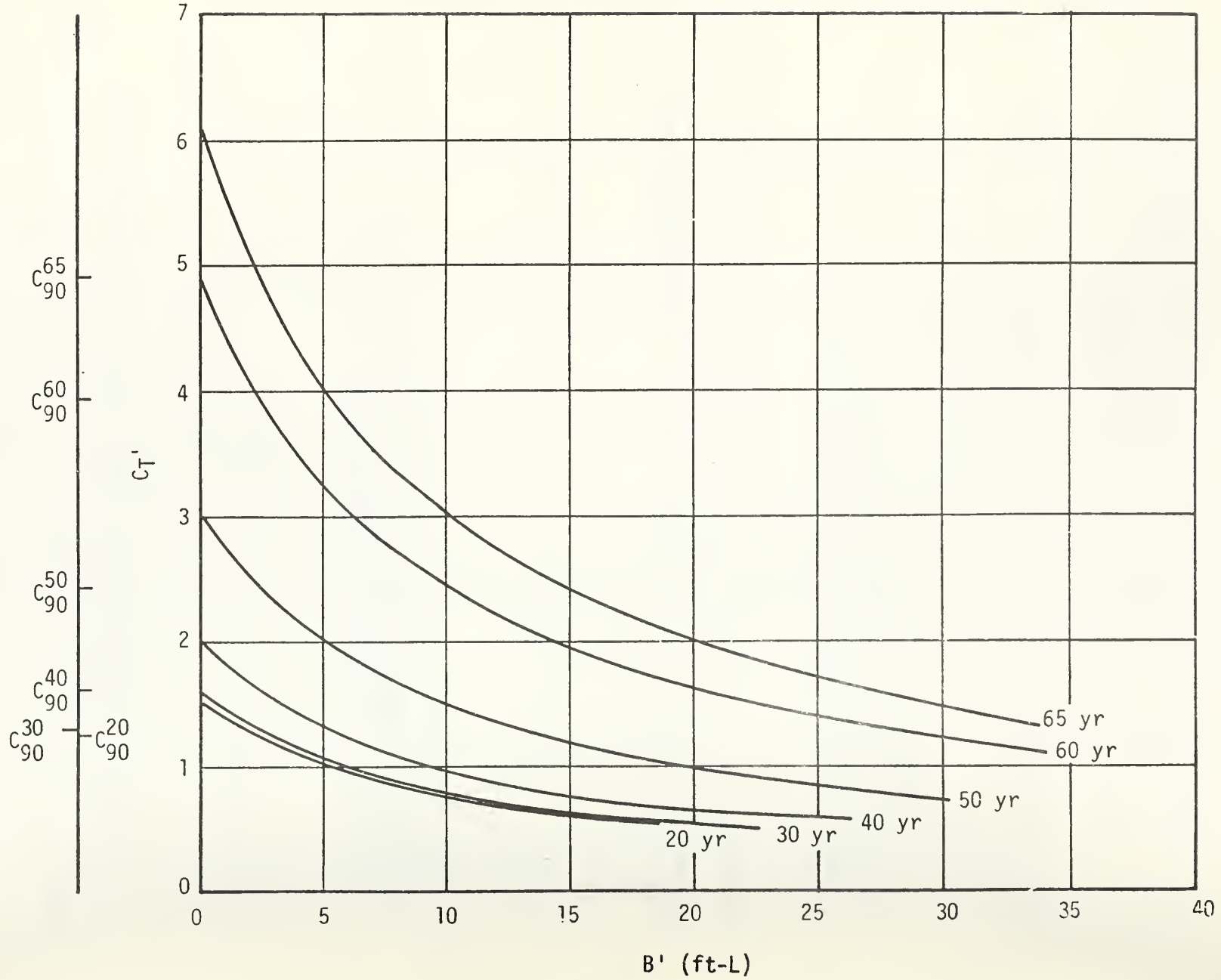

FIGURE 3. C_T' AS A FUNCTION OF B', B = 10 ft-L

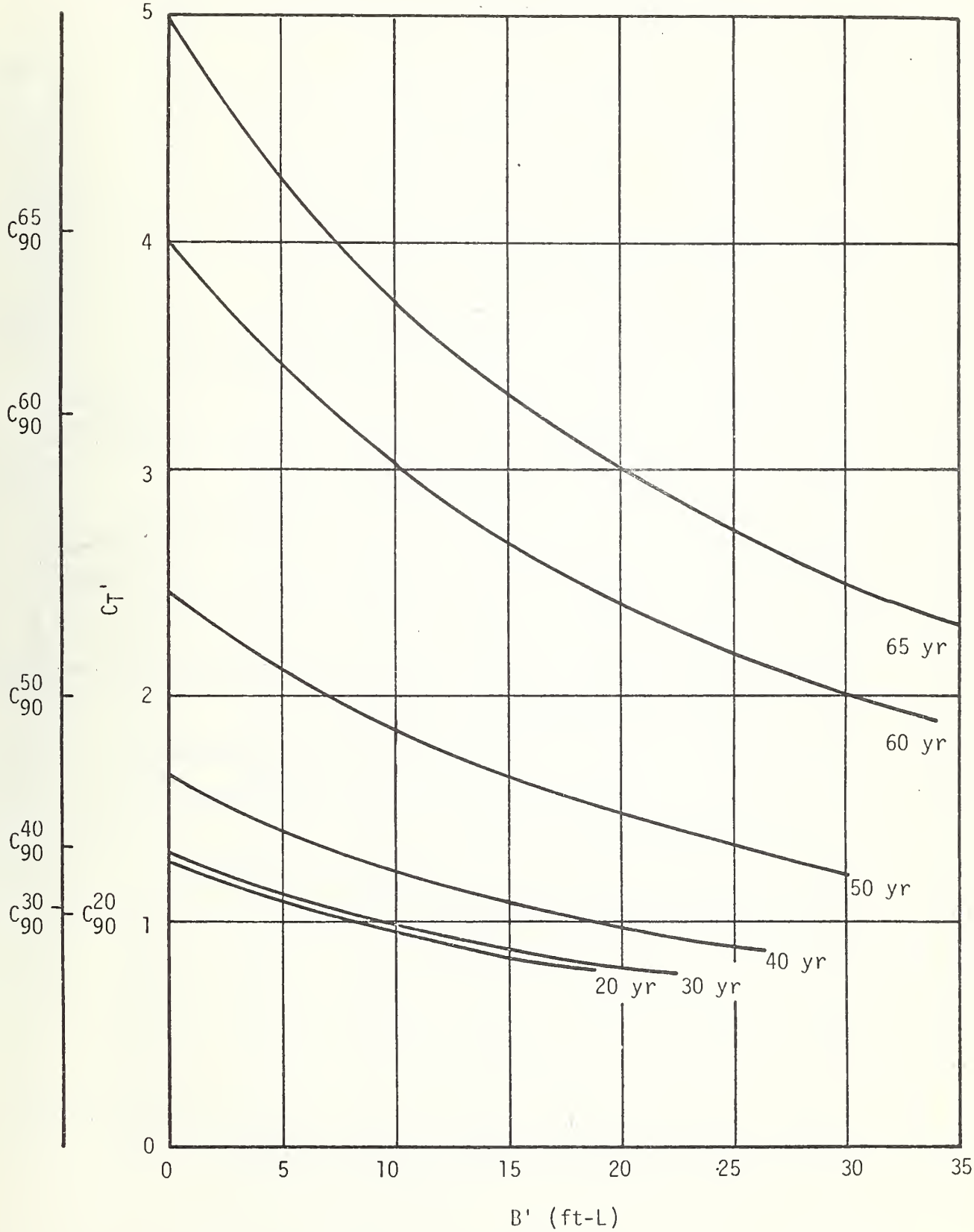

FIGURE 4. C_T' AS A FUNCTION OF B', B = 30 ft-L

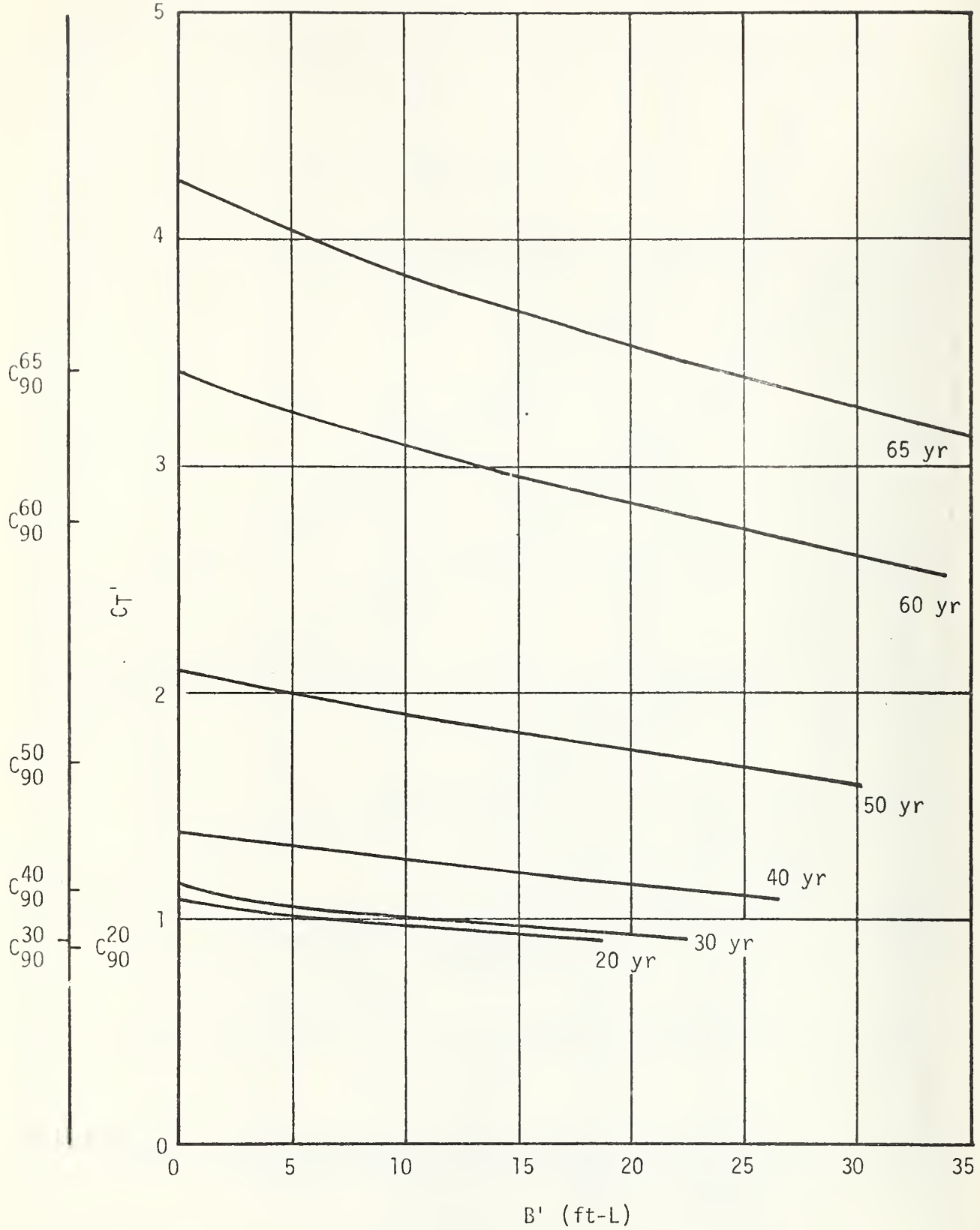

FIGURE 5. C_T' AS A FUNCTION OF B', B = 100 ft-L

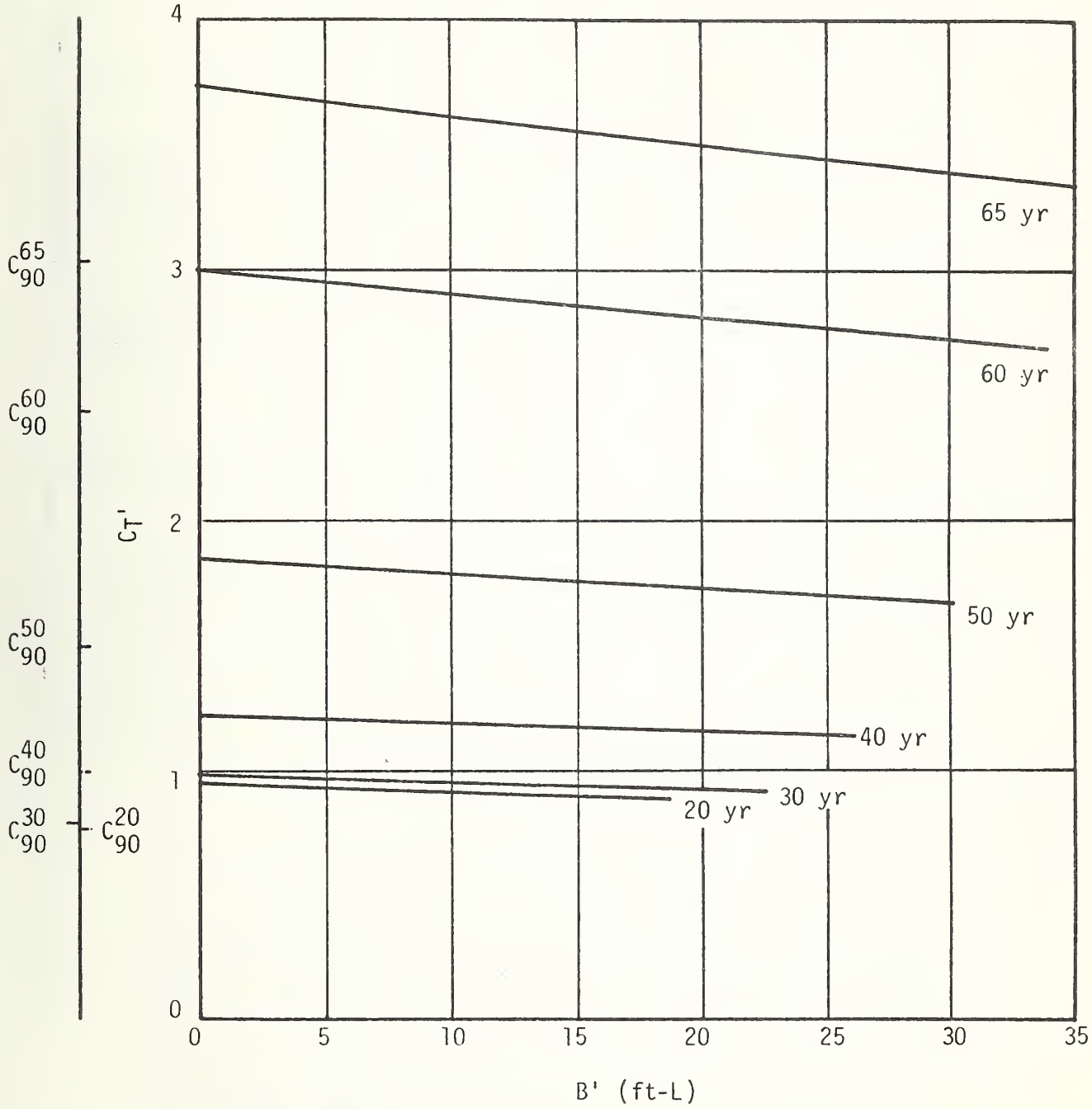

FIGURE 6. C_T' AS A FUNCTION OF B', B = 300 ft-L

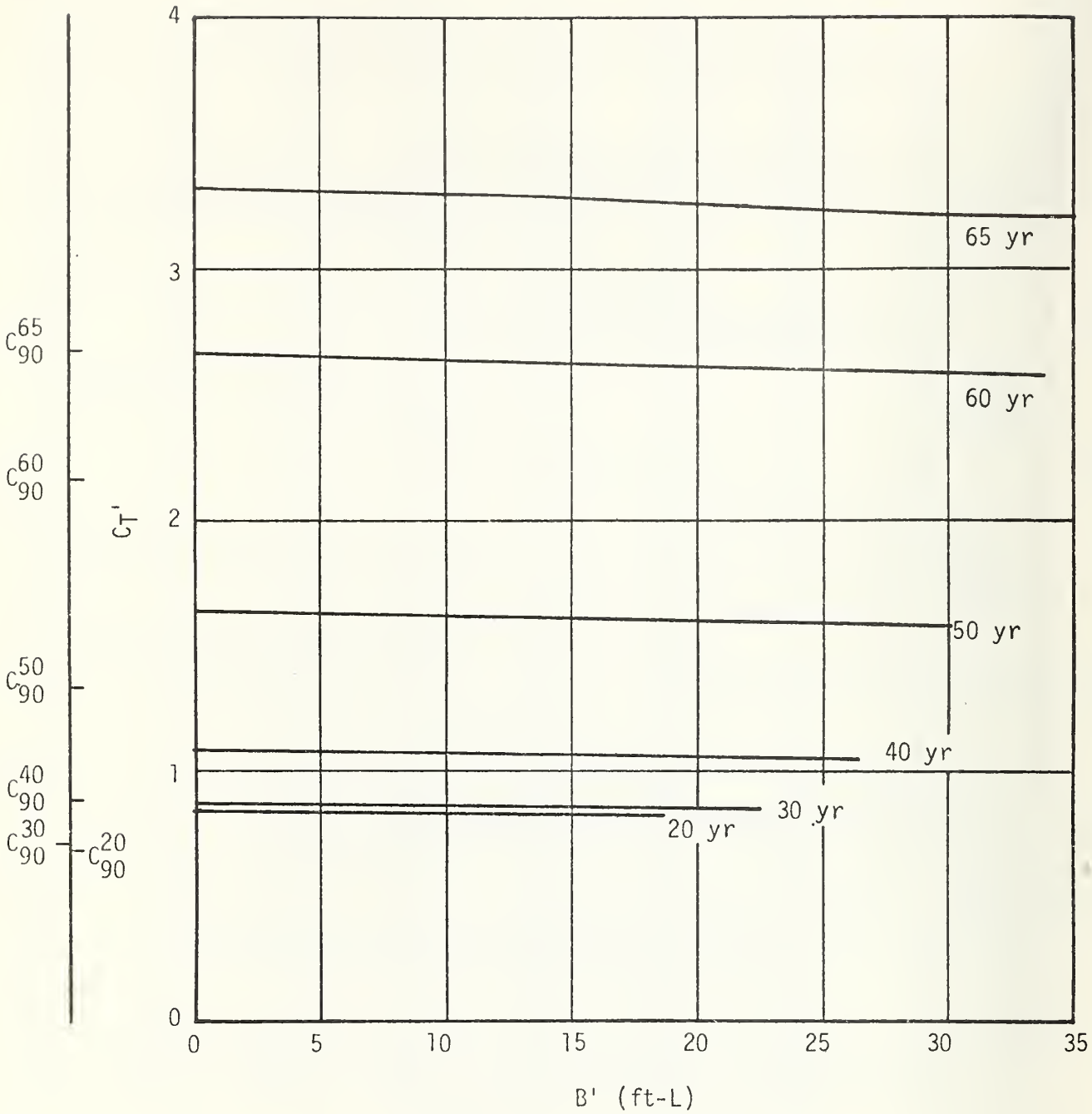

FIGURE 7. C_T' AS A FUNCTION OF B', B = 1,000 ft-L

of E and 0 values was made so as not to exceed too greatly the values used in the experiments made to derive the equation for B'. Further extrapolations were sometimes necessary to derive glare levels for the larger background luminances; they were made by linear extrapolation of the values shown in Figures 6 and 7.

The marks in the left-hand margins of Figures 3 through 7 show the positions of the 90-percent probability contrast values: $C_{90}{}^{50}$ is the 90-percent probability contrast for age 50, and so on. The allowable glare values are the values of B' for which the plotted values of C_T' are greater than the value of C_{90} for the age in question. It can be seen at once from the plots that the C_{90} level for each background luminance is essentially independent of age, so the only age-dependent quantity which will affect the glare criterion is the perceived glare luminance, B'. The absolute value of perceived glare luminance is greatest for the 65-year-old driver, so the values for these individuals will determine the glare luminance standard. The maximum "allowable glare" luminance levels for 65 year olds are shown in Table 6. The "allowable levels" are maximum luminance anywhere in the driver's field of view due to a glare source; they are determined at the driver's eye position.

TABLE 6. "ALLOWABLE" GLARE LUMINANCES FOR 65 YEAR OLDS

BACKGROUND LUMINANCE (ft-L)	GLARE LUMINANCE AT EYE POSITION (ft-L)
10	2.5
30	7.0
100	25.0
300	60.0*
600	120.0*
1,000	200.0*

*These values were found by linear extrapolation of the plotted values; the values for B = 600 ft-L were calculated separately by the same methods used for the other values but were not plotted.

To compare these values with the measurements which form the remainder of this study, allowance must be made for the fact that the measured values are calibrated to match Fry's relation (Equation 2). This can be done either by deriving a new measurement calibration constant or by converting the values in Table 6 to the scale of the present constant. The second alternative was chosen to reduce the number of operations in the data reduction.

The rescaling was done by comparing the glare luminance values predicted by the Fry and Fisher-Christie equations for the same glare conditions. The condition chosen was a glare source providing illumination E at the observer's eye and located at an angular distance of 5 degrees from the observer's line of sight. The value of 5 degrees was chosen because it was the value of θ used by Fry in scaling his equation and because it is almost equal to one of the glare source locations used in Fisher and Christie's experimental work (their experimental value was $\theta = 4$ degrees). Therefore, both equations should predict the glare luminance at $\theta = 5$ degrees with the best accuracy of which they are capable. For re-scaling, the value of k for a 65-year-old observer was used with the Fisher-Christie form, and Fry's value of 33.4 was used in the numerator of the Fry equation. The ratio of glare luminance predicted for the 65-year-old observer to the value measured with the Fry lens is then

$$R = \frac{\dfrac{\left[(0.2)\,(65) + 5.8\right]\pi E}{5^{2.3}}}{\dfrac{33.4\,E}{5(1.5 + 5)}}$$

$$R = 1.419 \quad .$$

The glare criterion of Table 6 is then re-expressed in Table 7 in terms of the measured values by dividing the glare luminance values by 1.419. (The values in the table have been rounded off to the nearest foot-lambert.)

TABLE 7. GLARE CRITERION LEVELS FOR MEASUREMENTS WITH FRY LENS

BACKGROUND LUMINANCE (ft-L)	MAXIMUM GLARE LUMINANCE (ft-L)
10	2
30	5
100	18
300	42
600	85
1,000	140

The values in Table 7, then, are the ones with which the measured values are to be compared.

METHODOLOGY FOR EXPERIMENTAL DETERMINATION

Development of Rationale

Glare (as defined in the preceding section) which is a result of reflection of light energy from the driver's own vehicle may be considered to be generated by two general classes of sources: collimated and diffuse. During daylight hours, the period during which these investigations were designed to provide guidelines for allowable glare, these sources are primarily the sun (the collimated source) and the sky and immediate surround of the vehicle (the diffuse source).

If laboratory measurements are to be made with no preconceived notions of the relative importance of various contributions to the total glare from the vehicle, they must be made so as to include all components of the glare sources.

A collimated source of light produces a beam of energy in which all the rays emerge parallel from the source. No acceptable alternatives to having a collimated source could be conceived. Since the light rays must emerge parallel, the size of the source must be the same size as the illuminated area. In addition, the source must be movable to illuminate the vehicle from all possible angles for which the reflected energy is likely to be a problem.

A diffuse source, however, must produce illumination at the vehicle that is essentially independent of viewing angle at the point of incidence. (An exception to this is that for the dashboard a major portion of the upper hemisphere is masked by the vehicle interior.)

Two pieces of equipment were constructed under a previous contract and are described completely in Reference 1. The collimated source is shown in Figure 8. The source moves along an aluminum track with a 12-foot radius. The track, in turn, pivots about an axis through the center of curvature. The system is controlled through a unit shown in the foreground of Figure 8. The diffuse illumination apparatus is shown in Figure 9. It consists of twenty, 8-foot-long fluorescent lamps mounted in a single plane and six lamps in each of two additional planes mounted at each side of the control plane and at an angle of 22 degrees to it. Aluminum foil is mounted behind the lamps to direct most of the light energy forward, and a frosted 4-mil-thick Mylar diffuser is mounted 12 inches in front of the lamps.

The scaling factors used for this work were as derived in Reference 1. Angular relationships used for scaling to direct solar illumination are shown in Figure 10. The veiling luminance measured with a photometer with a Fry lens is scaled by the equation

$$L_{SV} = R_S\ (\Psi,\Phi)\ K_{SL}\ C_{AS}\ T_S$$

where K_{SL} scales the illuminance of the solar simulator to maximum solar illuminance, C_{AS} corrects for solar altitude, and T_S corrects for temporal variations in atmospheric transmission. In this equation, $R_S\ (\Psi,\Phi)$ is the photometer reading with the solar simulator. The diffuse illumination must be scaled in two parts. The hood is considered to act as a specularly reflecting surface. The dashboard is assumed to be diffusely reflecting. Other sources on the vehicle, e.g., side mirrors and interior trim, are assumed to contribute negligible amounts of glare to the driver when illuminated by the diffuse source. The final scaled diffuse veiling luminance, L_{DV}, is represented by

$$L_{DV} = R_{DH}\ (\Psi,\Phi)\ K_{DL}\ C_{AD}\ D_F + R_{DD}\ (\Psi,\Phi)\ K'_{DL}\ C_{AD}\ D_F$$

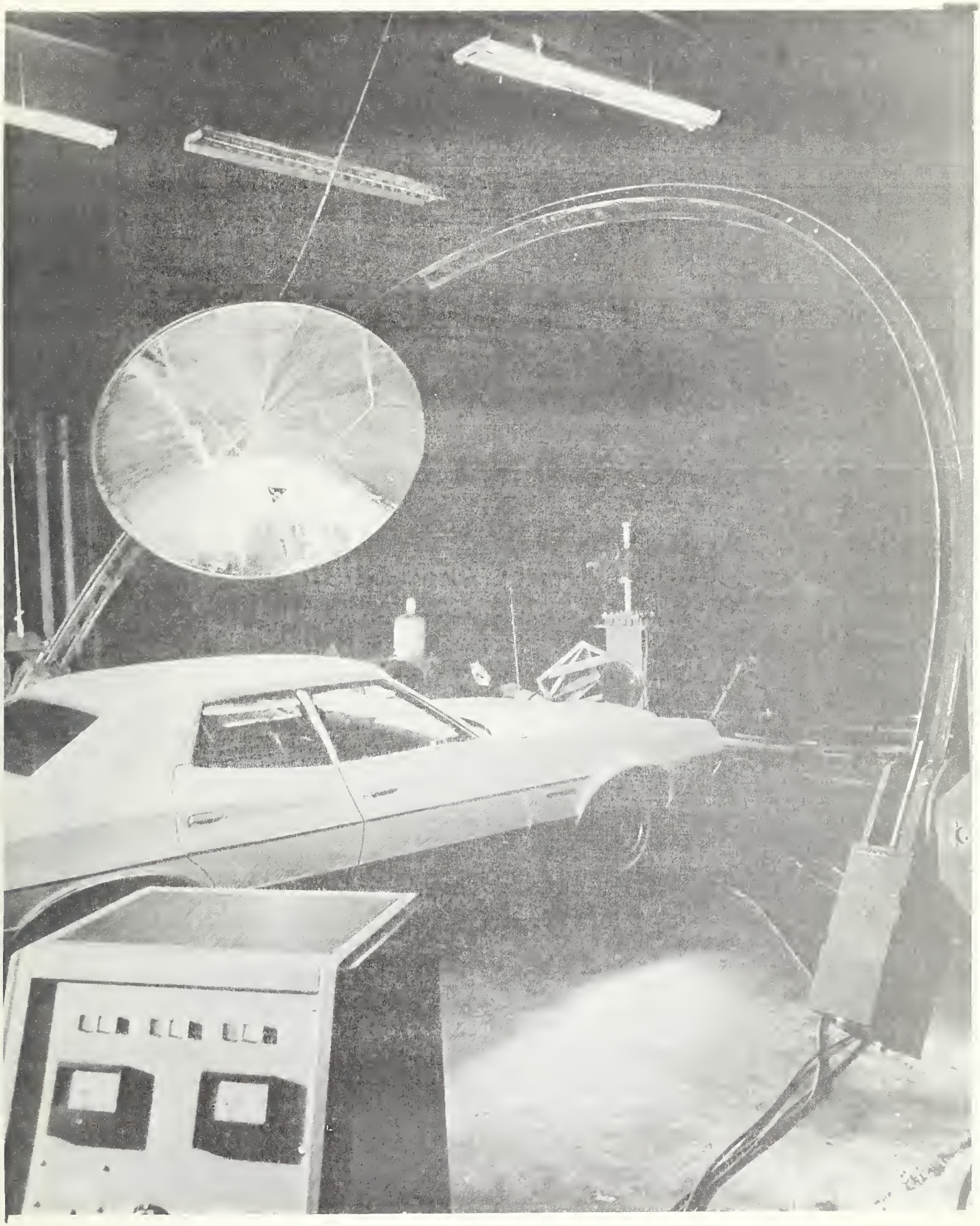

FIGURE 8. COLLIMATED SOURCE USED AS SOLAR SIMULATOR

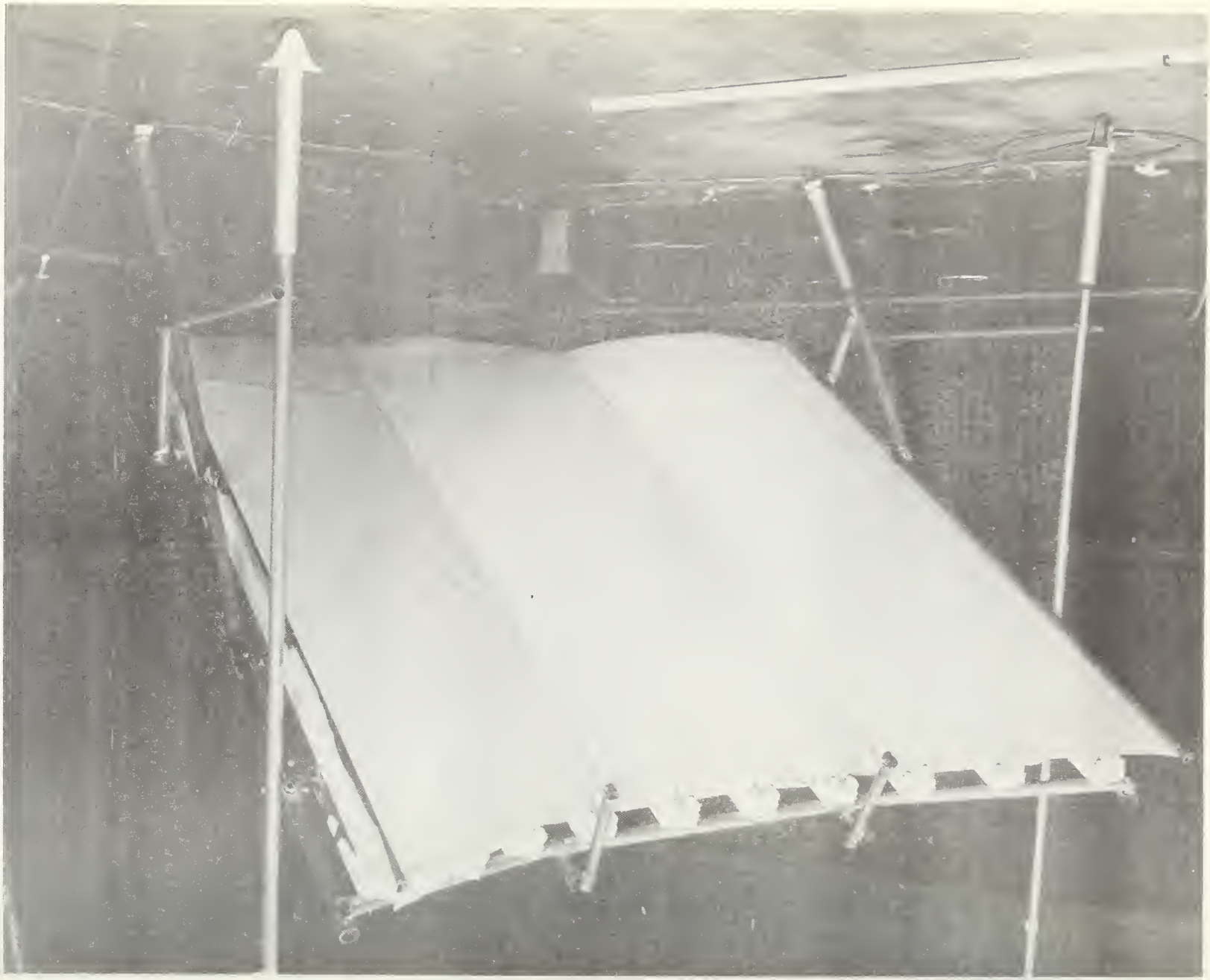

FIGURE 9. DIFFUSE RADIATION SOURCE FOR MOTOR VEHICLE TESTING

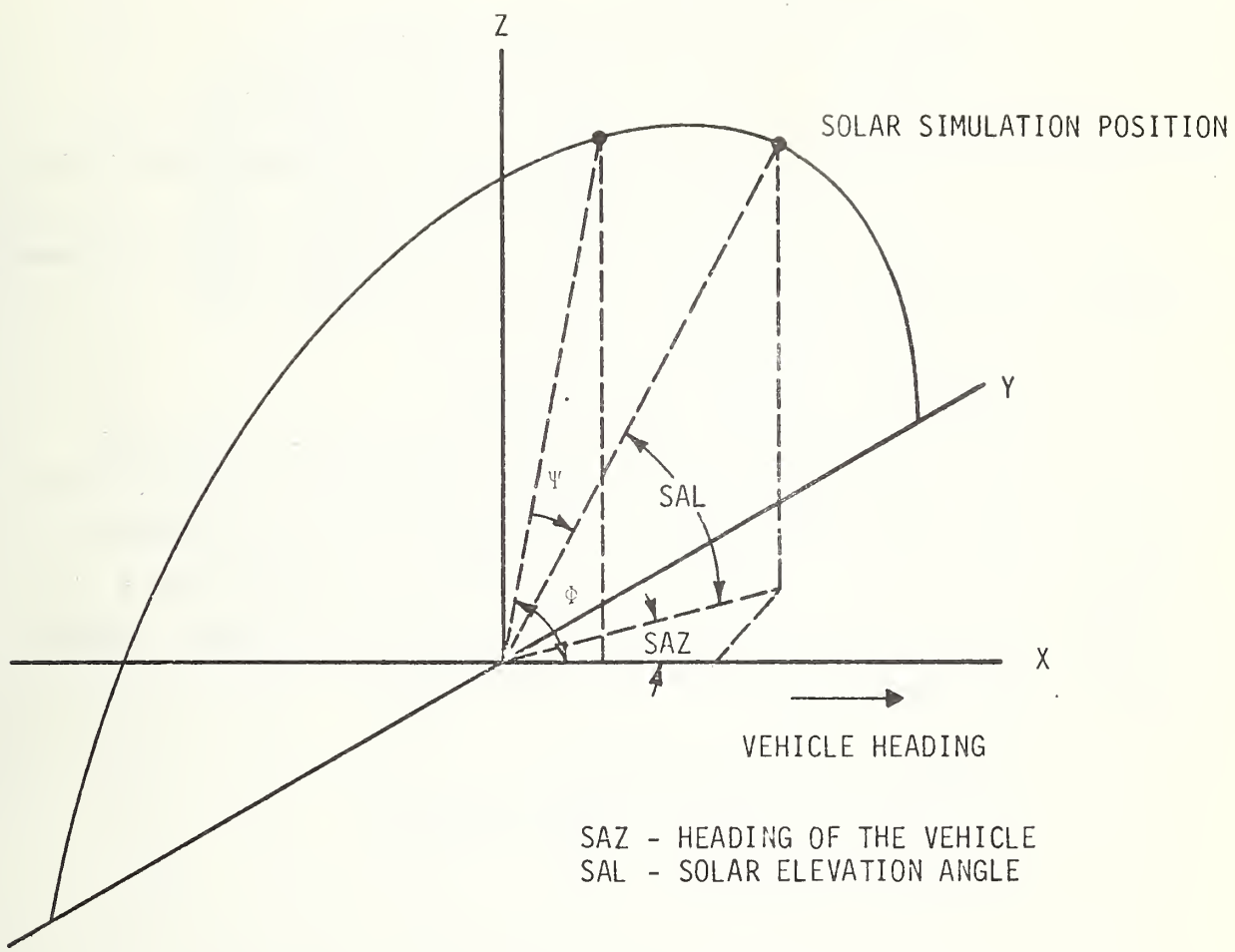

FIGURE 10. ANGULAR RELATIONSHIPS USED WITH SOLAR SIMULATOR

where

R_{DH}, R_{DD} - readings obtained from the hood and dashboard, respectively

K_{DL}, K'_{DL} - scaling factors to sky luminance

C_{AD} - a correction factor for Sun elevation

D_F - a correction factor for vehicle travel direction with respect to the Sun.

The solar altitude correction factor, C_{AS} T_S, and the direction of travel factor D_F are shown in Figure 11.

Modification to Paraboloid Reflector

The paraboloid reflector originally installed on the solar simulator had an unacceptably large angular subtense for the source and nonuniformities in the illumination it produced. Minimum acceptable specifications for the dish were arrived at by considering effects of geometrical variations from the paraboloidal shape. The specification for the current dish is

- Diameter: 8 ft, nominal
- Focal Length: 4 ft, nominal
- Surface: ±0.010 in. from paraboloid
- Error: Random
- Weight: 110 lb.

As it turned out, this specification is about the best that can be obtained within the weight and cost constraint. Weight is constrained by the structural limitations of the positioning apparatus. Cost of obtaining any closer tolerance working with lightweight dishes would be, in our opinion, prohibitive for this use. In a later section, the limitation imposed by the apparatus, as it now stands, is discussed.

Relationship of Photometric Measurements on Illuminated Vehicle to Glare

The supposition has been advanced in this section that the luminance, as measured with a photometer, may be scaled to daylight conditions to obtain a glare luminance value. The theoretical

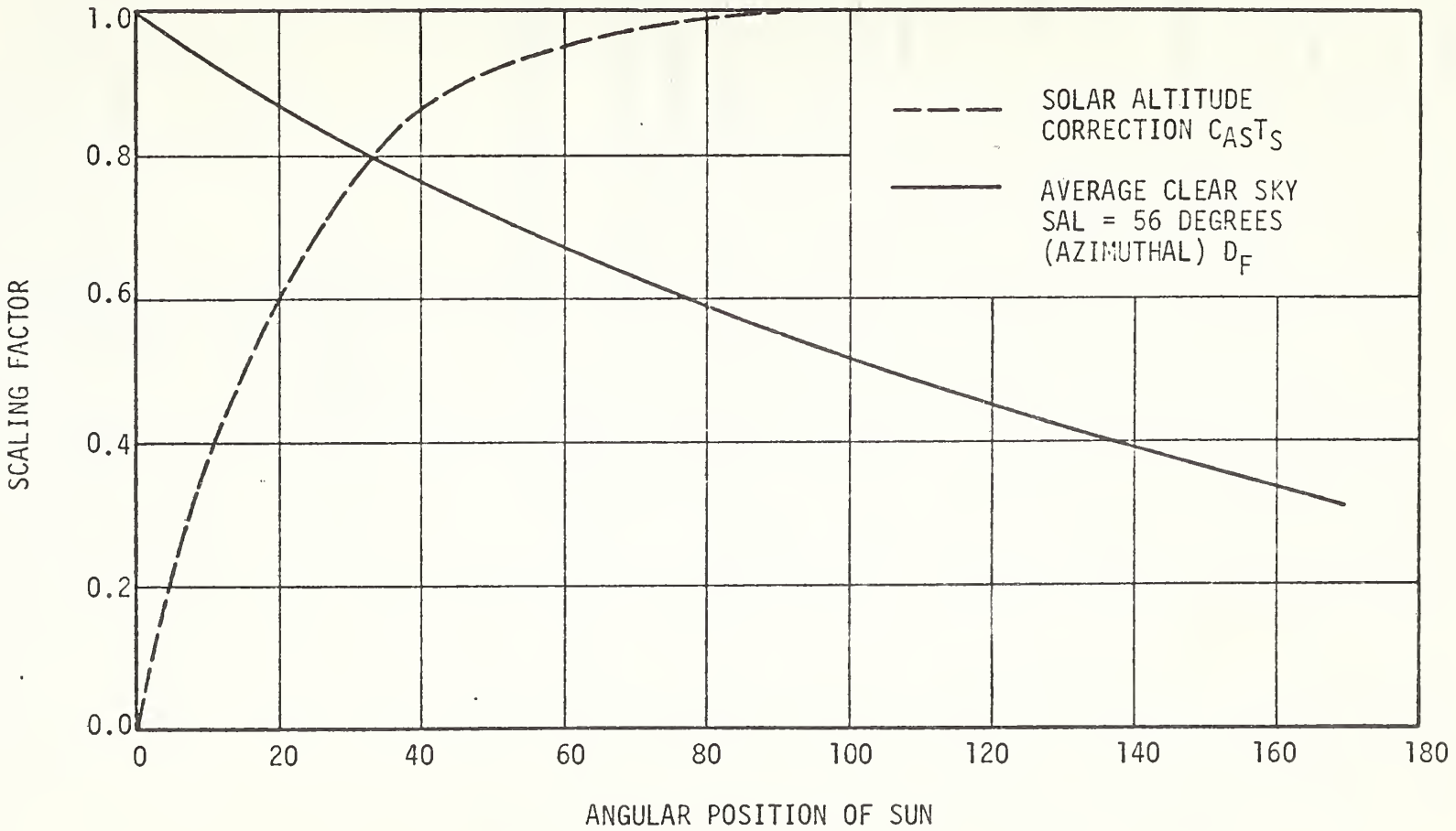

FIGURE 11. SCALING FACTORS FOR SOLAR POSITION FOR DIFFUSE AND SOLAR GLARE

development in this section presupposes that the photometric measurement is performed such that the contributions to the measured value as a function of angular position of the source to the line of sight are integrated according to the Fry relationship. Under daylight conditions, the driver's vehicle is a normal part of the "background" against which he sees a target. An estimate must be made of the overall effect of a constant luminance equal to the background luminance upon the measurement.

To estimate the luminance that may be attributed to the veiling luminance that is caused by illumination of the vehicle hood to a level of luminance equal to the rest of the background, the driver's field of view was assumed to be described by the very simple model shown in Figure 12. In Figure 12, D is the distance from the driver's eye to the end of the hood. The hood is thus treated as a portion of a vertical plane, at distance D from the eye, occupying one-third of the driver's field of view. The hood is assumed to have uniform luminance B. The intersection of the line of sight with the vertical plane is point A, assumed to be centered laterally in the field of view. Point A is a distance h above the hood line. The angle θ is the angle between the line of sight and a point on the hood; Φ is the angle between the point on the hood and a vertical line through A.

The veiling glare B_V which will be experienced from the hood luminance B is then given by

$$B_V = \int_0^{2\pi} \int_0^{\pi/2} \frac{9.2\ B \cos\theta \sin\theta\ d\theta\ d\Phi}{57.3\ \theta(1.5 + 57.3\ \theta)} \qquad (8)$$

The notation of Equation 8 is that used by Fry et al. (Ref. 16). The angle θ is expressed in radians.

The contribution of the hood to veiling glare in the field of view can be found by expressing the glare contribution from an incremental area da and integrating over the entire hood area. The integration can be most conveniently carried out in rectangular coordinates.

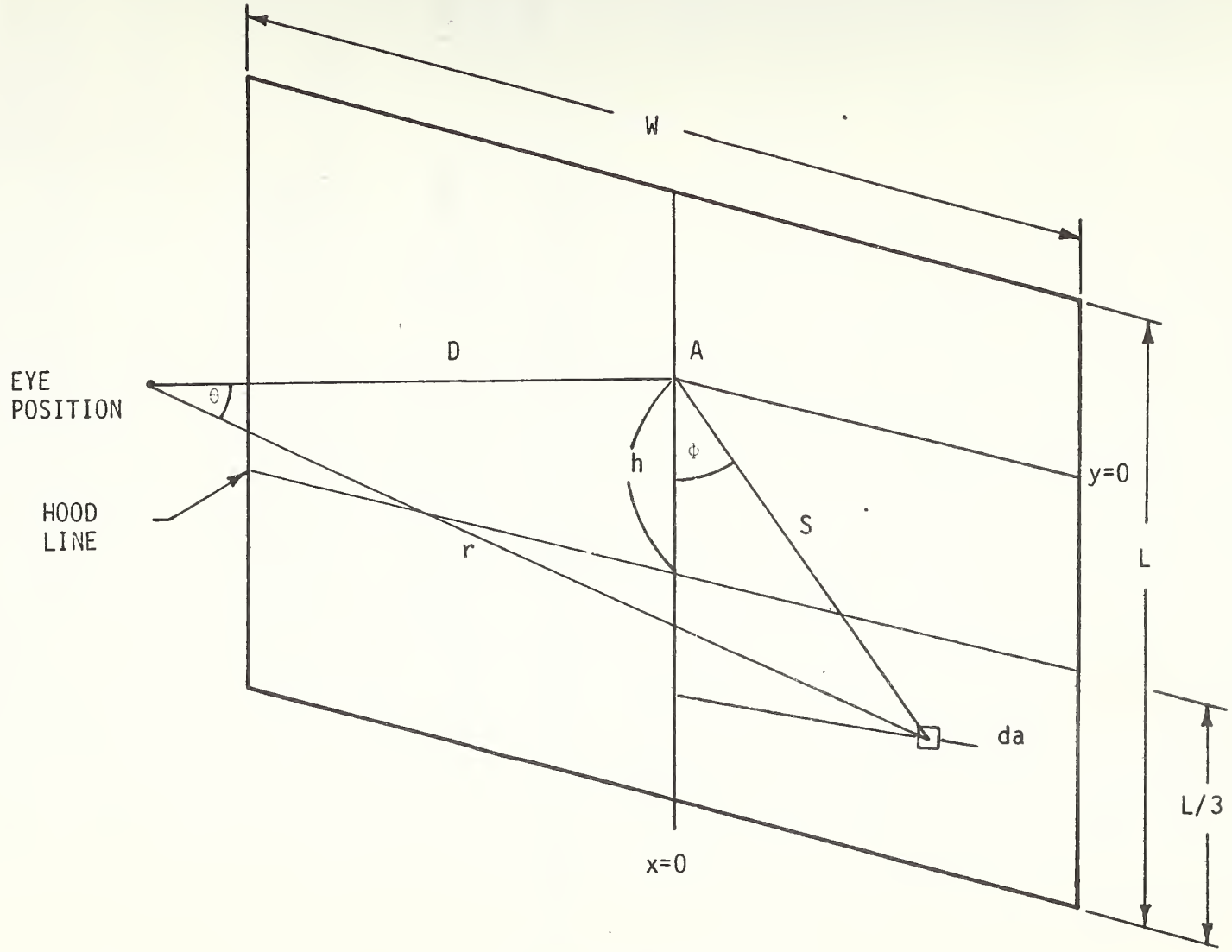

FIGURE 12. DRIVER'S FIELD OF VIEW

$$\frac{S}{D} = \tan \theta$$

$$ds = D \sec^2 \theta d\theta$$

and

$$dy = ds \cos \Phi$$

so

$$dy = D \frac{\cos \Phi}{\cos^2 \theta} d\theta$$

and

$$d\theta = \frac{\cos^2 \theta}{D \cos \Phi} dy$$

$$\frac{x}{y} = \tan \Phi$$

$$dx = y \sec^2 \Phi \, d\Phi$$

$$d\Phi = \frac{\cos^2 \Phi}{y} dx.$$

Then Equation 8 can be rewritten with the appropriate limits as

$$B_v = 2 \int_{x=0}^{W/2} \int_{y=h}^{2L/3} \frac{9.2 \, B \cos^3 \theta \sin \theta}{57.3 \, \theta \, (1.5 + 57.3 \, \theta)} \frac{\cos \Phi}{Dy} \, dy \, dx \quad . \qquad (9)$$

To integrate this numerically, values must be supplied for the variables W, L, h, and D. The following values were assumed:

W = 72 in

L = 72 in

D = 48 in.

The upper limit to values of veiling glare which can be expected in practice will be found for θ = 10 deg = 0.1745 radians. Contributions to veiling glare will come from portions of the hood for which $\theta \geq 10$ deg, extending to the edges of the field of view. For most drivers, the

smallest value of θ will be greater than 10 degrees. This value was chosen because it was considered to be the smallest line-of-sight angle with the hood for which the driver would be tall enough to see over the steering wheel. The choice of the limiting value of θ determines the value of h

$$h = D \tan \theta = 8.46 \text{ in.}$$

Equation 9 becomes

$$B_v = 2 \int_{x=0}^{36} \int_{y=8.46}^{48} \frac{9.2\ B \cos^3 \theta \sin \theta}{57.3\ \theta(1.5 + 57.3\ \theta)} \frac{\cos \Phi}{48y}\ dy\ dx \qquad (10)$$

where dimensions are given in inches and angles in radians.

Numerical integration of Equation 10 over the limits shown yields

$$B_v = 0.00581\ B.$$

The upper limit to veiling glare luminance from a hood of uniform luminance B is therefore about 0.6 percent of B; if the hood luminance is low it will not contribute appreciably to the glare luminance of the visual scene.

EXPERIMENTAL ENVIRONMENT AND PROCEDURES

EXPERIMENTAL ENVIRONMENT

The solar simulator is installed in a rectangular metal frame building. The diffuse illumination apparatus is also used in this same building. Total working area required for operation is 40 by 40 feet. The apparatus, walls, and ceiling of the room all are blackened. The following power requirements are necessary for operation:

- Electrical Power Supply
  - 440 Vac, 35 amperes
  - 220 Vac, three-phase, 3 amperes
  - 120 Vac, 5 amperes
- Hydraulic Power Supply
  - 2,500 psi working pressure at 3 gal/min.

Items of equipment required are:

- Solar simulator with hydraulic pump and control console
- Diffuse illumination apparatus
- Prichard Photometer with right-angle viewing attachment, Fry lens, and amplifier
- x-y recorder (Houston Scientific Model HR-97)
- Monostand mount for photometer
- Luminance meter (Weston).

POSITIONING OF VEHICLE AND PHOTOMETER

The vehicle is placed such that the hood and dash are entirely illuminated by the solar simulator with the dish in a raised position. This is accomplished by first positioning the dish to azimuth 0 degree and raising the frame to a relatively high elevation, 80 to 90 degrees. The vehicle is placed with its longitudinal axis perpendicular to the frame axis and exactly midway between the frame ends (passing through the center of the illuminated area). For vehicles having very long

hoods, where it is impossible to cover the hood and dash completely with the light pattern, all but the front tip of the hood is filled. This is done since it has been experimentally verified that the front end portion of the hood contributes in a negligible way to the overall veiling luminance.

All measurements with the solar simulator are carried out with the vehicle so located. Measurements with the diffuse illumination apparatus are also performed with the vehicle in this position.

The photometer is positioned with the center of the Fry lens front face at the eyellipse centroid. The eyellipse centroid is a standard point used in vehicle body design. It is located approximately 25 inches above the seating reference point (SRP), which is the rearmost position of the H point. For our work the exact position of the eyellipse centroid was taken from the Society of Automotive Engineers Data Sheet J941c (Ref. 17). The exact location of the point depends somewhat upon seat travel and back angle as given in the SAE data. Data sufficient for determination of the SRP relative to fixed identifiable points on the vehicles were obtained from the manufacturers. Since each manufacturer specified location of this point in a different way, a detailed review of eyellipse centroid location is not given here. In each case the eyellipse centroid location was very nearly independent of vehicle loading and was felt to be accurate to one-fourth inch. The Fry lens was pointed in the forward direction with its optic axis parallel to the longitudinal axis of the vehicle. Measurement of direct luminances and inside vehicle photographs were made from the approximate eyellipse centroid location.

LUMINANCE MEASUREMENTS

For measurements with the diffuse source this apparatus was rolled over the hood of the vehicle. This source was positioned with its Mylar surface at a perpendicular distance from the hood-windshield intersection of approximately 1 meter and extending an equal distance over the vehicle on both sides. The actual hood-diffuse source distance is not critical

since a measurement was taken separately of the hood and dash illuminance with the Weston meter for each vehicle. A problem arose with the two larger trucks and the bus in that the diffuse source could not be extended much beyond the end of the hood. The diffuse source measurements with these vehicles are probably erroneous and are indicated by question marks in Table 9, which appears later in this report.

Veiling luminance measurements with the diffuse source were taken with the Prichard photometer fitted with the Fry lens. Readings were taken with the vehicle uncovered, the dash covered, the hood covered, and the hood and dash covered with nonreflecting black cloth. Traces of the direct luminance reflected by the black cloth from the solar simulator have been recorded and do in fact indicate that the reflectance of this material is 0.1 percent or less. Differences between readings taken with the vehicle uncovered and covered represent veiling luminance values for the vehicle. Also, direct luminance readings were taken of light reflected by the windshield from the dash with the diffuse source. This was done by pointing the photometer, without the Fry lens, directly ahead at the windshield and recording values with and without the dash covered with black cloth. The calibration was done according to the photometer instruction manual.

For each vehicle studied in the program an extensive set of veiling luminance data was recorded with the solar simulator. The x-y recorder was used for this. The amplifier output from the photometer provided the input for the y-axis. The x-axis of the recorder indicated the frame elevation. This was achieved by a potentiometer geared to the frame drive shaft, which served as a voltage divider for a supplied dc voltage. The voltage output of the potentiometer served as the input for the x-axis. The record made with the x-y recorder was calibrated to yield veiling luminance in foot-lamberts as a function of frame elevation in degrees.

Four curves of veiling luminance as a function of frame elevation were recorded at each dish position Ψ (Figures 13 through 23). One was taken with the vehicle uncovered, one with the hood covered, one with the dash covered, and one with both hood and dash covered. The traces were begun with the dish at the center of the frame (Ψ = 0 deg) and extended

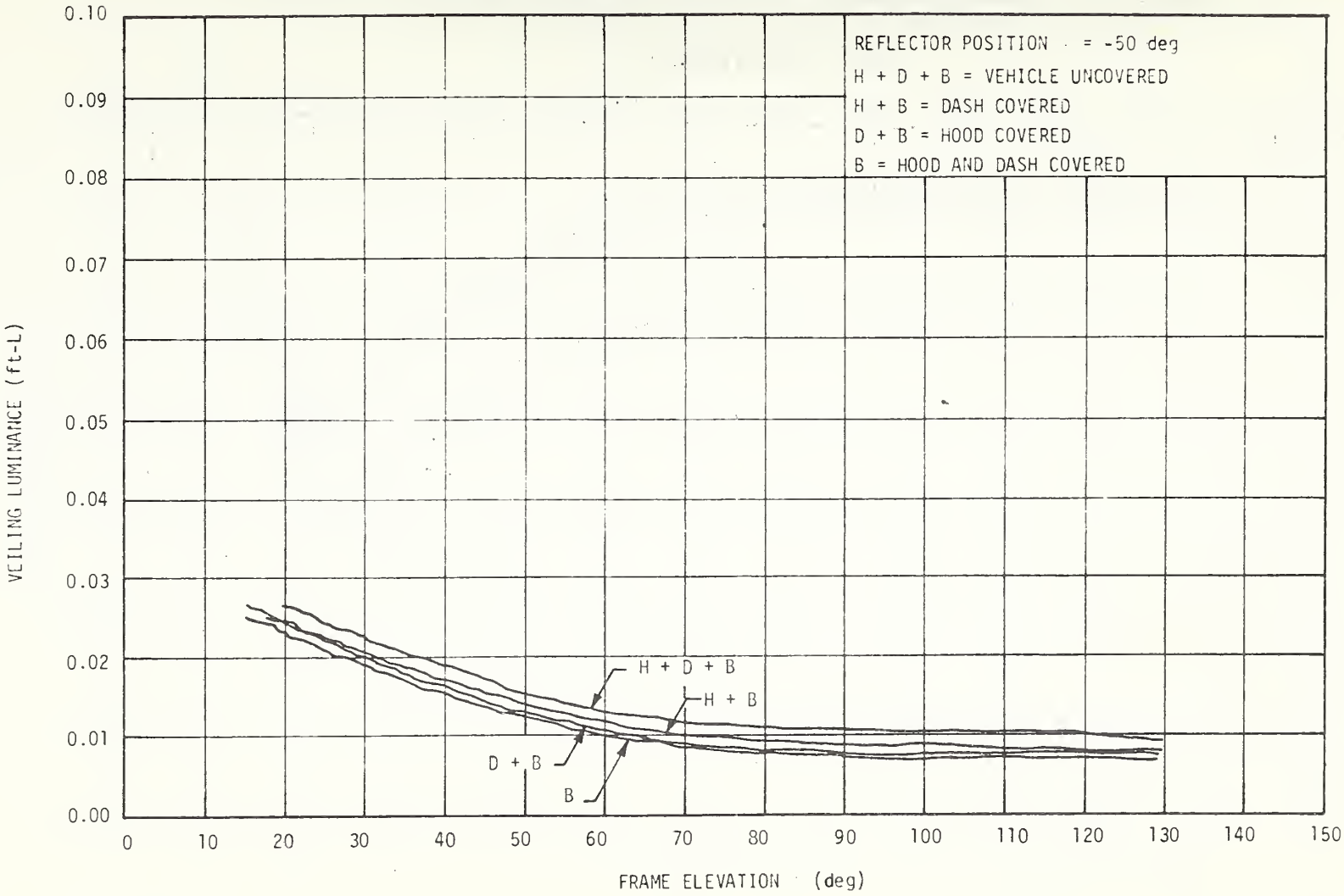

FIGURE 13. VEILING LUMINANCE DATA FOR THE MERCURY CAPRI, Ψ = -50 deg

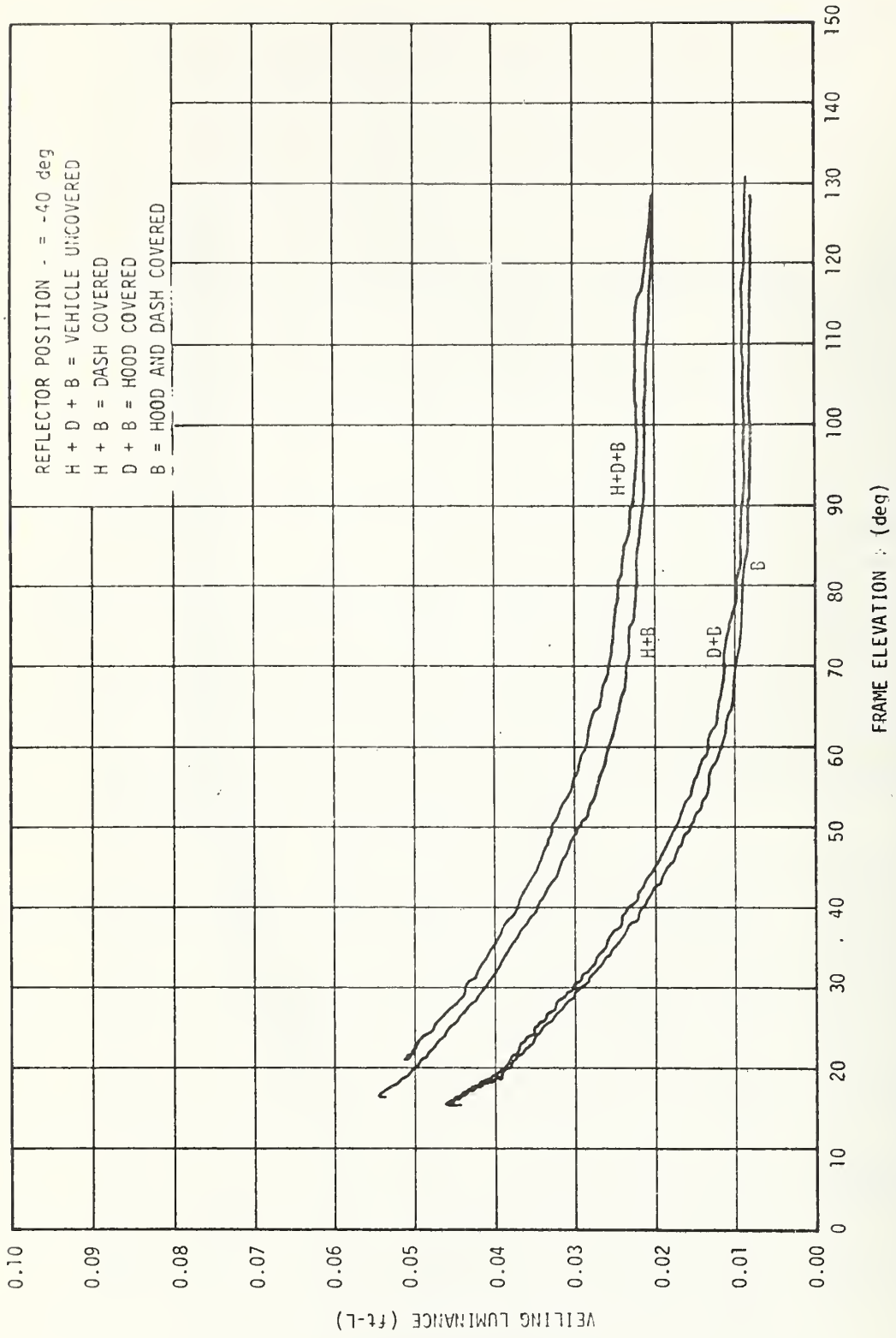

FIGURE 14. VEILING LUMINANCE DATA FOR THE MERCURY CAPRI, Ψ = -40 deg

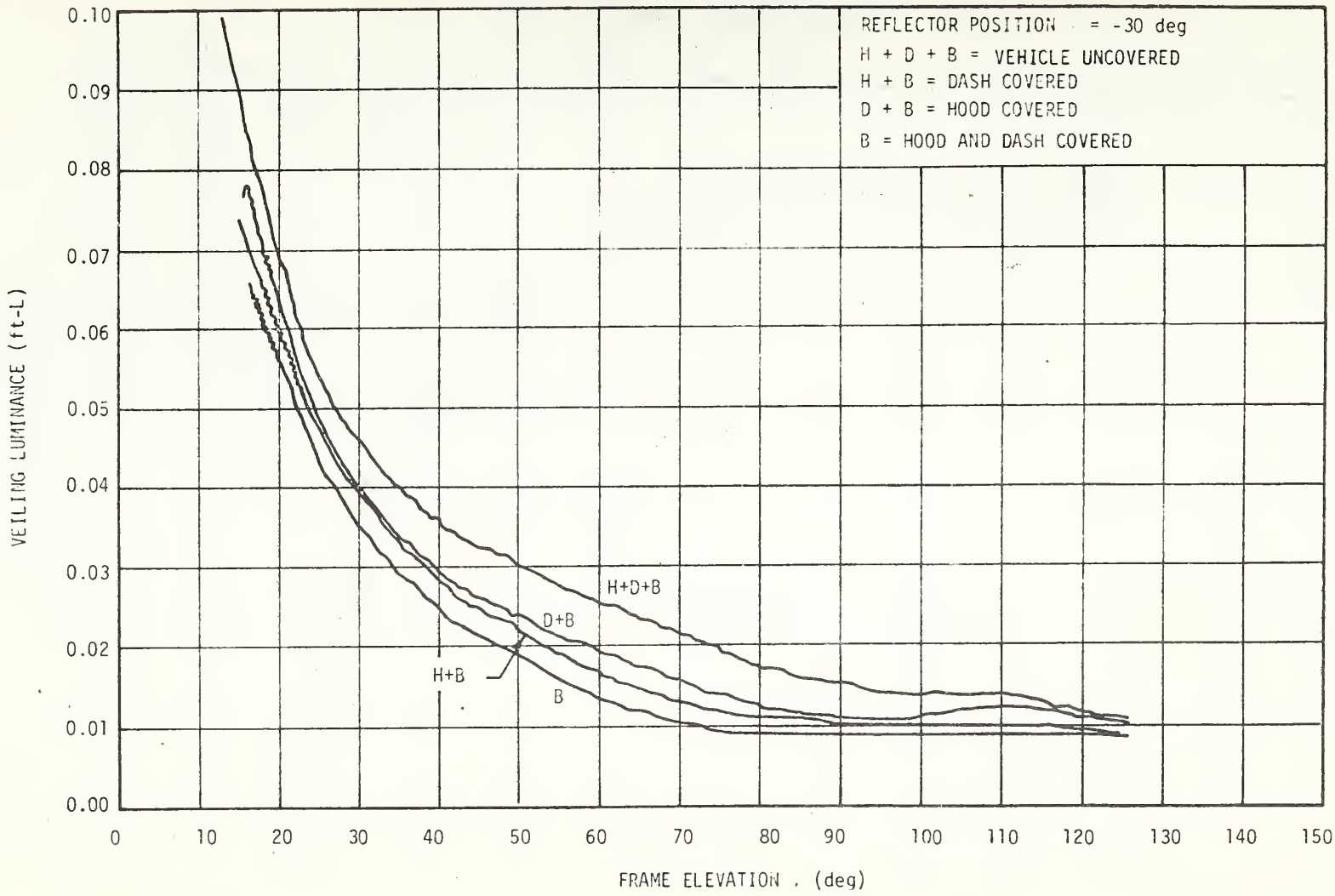

FIGURE 15. VEILING LUMINANCE DATA FOR THE MERCURY CAPRI, Ψ = -30 deg

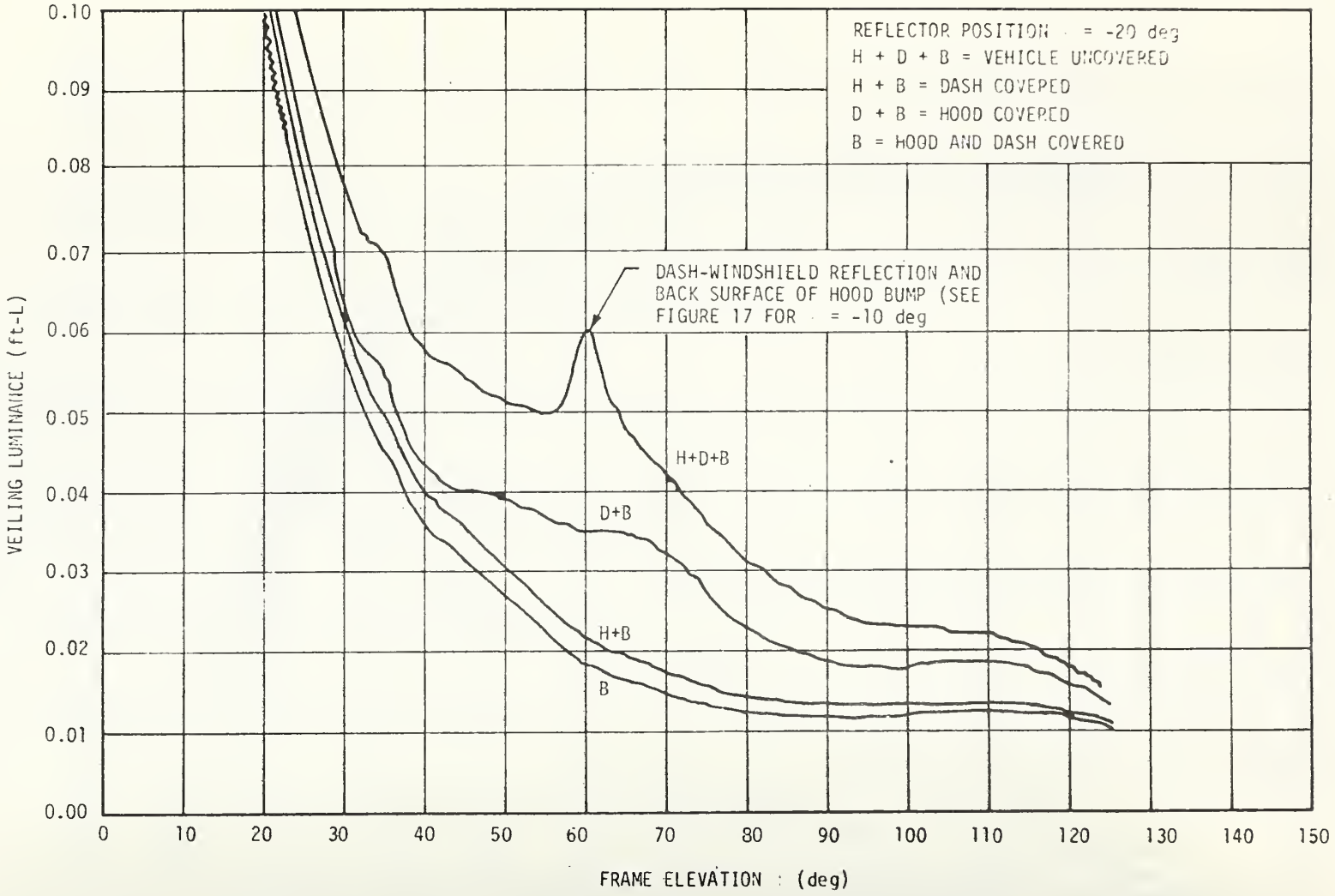

FIGURE 16. VEILING LUMINANCE DATA FOR THE MERCURY CAPRI, Ψ = -20 deg

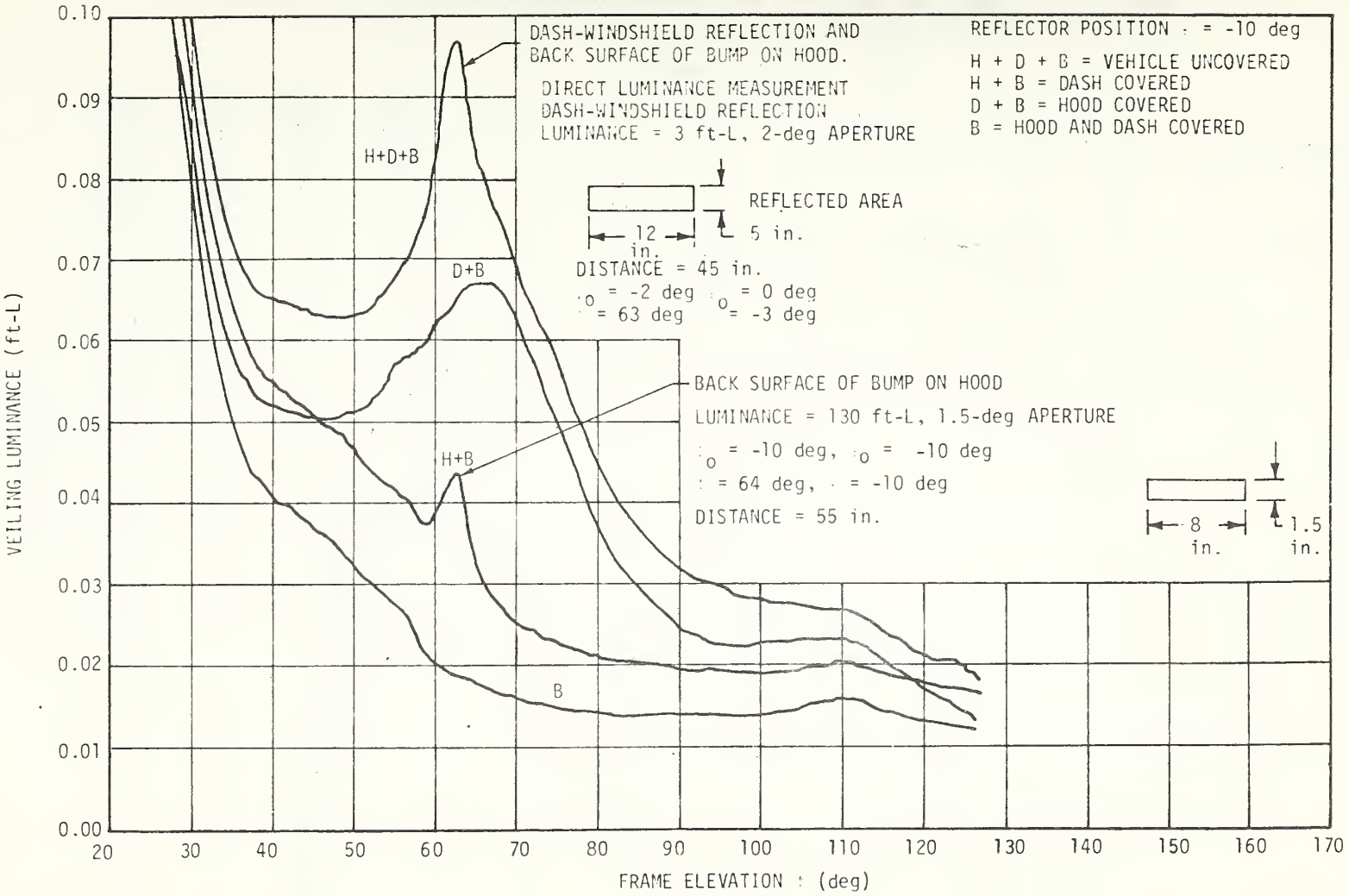

FIGURE 17. VEILING LUMINANCE DATA FOR THE MERCURY CAPRI, Ψ = -10 deg

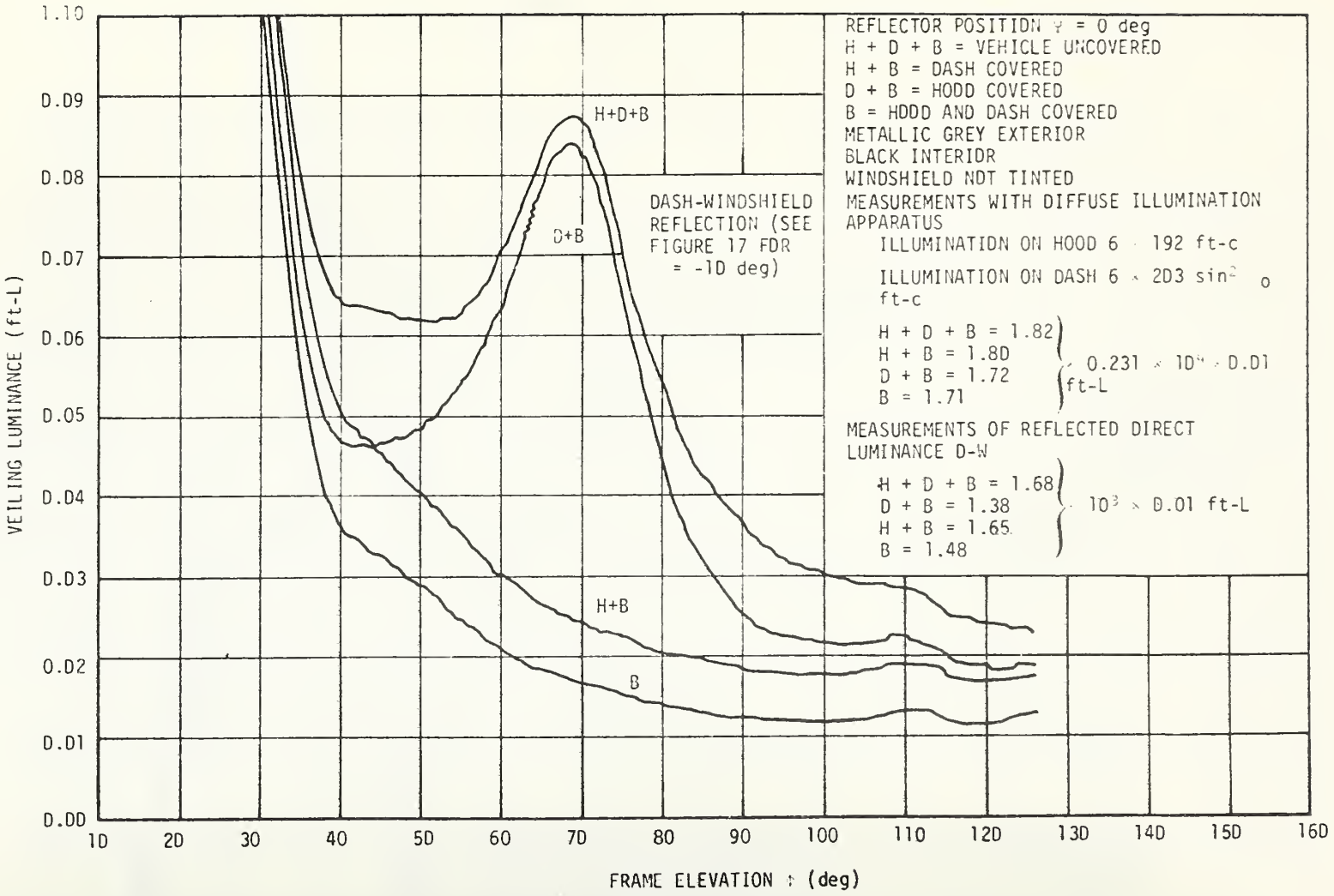

FIGURE 18. VEILING LUMINANCE DATA FOR THE MERCURY CAPRI, Ψ = 0 deg

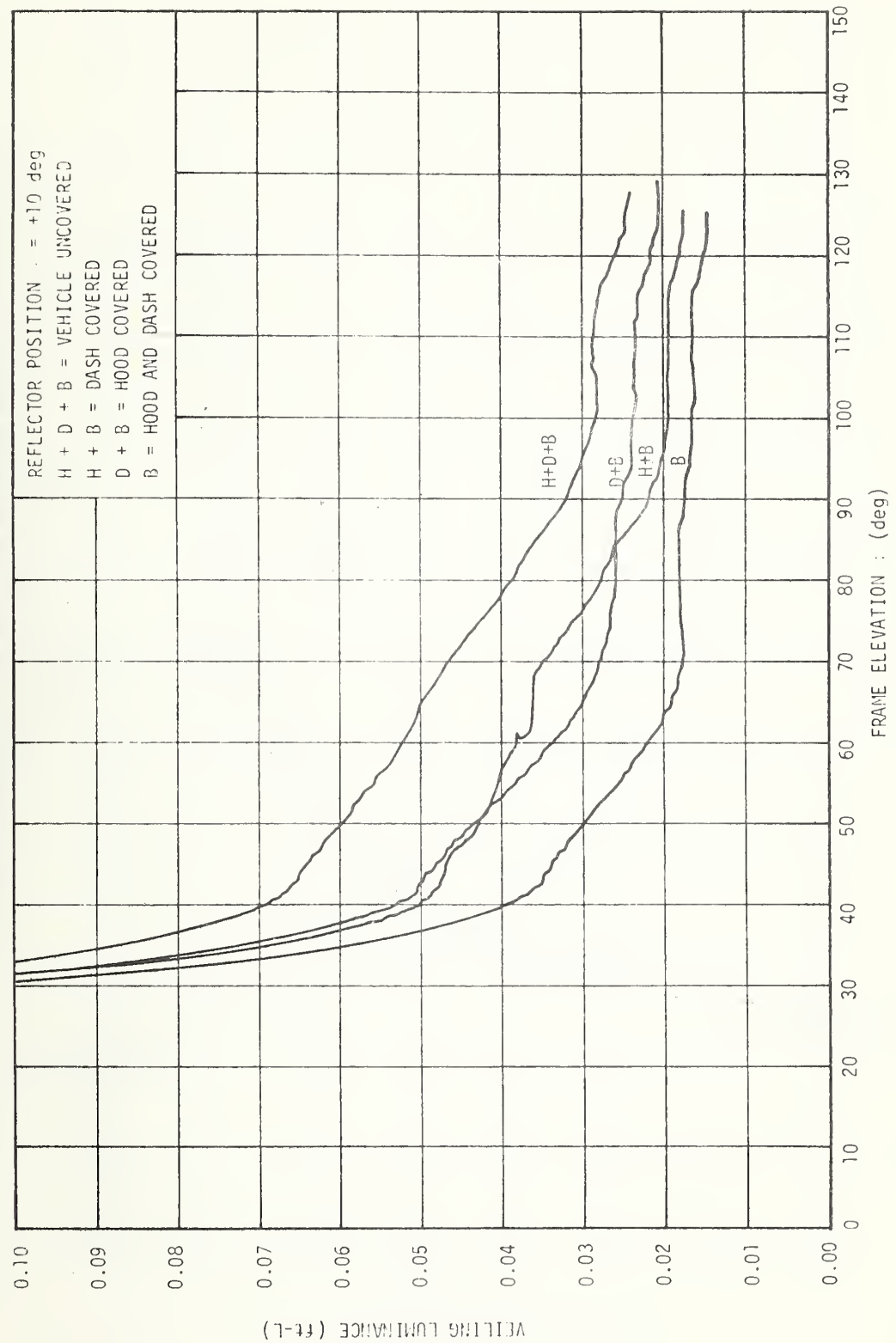

FIGURE 19. VEILING LUMINANCE DATA FOR THE MERCURY CAPRI, Ψ = +10 deg

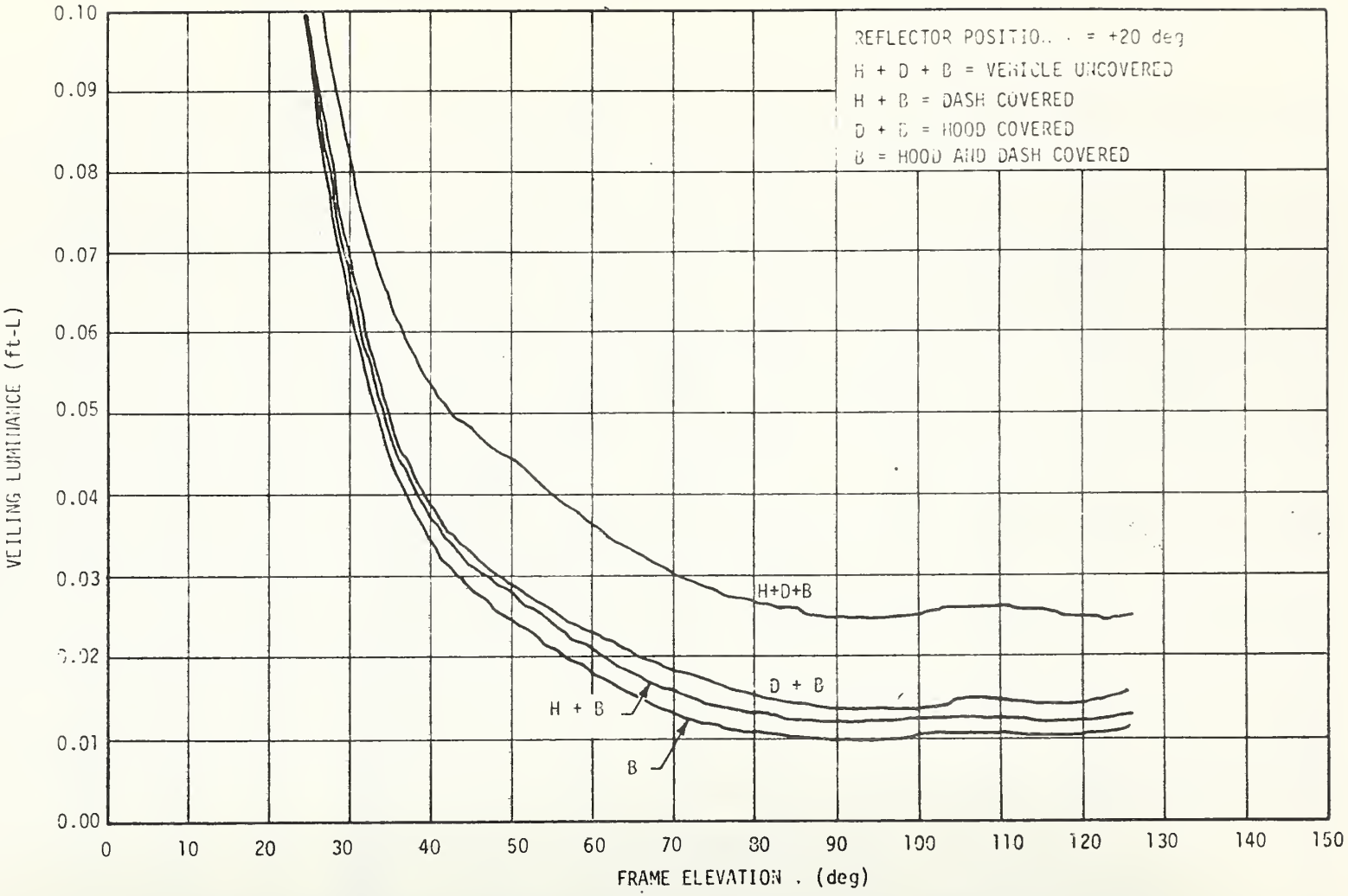

FIGURE 20. VEILING LUMINANCE DATA FOR THE MERCURY CAPRI, Ψ = +20 deg

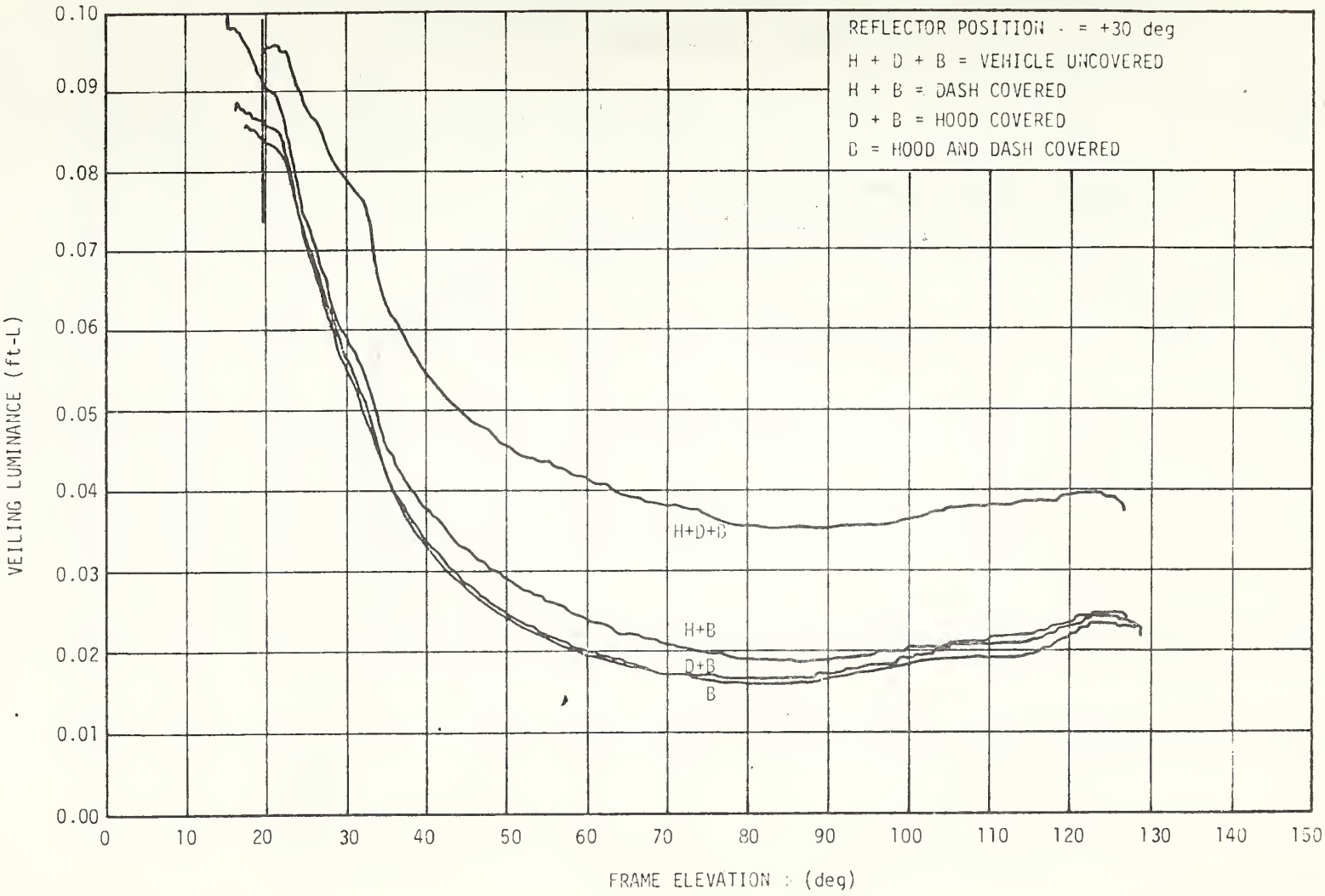

FIGURE 21. VEILING LUMINANCE DATA FOR THE MERCURY CAPRI, Ψ = +30 deg

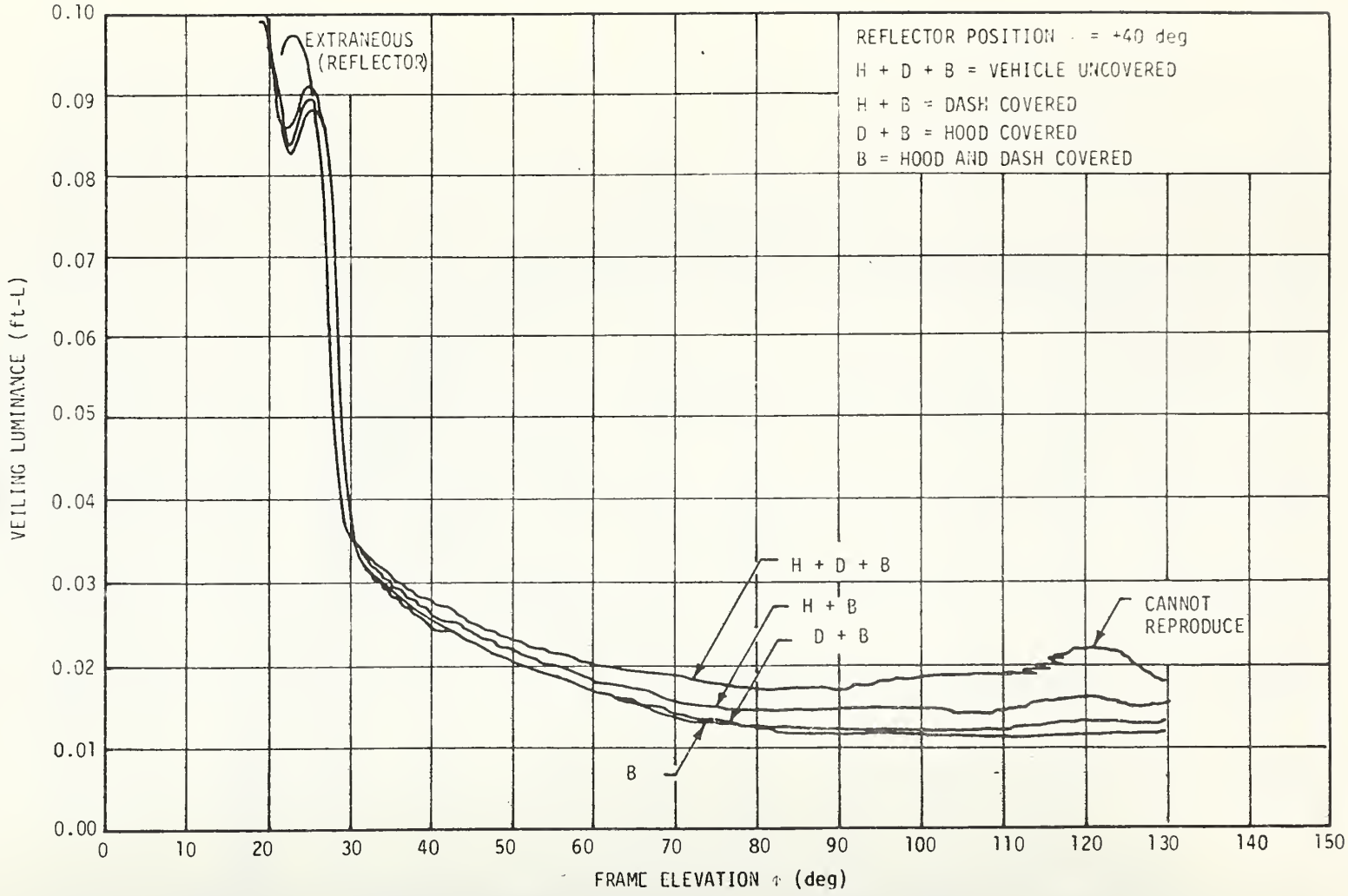

FIGURE 22. VEILING LUMINANCE DATA FOR THE MERCURY CAPRI, Ψ = +40 deg

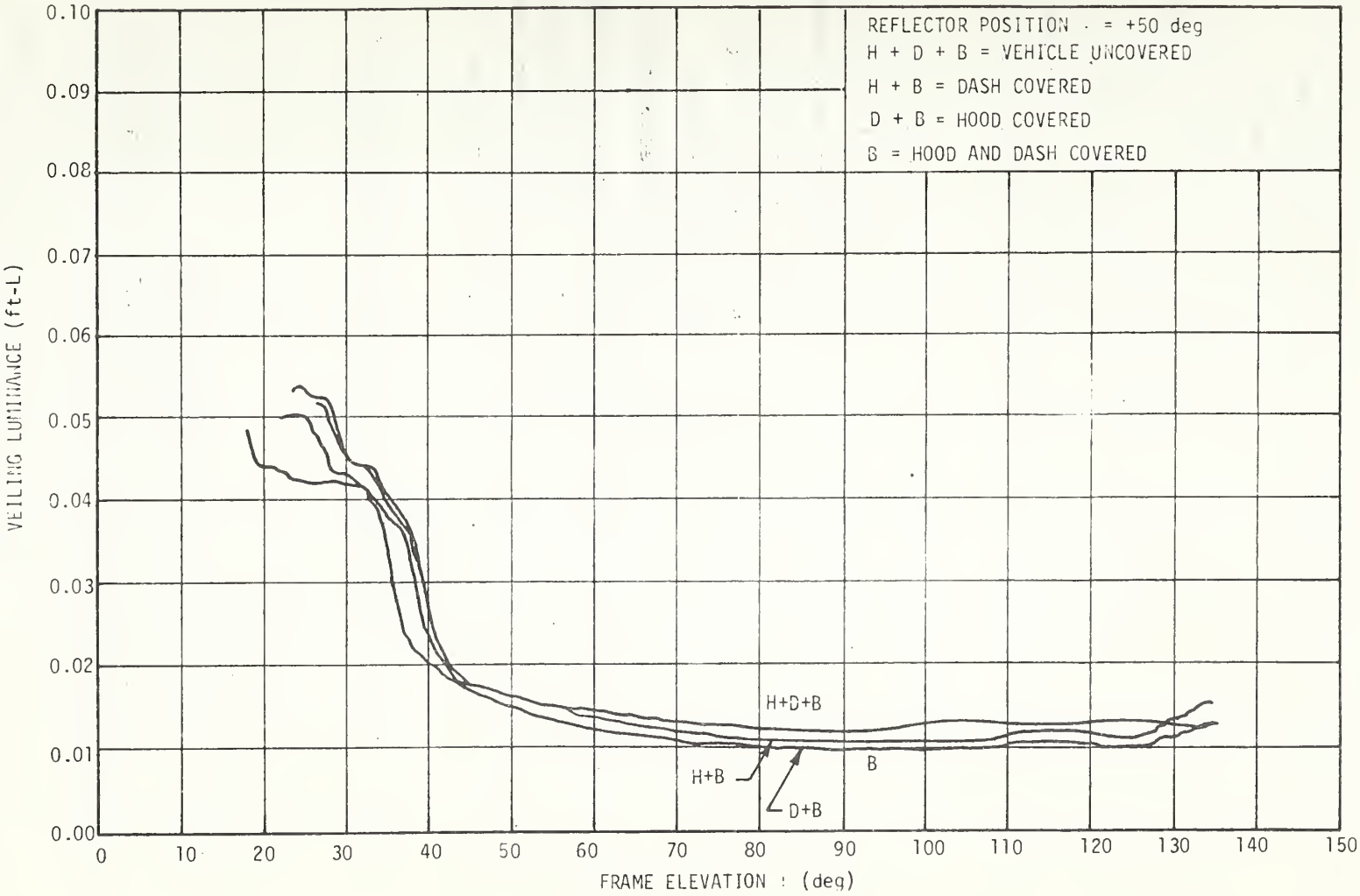

FIGURE 23. VEILING LUMINANCE DATA FOR THE MERCURY CAPRI, Ψ = +50 deg

in 10-degree increments of Ψ on both sides to approximately $\Psi = \pm 50$ degrees. One sheet was recorded at each position Ψ. Thus, eleven sheets were recorded at the positions $\Psi = 0, \pm 10, \pm 20, \pm 30, \pm 40$, and ± 50 degrees. The smallest range recorded for any vehicle was to $\Psi = \pm 30$ degrees, the largest was to ± 60 degrees. Generally, traces were recorded to Ψ values large enough that they finally took on a low horizontal shape. For 20 vehicles measured and one remeasured to check reproducibility (which was generally within 20 percent), the total number of sheets recorded during the routine measurements was 226. A typical set of data sheets is shown in Figures 13 through 23.

Occasionally, peaks were observed in the traces. These were generally due to "spot" glare sources such as chrome strips, chrome mirror mounts, and windshield wiper blades. Direct luminance measurements were taken of such sources at the dish position showing the maximum luminance. For these the photometer was used without the Fry lens at the approximate eyellipse centroid location. A spot glare source approximates a "point" source, the brightness of which is specified by an illuminance. Data on the size, shape, and distance of each spot source were recorded so that luminance readings could be corrected to illuminance values. The angular position of the source in the driver's field of view and the position of the dish at maximum source brightness were also recorded.

Finally, exterior and interior colors and windshield tint were recorded.

PROCEDURES FOR GLARE REDUCTION

Methods of glare reduction investigated were:

- Use of a nonreflecting covering material on the dash top
- Tilting the dash top
- Tilting the hood.

These are discussed below in sequence. In each case, direct luminance measurements as well as measurements of veiling luminance were taken so that the reduction in veiling glare might be independently verified.

The most obvious method of reducing glare is to use matte, low-reflecting covering materials, or even eliminate the glare-reflecting surface itself. In the process of taking routine veiling luminance measurements on the 20 vehicles used in the program, each vehicle was in effect measured for the reduction in veiling luminance resulting from covering the hood and dashboard.

Additional studies of glare reduction by dash top coverage were carried out on a 1975 American Motors Gremlin (Figure 24). Material used for covering the dash was the same used in the routine veiling glare measurements. Traces of the direct luminance reflected by this material from the solar simulator as a function of frame elevation were recorded and indicate a reflectivity of 0.1 percent or less. Veiling glare reflected by the dash top may be divided into two parts: light reflected directly by the dash into the field of view of the driver, and light reflected by the windshield from the dash (Figure 24). In addition to veiling luminance measurements, direct luminance measurements were recorded for these two components. For each of these components, three traces were recorded (luminance as a function of frame elevation) with the solar simulator. Three traces were recorded of direct luminance reflected by the windshield, and three of the dash, the directions being at various angles to the line of sight (the straight-ahead direction, Figure 25). The traces were taken both with the dash uncovered and covered with the black cloth. Sufficient linear dimensions were also recorded to allow computation of solid angles and angles off the line of sight.

Reduction of veiling glare was studied by tilting the dash top of a 1975 Ford Mustang II. The driver's view of this automobile is shown in Figure 26. The model studied had a medium-blue vinyl dash top. Blue vinyl material similar to this was purchased, and veiling luminance measurements were made of the original dash and the dash covered with the blue vinyl. These measurements indicated a reflectivity difference in the material of 10 percent or less. A new dash top was then fabricated from heavy corrugated cardboard. It was formed in such a way that when

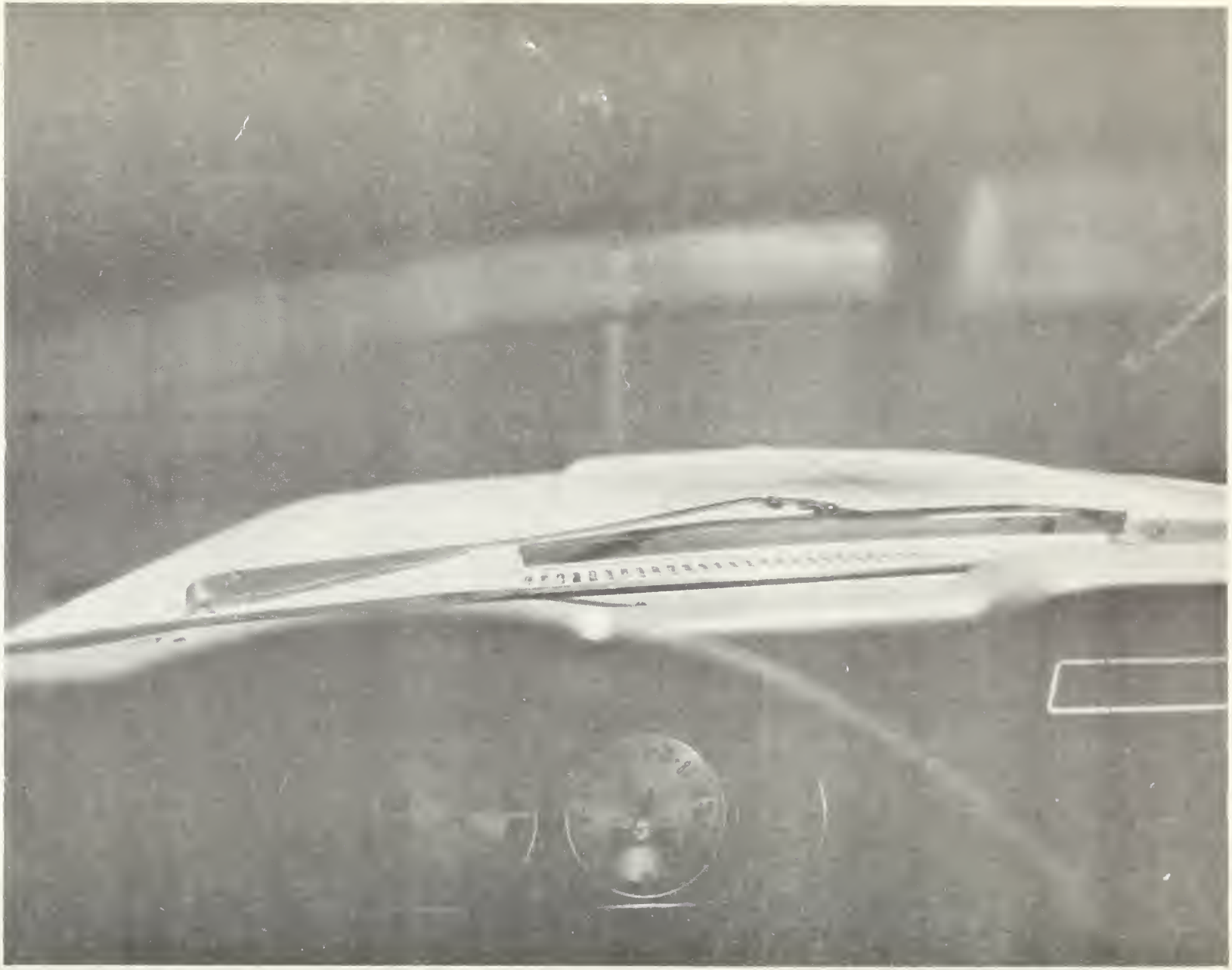

FIGURE 24. DRIVER'S VIEW OF THE 1975 AMC GREMLIN

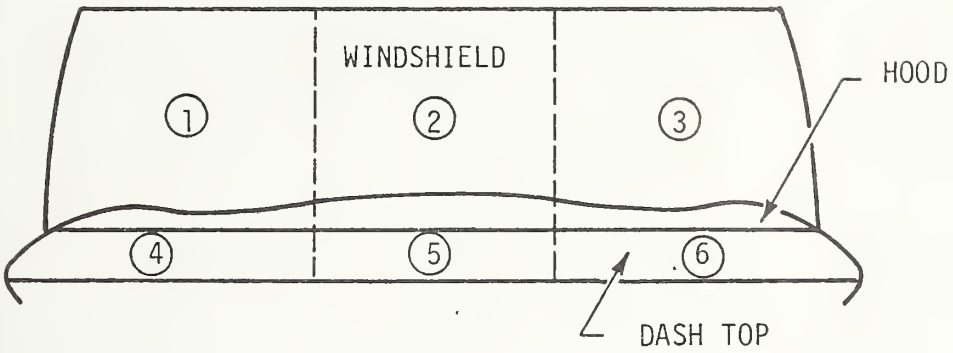

FIGURE 25. SKETCH OF DRIVER'S VIEW OF THE 1975 AMC GREMLIN (The circled numbers indicate the approximate locations of direct luminance traces.)

FIGURE 26. DRIVER'S VIEW OF THE 1975 FORD MUSTANG II

placed atop the original dash of the Mustang the rear dash surface (toward the driver) was elevated above the former surface by 2 inches, with the forward dash surface coincident with the former surface. The modified dash was then covered with the purchased blue vinyl material so that its surface covering would resemble the original.

The top of the modified dash installed was effectively tilted so that its surface was not directly visible from the eyellipse centroid (Figure 27). Veiling glare from the original dash consists of light reflected by the dash top directly into the driver's field of view and light reflected by the windshield from the dash top. Veiling glare reflected by the tilted dash top consists also of a portion reflected by the windshield as well as an illuminated rim at the rear of the dash which the driver views directly.

A complete set of veiling luminance data, with the solar simulator and the diffuse illumination apparatus, was recorded with the original dash and the modified dash. In general, the modified dash showed less veiling luminance than the original dash (Figure 28). Traces of the direct luminance as a function of frame elevation with the solar simulator at $\Psi = 0$ degree were recorded for the original dash top, the illuminated rim of the modified dash top, and the original and modified dash tops reflected in the windshield. These were recorded for various angles off the line of sight with the photometer objective lens located at the approximate position of the eyellipse centroid. Sufficient linear dimensions were also recorded so that solid angles and angles off the line of sight (the straight-ahead direction) could be calculated.

Reducing veiling luminance by tilting the hood was also studied. A 1975 Gremlin was used as the subject; a photograph of the driver's view of this automobile is shown in Figure 24. The hood of the vehicle was modified by first building up the rear portion of this surface with pieces of thick corrugated cardboard. This was covered with a sheet of Celotex the size of the hood and having the approximate curvature of the hood. On top of this was fastened a large piece of Mylar, painted and waxed to resemble the outside finish (arctic white). This modified hood

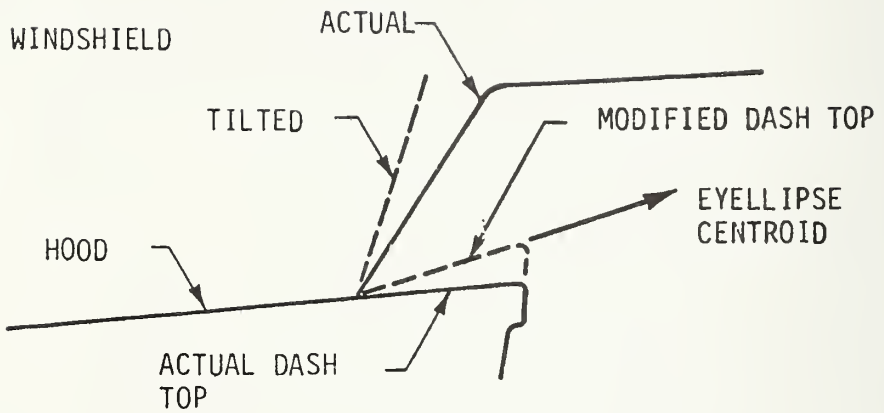

FIGURE 27. GLARE REDUCTION BY MODIFICATION OF DASH SHAPE

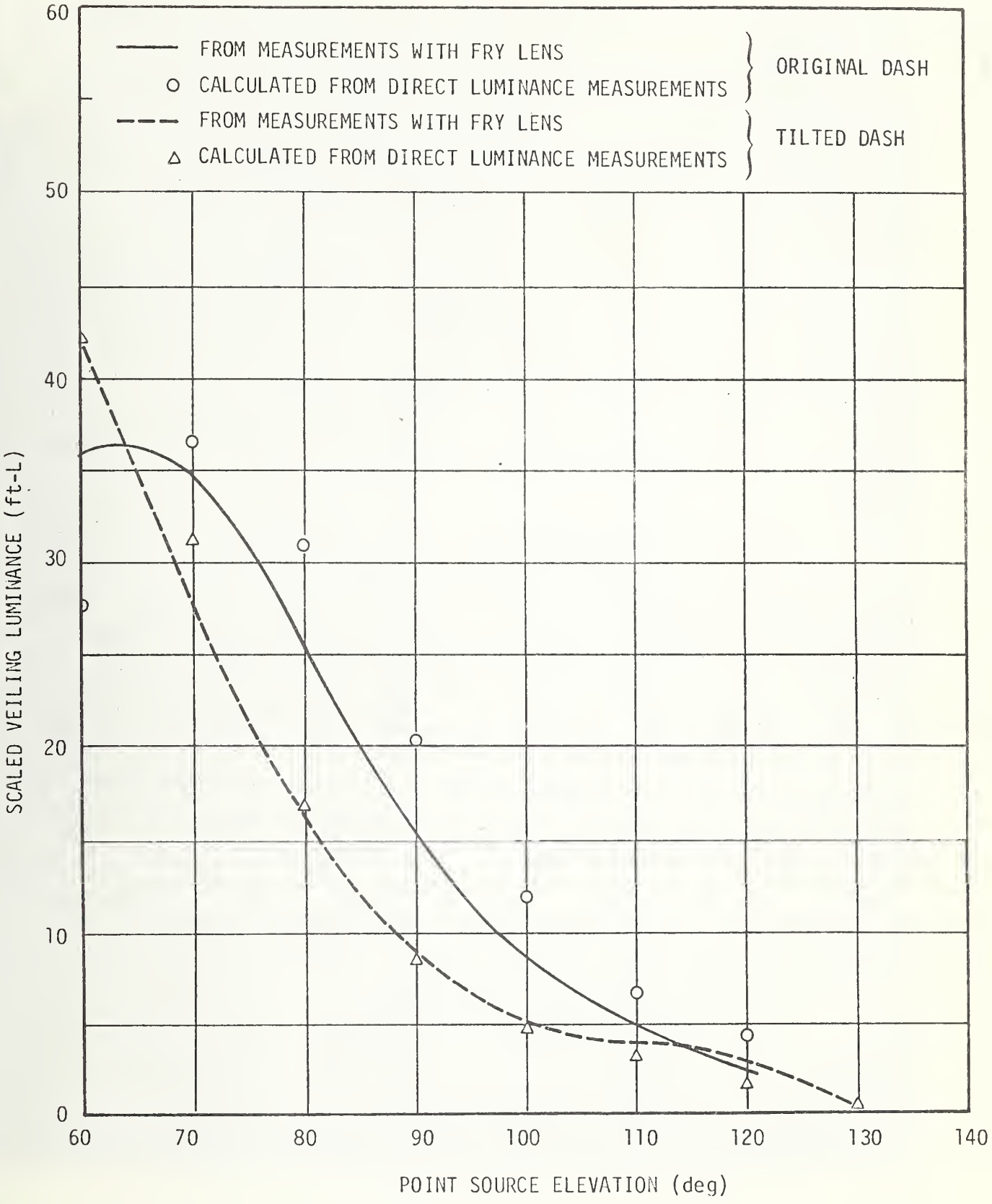

FIGURE 28. VEILING LUMINANCE FROM ORIGINAL AND TILTED DASH TOP IN THE 1975 FORD MUSTANG II, BLUE VINYL, AZIMUTH = 0 deg

was coincident with the original hood at the front, but elevated 5 inches above it at the windshield. This modified hood surface is shown in Figures 29 and 30. The effect is that the surface of the modified hood is not seen from the eyellipse centroid (Figure 31). A photograph of the driver's view with the modified hood in place is shown in Figure 32.

A complete set of veiling luminance measurements, with both the solar simulator and the diffuse illumination apparatus, was taken for both the original hood and the modified hood. All measurements with the modified hood were less than those with the original hood (Figure 33). Since all measurements represent the difference between the hood uncovered and covered, no effect of shadowing of the dash is present in the veiling luminance data.

Traces of direct luminance due to the hood as a function of frame elevation were also recorded with the solar simulator at $\Psi = 0$. Veiling luminance reflected by the hood is seen directly by the driver and as light reflected by the hood and scattered by the windshield. Direct luminance traces were taken of the hood and the windshield with the original hood, and of the windshield with the modified hood. These were recorded with the hood uncovered and covered with nonreflecting cloth at various angles to the line of sight (the straight-ahead direction). Sufficient linear dimensions were also recorded so that solid angles and angles off the line of sight could be calculated.

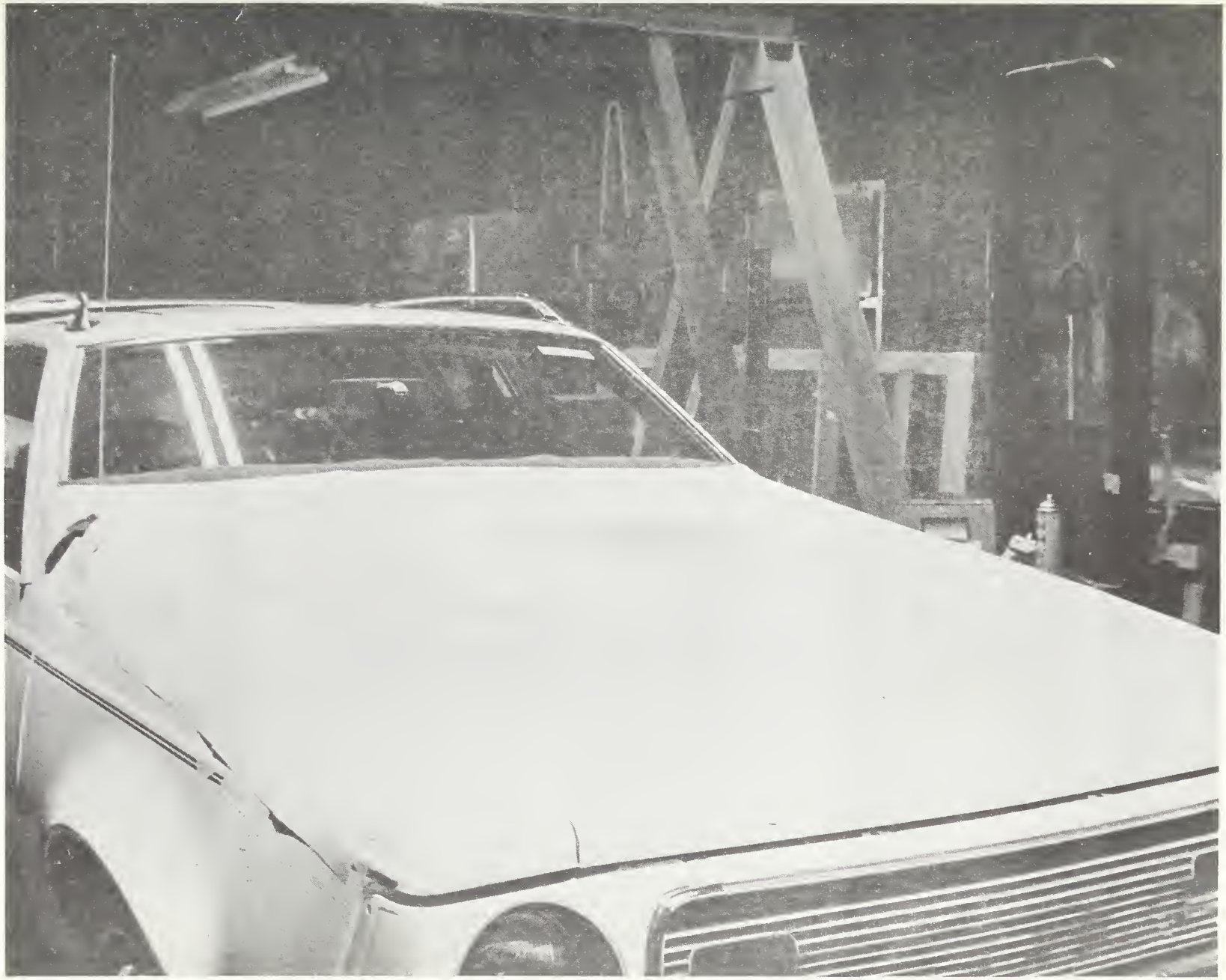

FIGURE 29. OUTSIDE VIEW OF THE MODIFIED HOOD, 1975 AMC GREMLIN

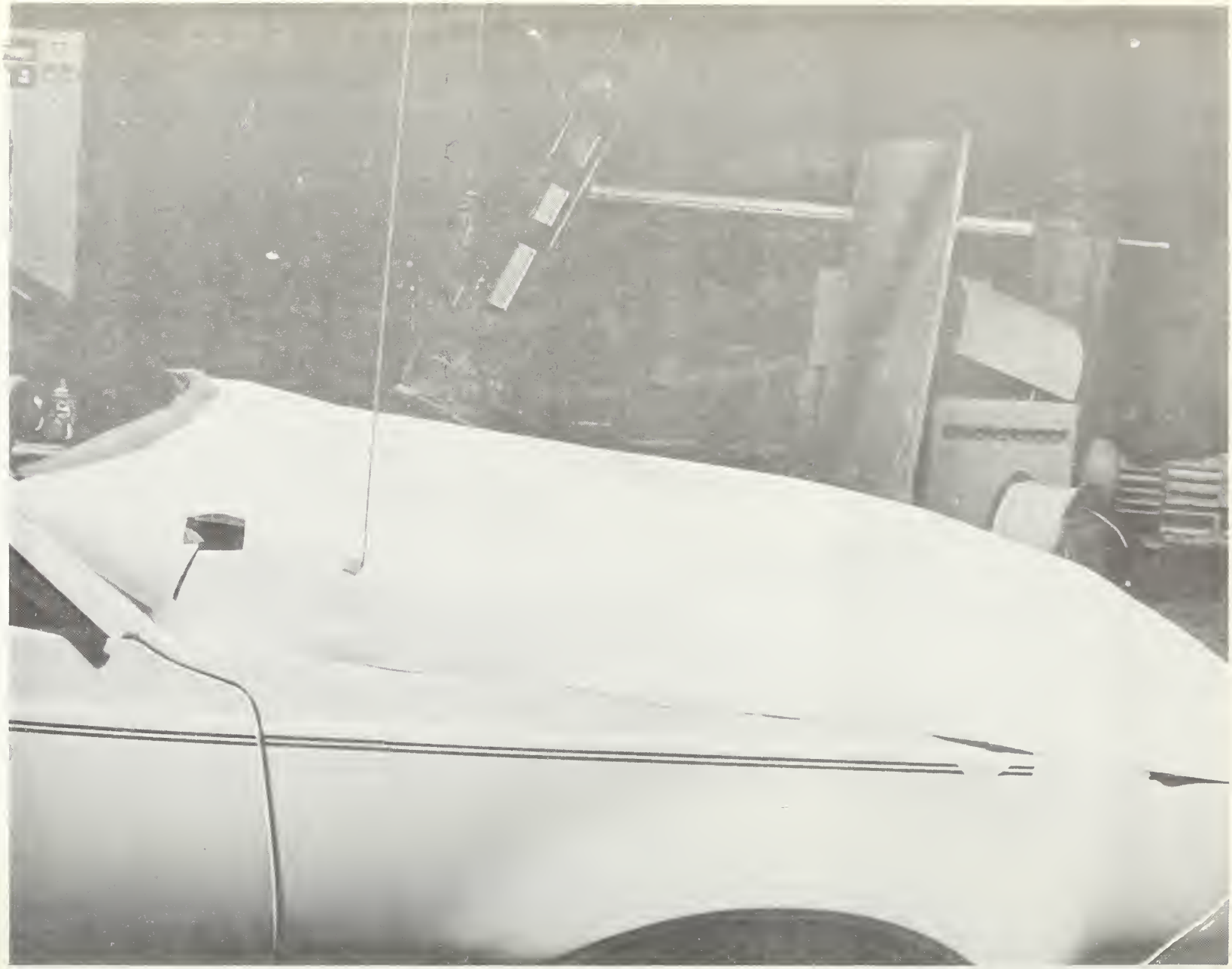

FIGURE 30. OUTSIDE VIEW OF THE MODIFIED HOOD, 1975 AMC GREMLIN

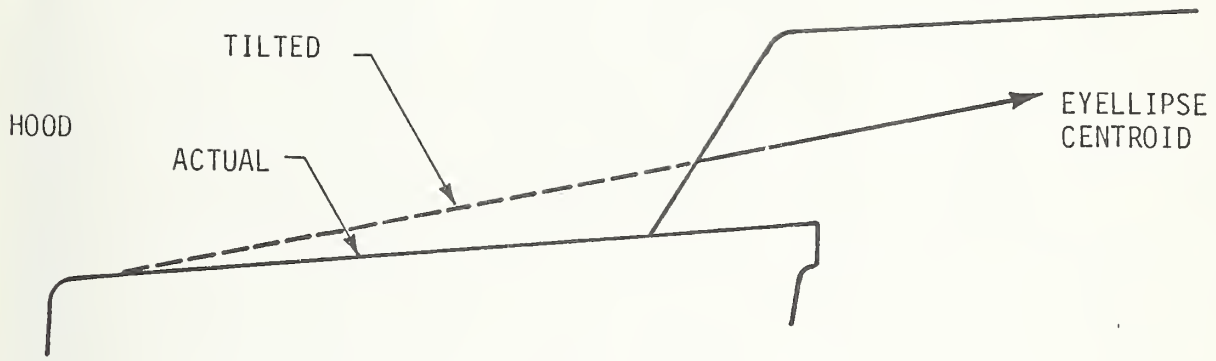

FIGURE 31. GLARE REDUCTION BY MODIFICATION OF HOOD ANGLE

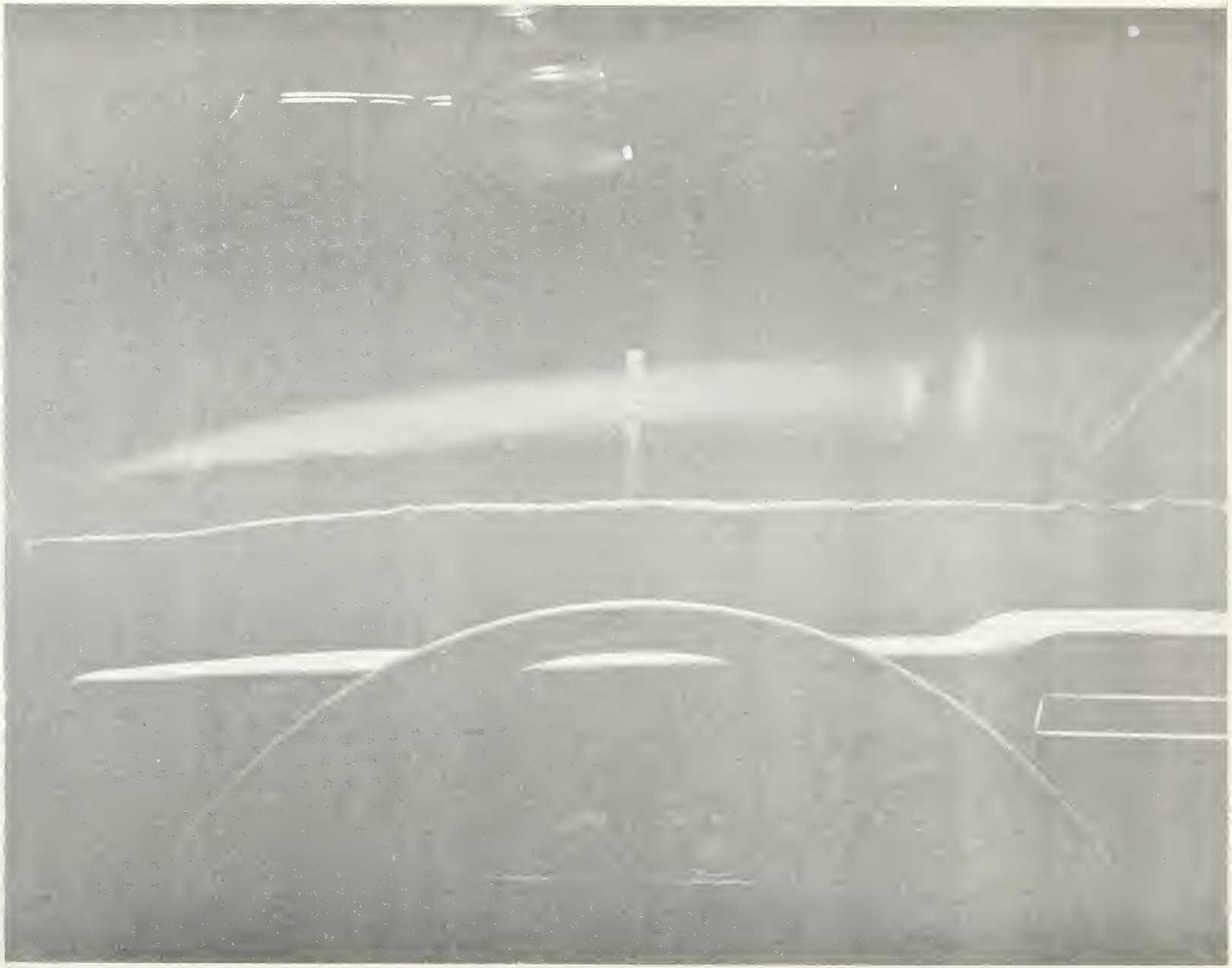

FIGURE 32. DRIVER'S VIEW WITH MODIFIED HOOD IN PLACE, 1975 AMC GREMLIN

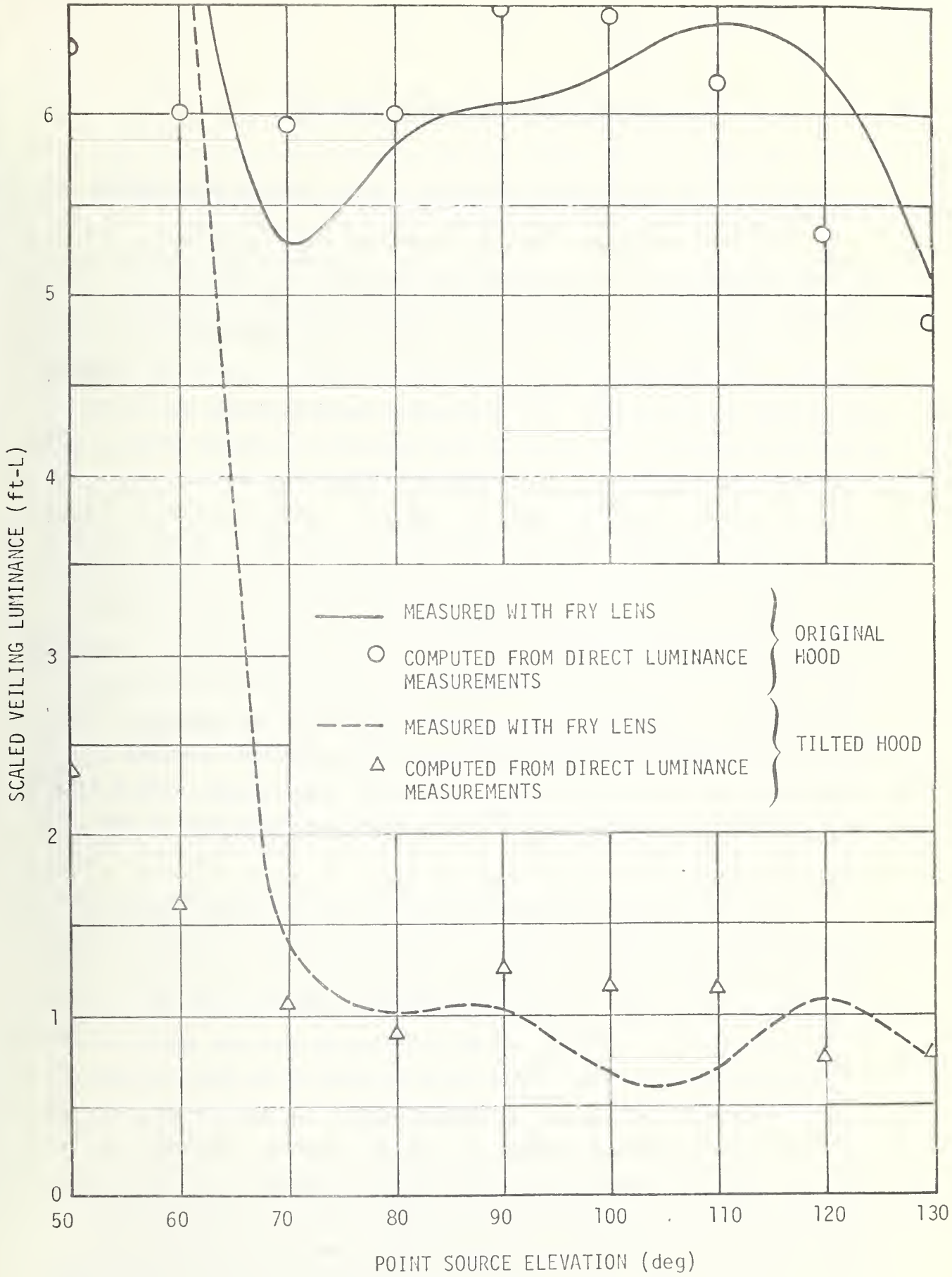

FIGURE 33. VEILING LUMINANCE REDUCTION DUE TO TILTING OF HOOD OF THE 1975 AMC GREMLIN, EXTERIOR ARCTIC WHITE, POINT SOURCE, AZIMUTH = 0 deg

EXPERIMENTAL AND TEST RESULTS

EVALUATION OF GLARE MEASUREMENT APPARATUS - MOTOR VEHICLE MEASUREMENTS

To test the glare measurement apparatus and scaling laws, the equivalent veiling luminances reflected by the hood and dash for two automobiles have been measured both in natural daylight and with the daylight simulation apparatus. Recent model automobiles were chosen so that the effects of age degradation of the paint finish and windshield transparency were minimized. A 1973 Pontiac Catalina Sedan was chosen as the first subject. The color of this automobile is burnt umber. Although the equivalent veiling luminance reflected by the hood was smaller than what would have been preferable for comparative purposes, the equivalent veiling luminance reflected by the dash was large enough that a satisfactory overall comparison was possible. The measurements were carried out with the Prichard Photometer with Fry lens attachment. This was placed in the estimated location of the driver eyellipse centroid: 3 inches below top of driver's window, 9.75 inches forward from rear of same window, in the vertical longitudinal plane of the steering wheel center. This estimated location of the centroid is adequate because we are only interested in a comparative measurement. The Y filter, which provides a relative spectral responsivity matching that of the human eye, was used.

The measurements with the Catalina made in natural daylight were recorded on November 30, 1974. The automobile was located north of the high bay wing of the Manufacturing Building at Teledyne Brown Engineering. The vehicle was pointed south (toward the high bay) and was located sufficiently close to the building so that the north building wall (shaded) occupied much of the field of view of the Fry lens and served to minimize extraneous background light. The sky on this day was clear, and the measurements began at 19^h 15^m U.T. and concluded at 21^h 19^m U.T. Before the measurement series, the automobile was placed just inside the shadow of the bay for measurement of the veiling luminance reflected by the hood and dash from the sky. Background values were obtained by covering selected portions of the vehicle with nonreflecting

black cloth. Since the sky was still largely unobstructed, these readings constituted measurements of the diffuse source (sky) contribution. The values were equal for the hood and dash and were 0.5-foot-lambert at 19^h 15^m U.T. This value was adjusted for the solar elevation and azimuth with the computed sun angles for the remainder of the afternoon. These adjusted values were subtracted from the values measured with the automobile in sunlight to give the point source (sun) veiling luminance values.

The uncorrected meter readings taken throughout the afternoon are shown in Figure 34. As before, various portions of the automobile were covered with nonreflecting black cloth to obtain background values. Readings were taken as a function of time with the vehicle uncovered (Curve 1), the hood covered (Curve 2), the dash covered (Curve 3), and with both the hood and dash covered (Curve 4). The hood and dash values may each be obtained in two ways from these four curves. The veiling luminance due to the hood reflection may be obtained by taking the difference between Curve 1 and Curve 2, or between Curve 3 and Curve 4. Similarly the dash value is given by Curve 1 minus Curve 3, or by Curve 2 minus Curve 4. Differences in the hood and dash values obtained in these two ways are due to time variations in sky transparency, drift of the photometer sensitivity, and small variations in coverage of the vehicle with the black cloth. Since two sets of readings taken with the solar simulation apparatus are in excellent agreement, sky transparency variations are indicated as the major cause for the dash variations. The overall variations range up to 25 percent for the dash values and to 70 percent for the hood values and are so indicated in Figure 35.

The values of equivalent veiling luminance for the dash and the hood were obtained by taking the average of the differences of the two sets of curves. These values are shown in Figure 35 as a function of negative azimuth (360 deg-SAZ) for the dash (solid curve) and hood (dashed curve). The solar azimuth, SAZ, is measured relative to the vehicle heading direction and has been defined earlier in this report. The corresponding values of solar elevation, SAL, are also indicated on the plot by the dot-dash curve.

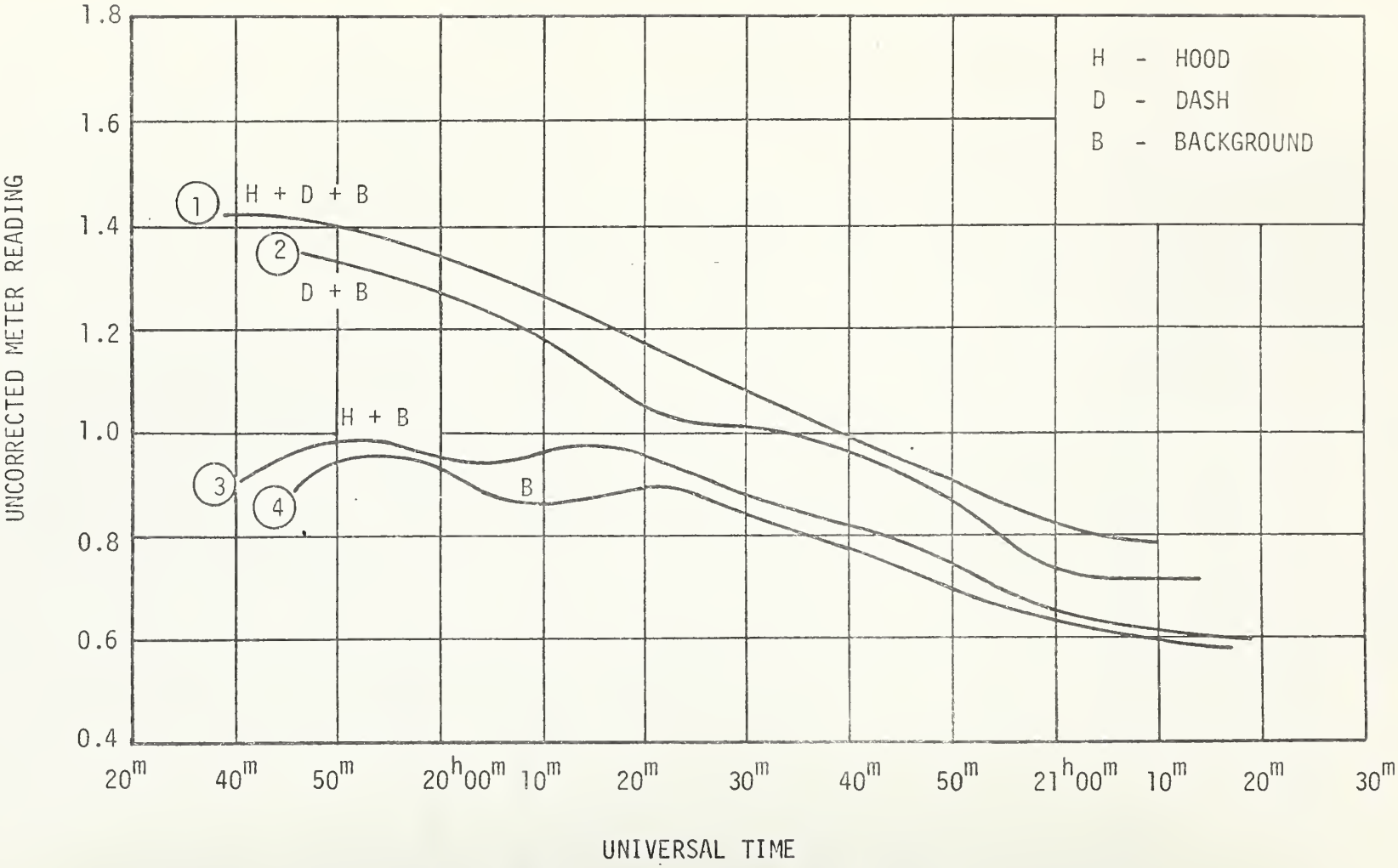

FIGURE 34. UNCORRECTED READINGS OF EQUIVALENT VEILING LUMINANCE WITH A 1973 PONTIAC SEDAN, COLOR BURNT UMBER, ON NOVEMBER 20, 1974

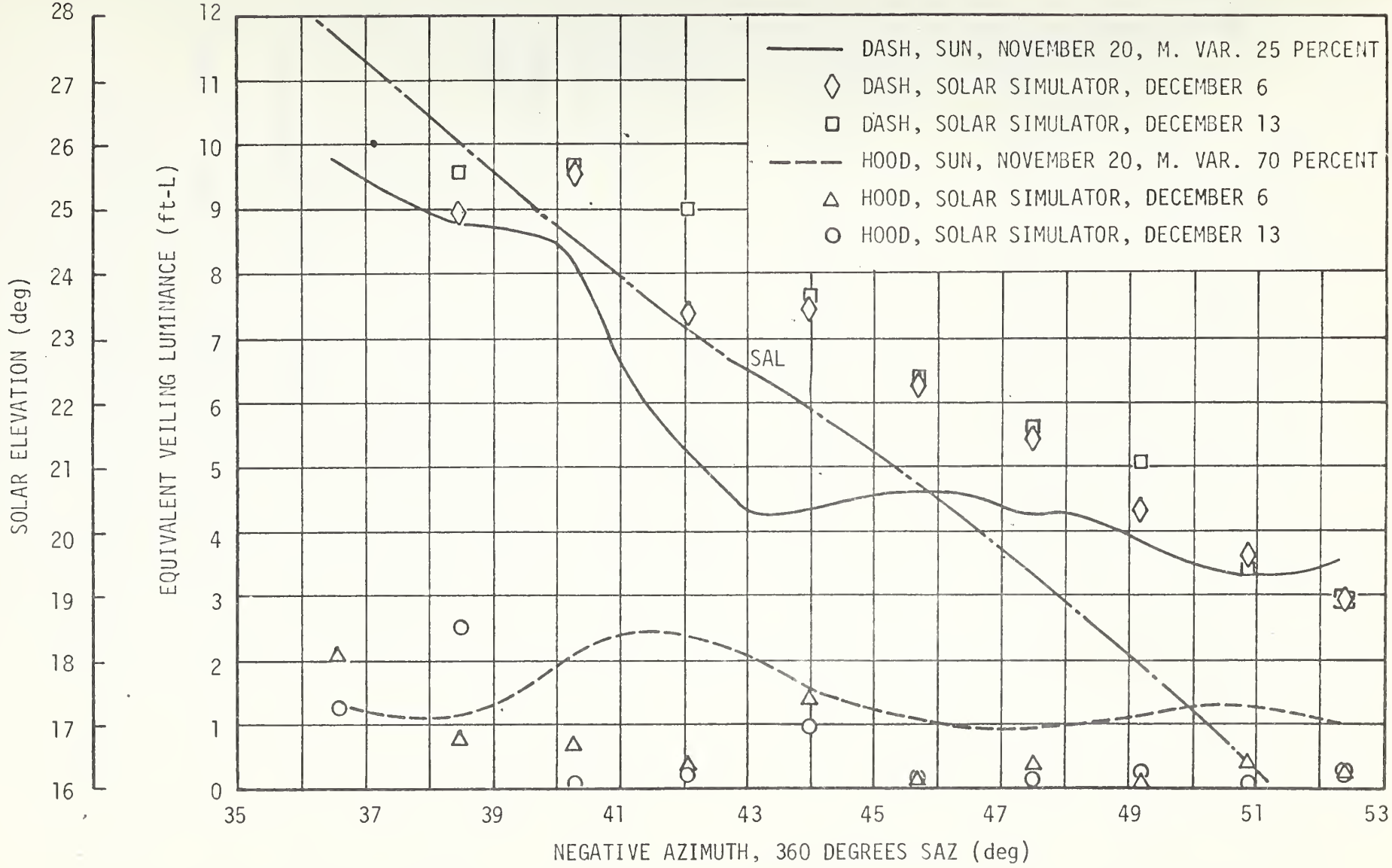

FIGURE 35. COMPARISON OF MEASURED VEILING LUMINANCE REFLECTED BY THE DASH AND HOOD OF A 1973 PONTIAC SEDAN, COLOR BURNT UMBER, FROM A POINT SOURCE

The values of solar azimuth and elevation were obtained from the time values, the geocentric coordinates of Huntsville, and data tabulated in the American Ephemeris and Nautical Almanac (Ref. 18). With the time values the Greenwich Sidereal Time (G.S.T.) was interpolated from the Ephemeris. The Local Sidereal Time (L.S.T.) was obtained by subtracting the longitude for Huntsville from the G.S.T. The solar hour angle, $h_\odot$, could then be found by subtracting the solar right ascension (Ephemeris) from the L.S.T. The celestial spherical triangle formed by the celestial pole, the local zenith, and the sun indicates that the solar elevation, SAL, is given by

$$\sin (SAL) = \sin (lat) \sin \delta_\odot + \cos (lat) \cos \delta_\odot \cos h_\odot , \qquad (11)$$

where (lat) is the local geometric latitude and $\delta_\odot$ is the solar declination (Ephemeris). For the vehicle heading south, the solar azimuth, SAZ, is given by

$$\cos (SAZ) = \frac{\sin (SAL) \sin (lat) - \sin \delta_\odot}{\cos (SAL) \cos (lat)} \qquad (12)$$

from consideration of the same spherical triangle. The sign of SAZ is opposite to that of $h_\odot$.

Veiling luminance reflected by the hood and dash of the Catalina with the diffuse illumination apparatus was measured on December 10, 1974. The apparatus was rolled over the hood and dash of the automobile so that the Mylar front of the apparatus was positioned at a perpendicular distance from the central point of the intersection of the windshield and hood of 1 meter. Actually, this distance is not critical since for each measurement of the equivalent veiling luminance produced by the hood and dash, the illuminances upon the hood and dash are also measured. Equivalent veiling luminance for the hood was measured to be 1.10 foot-lambert and for the dash it was measured to be 0.52 foot-lambert. A Weston luminance meter was used for reading the luminance of the diffuse illumination apparatus at the positions of the hood and dash, and the illuminance values at these positons were estimated from these. At the

hood position the luminance of the diffuse illumination apparatus measured 1,500 foot-lamberts. As viewed from this position, the diffuse illumination apparatus approximates a uniformly luminous, concave hemisphere. Since the illuminance in foot-candles upon a surface at the center of a uniformly luminous, concave hemisphere is numerically equal to the luminance of the hemisphere in foot-lamberts, the illuminance upon the hood was estimated to be 1,500 foot-candles. At the dash position the luminance of the diffuse illumination apparatus measured 900 foot-lamberts. Since the dash was only illuminated through the windshield of the automobile, the illuminance upon the dash in foot-candles was estimated to be numerically equal to 0.4 of this or 360 foot-candles.

These values of equivalent veiling luminance measured with the diffuse illumination apparatus were scaled to the natural daylight conditions for the date and time of the measurements outside. The scaling equations given earlier were used for this. For the hood, the equation for the equivalent veiling luminance scaled to outside conditions is

$$L_{DH} = R_{DH} K_{DL} C_{AD} D_F \quad , \tag{13}$$

where R_{DH} is this luminance measured with the diffuse illumination apparatus, K_{DL} is the scaling factor [equal to the illuminance on a horizontal surface outside (with sky) divided by illuminance upon the hood with the diffuse illumination apparatus], C_{AD} is a correction factor for sun elevation, and D_F is a correction factor for sun azimuth. For the date and sun elevation of the measurement outside, the IES Lighting Handbook (Ref. 19) indicates the illuminance upon a horizontal surface to be 934 foot-candles (interpolated). From Figure 11, D_F (at 360 deg - SAZ = 33 deg) is equal to 0.8. The factor C_{AD} is unity since correction for sun elevation is contained in the horizontal illuminance taken from the IES Handbook. Thus

$$L_{DH} = 1.10 \left(\frac{934}{1,500}\right) 0.8 = 0.55 \text{ ft-L.}$$

For the dash, the scaling equation is

$$L_{DD} = R_{DD}\, K'_{DL}\, C'_{AD}\, D_F \quad , \tag{14}$$

where L_{DD} is the equivalent veiling luminance for the dash scaled to outside conditions, R_{DD} is this luminance measured with the diffuse illumination apparatus, K'_{DL} is the scaling factor for the dash, and C'_{AD} is a correction factor for sun elevation which includes a window aperture factor (1/2, analogous to the factor of 0.4 used above). The scaling factor K'_{DL} is defined in an analogous manner to the factor K_{DL}. By Equation 14, L_{DD} is computed to be

$$L_{DD} = 0.52 \left(\frac{934}{360}\right)\left(\frac{1}{2}\right) 0.8 = 0.54 \text{ ft-L} \quad .$$

These values and the values measured outside are summarized in Table 8. The agreement between inside and outside measured values is good.

Measurements on the Catalina with the solar simulator were conducted on December 6 and again on December 13, 1974. The measurements were conducted in a darkened room (except for the simulator) to minimize background illumination. For these measurements, the parabolic dish was located in a sequence of positions having the same orientation relative to the vehicle as the sun had when the measurements under natural conditions were recorded. Orientation of the solar simulator is specified by dish position, Ψ, and frame elevation, Φ, as defined above. The values of Ψ, Φ were computed from the angles SAZ, SAL by the transformation equations

$$\sin \Psi = \sin (SAZ) \cos (SAL) \quad , \tag{15}$$

and

$$\sin \Phi = \frac{\sin (SAL)}{\cos \Psi} \quad . \tag{16}$$

These computed values of Ψ, Φ were used for positioning the dish.

TABLE 8. COMPARISON OF VEILING LUMINANCE REFLECTED BY THE TEST VEHICLE FROM A DIFFUSE (EXTENDED) SOURCE MEASURED UNDER NATURAL AND ARTIFICIAL CONDITIONS

	MEASURED OUTSIDE (SKY) ON NOVEMBER 20, 1974 $19^h\ 15^m$ U.T.	SCALED FROM MEASUREMENTS INSIDE (WITH DIA) ON DECEMBER 10, 1974
Hood	0.5 ft-L	0.55 ft-L
Dash	0.5 ft-L	0.54 ft-L

The measurements with the solar simulator were scaled to outside conditions with the equations

$$L_{SH} = R_{SH}\ (\Psi,\ \Phi)\ K_{SL}\ C_{AS}\ T_S \tag{17}$$

for the hood, and

$$L_{SD} = R_{SD}\ (\Psi,\ \Phi)\ K_{SL}\ C_{AS}\ T_S \tag{18}$$

for the dash, where

L_{SH} - equivalent veiling luminance reflected by the hood and scaled to outside conditions

R_{SH} - this luminance read with the simulator

K_{SL} - the scaling factor (the ratio of the maximum solar illuminance, 9,000 ft-c, to the illuminance produced by the simulator)

C_{AS} - a correction factor for solar elevation

T_S - a correction factor for temporal variations in atmospheric transmittance (usually taken to be unity)

L_{SD} - the equivalent veiling luminance reflected by the dash and scaled to outside conditions

R_{SD} - this luminance measured with the simulator.

The illuminance produced by the solar simulator was found by taking a weighted average of the measured illuminance as a function of radius. The radial illuminance measurements were taken by observation with the Prichard Photometer (without Fry lens) of the luminance reflected by a white card placed in the light beam from the simulator. These measurements, taken as a function of radius, are shown in Figure 36. The card was oriented perpendicular to the beam and the measurements were taken at 30 degrees to the card normal. The average reflected luminance, weighted according to annulus area, was found to be

$$\bar{L} = \frac{1}{\pi r_o^2} \int_o^{r_o} L(r)\, 2\pi r dr = 17.6 \text{ ft-L.}$$

Here L(r) is the observed luminance reflected by the card (a function of radius, (r), and r_o = 48 inches. To obtain the corresponding illuminance value, it was necessary to determine the reflectance and reflecting properties of the card. This was done by observing sunlight reflected by the card with the photometer. This observation was carried out on December 18, 1974, at 16^h17^m U.T. Geometry was the same as for the simulator measurements. The observed reflected luminance was 7,769 foot-lamberts. From the computed solar elevation (28.6 deg) the solar illuminance was determined to 6,700 foot-candles. The fact that the observed value of 7,769 foot-lamberts is numerically larger than this illuminance value is explained by assuming that the card reflectance is non-lambertian. Assume that the luminance B_θ reflected by the card at the angle θ to the card normal is related to the luminance B_o reflected normally by

$$B_\theta = B_o \cos \theta$$

Let ρ be the card reflectivity. Then the illuminance E falling upon the card is related to B_o by

$$\rho E = \int_o^{\pi/2} \frac{B_o}{\pi} \cos^2 \theta 2\pi \sin \theta d\theta$$

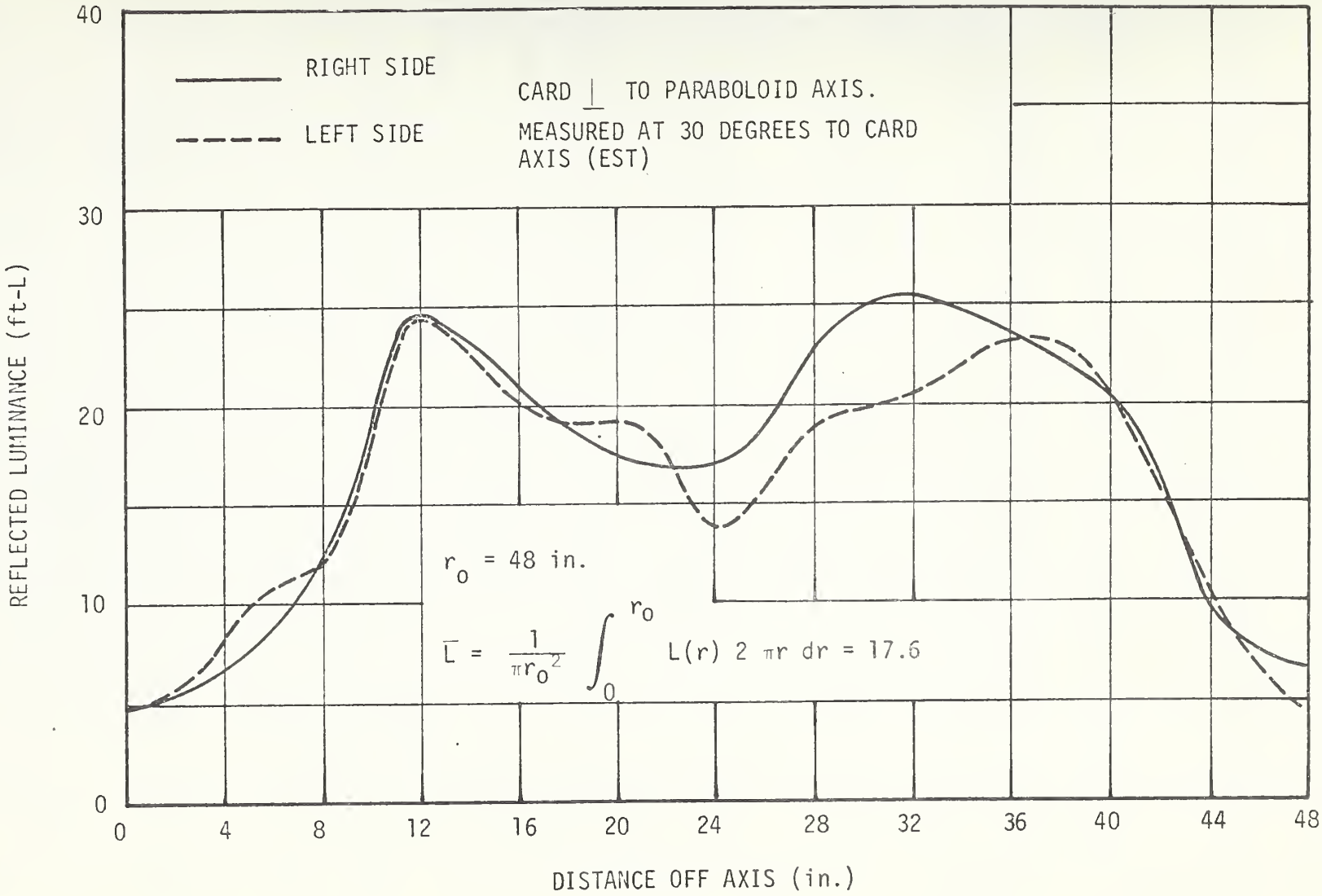

FIGURE 36. LUMINANCE REFLECTED FROM NUMBER 10 WHITE CARD ILLUMINATED BY SOLAR SIMULATOR

or

$$B_o = \frac{3}{2} \rho E$$

and thus

$$\frac{B_\theta}{\cos \theta} = \frac{3}{2} \rho E \quad . \tag{19}$$

If the values B_θ = 7,769 foot-lamberts, θ = 30 degrees, and E = 6,700 foot-candles are substituted into Equation 19, then ρ = 0.90, a reasonable value. Thus

$$E \text{ (solar simulator)} = \frac{2}{3} \frac{\bar{L}}{\rho \cos 30^\circ} = \frac{2}{3} \frac{(17.6)}{(0.9) \cos 30^\circ} = 15.0 \text{ ft-c.}$$

The values of $C_{AS}\ T_S$ were taken from Figure 11.

The resulting scaled values are shown as the plotted points in Figure 35. The reflected luminance from the hood of this vehicle was very small, and a reliable comparison is probably not possible here. However, the dash had adequate reflected equivalent veiling luminance, and a comparison is possible. The comparison between inside and outside measurements here is good, as it should be recalled that the curve measured under natural conditions had an uncertainty of 25 percent.

Data analogous to that taken for Figure 35 was also taken with the 1975 Ford Maverick. The colors of this automobile were white exterior and medium blue interior. These data are shown in Figure 37. The solid curves show separately the veiling luminance for the sun only for the hood and dash as a function of solar azimuth recorded outside under natural conditions. The dotted curve shows the solar elevation over the time period for the observations. The circled points represent veiling luminance scaled from observations with the solar simulator for the dash; the diamonds represent those for the hood. Agreement of the points with the curves is satisfactory.

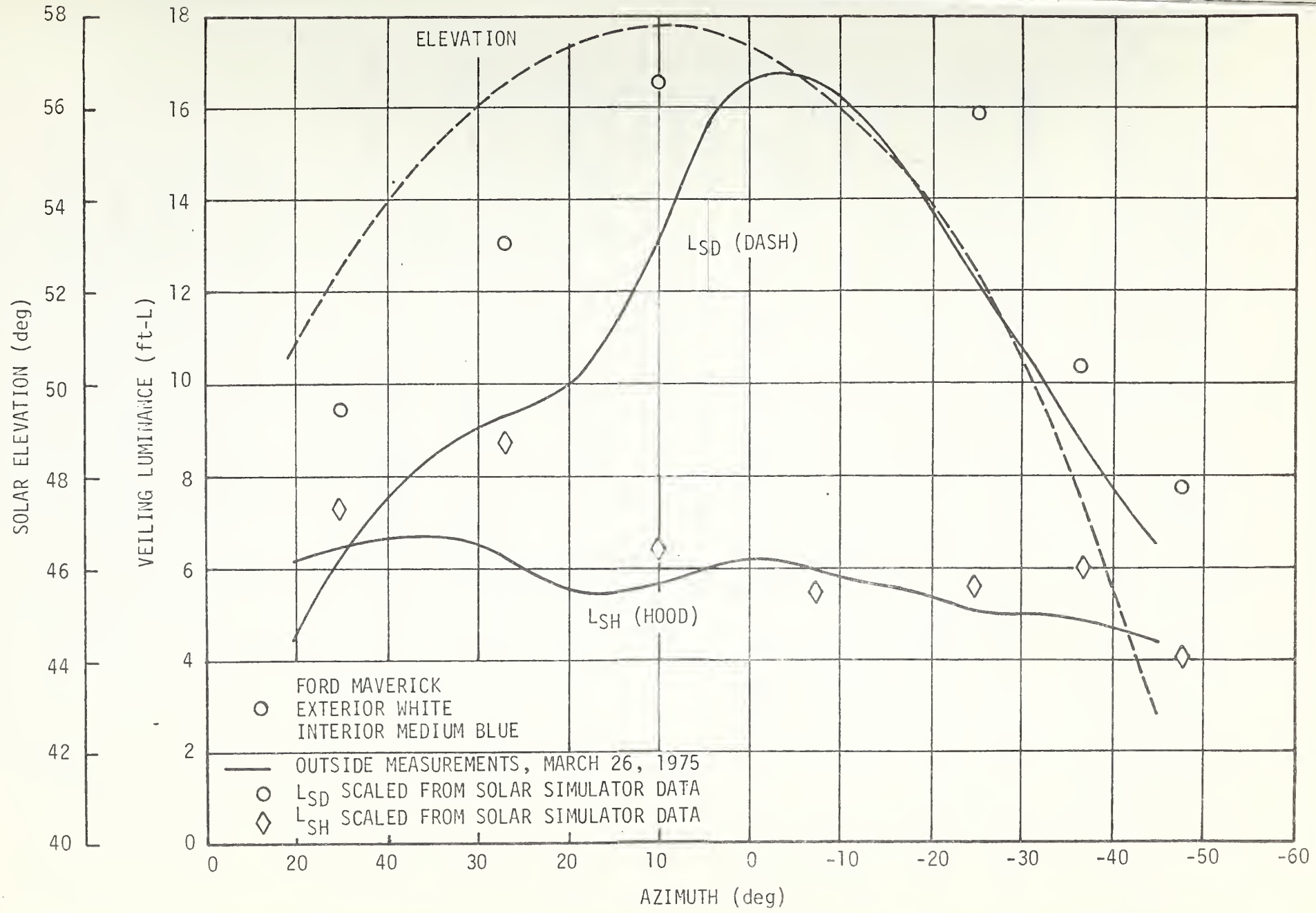

FIGURE 37. COMPARISON OF MEASURED VEILING LUMINANCE REFLECTED BY DASH AND HOOD FROM A POINT SOURCE

In summary, it may be concluded that the agreement between the equivalent veiling luminance values measured under natural conditions and those scaled from measurements with the daylight simulation apparatus is satisfactory in both the diffuse and point source cases.

EVALUATION OF GLARE MEASUREMENT APPARATUS SPECULAR REFLECTION MEASUREMENTS

Light reflection by the hood and dash of vehicles consists of both diffuse and specular components. To further test our glare measurement procedures and method of scaling, the equivalent veiling luminance reflected by a specular reflector from both the sun and the solar simulator have been measured. The procedure consists of reflecting sunlight (natural or artificial) directly into the Fry lens, which is attached to the Prichard Photometer. A purely specular reflection is particularly useful for a test since the equivalent veiling luminance expected may be computed with the Fry equation. A first-surface aluminized flat mirror was selected as the reflector, and this was masked by circular apertures of various diameters to obtain the effect of various mirror sizes. For all measurements the angle of incidence upon the mirror of rays from the source was 45 degrees, and the angle of incidence upon the Fry lens was also 45 degrees. The distance of the mirror from the Fry lens was 21 inches. The experimental procedure was more difficult than for measurements with the test vehicle, since for the smallest aperture sizes the light pattern could be barely seen upon the Fry lens. In all cases the mirror was adjusted so that a maximum reading was obtained on the meter. A background reading was obtained by tilting the mirror so that the reflection fell just off the Fry lens, and this reading was subtracted from the direct reflection reading.

Measurements with natural sunlight were recorded on January 2, 1975, at approximately 16^h50^m U.T. Background illumination of the Fry lens was minimized by directing the photometer into a darkened garage-type building. Readings were taken with aperture diameters of 2, 1, 1/2, and 1/4 inches. A reading was attempted with a 1/8-inch-diameter aperture, but the value was too small to be separated from the spurious variations. These readings are shown in Figure 38 plotted as a function of mirror

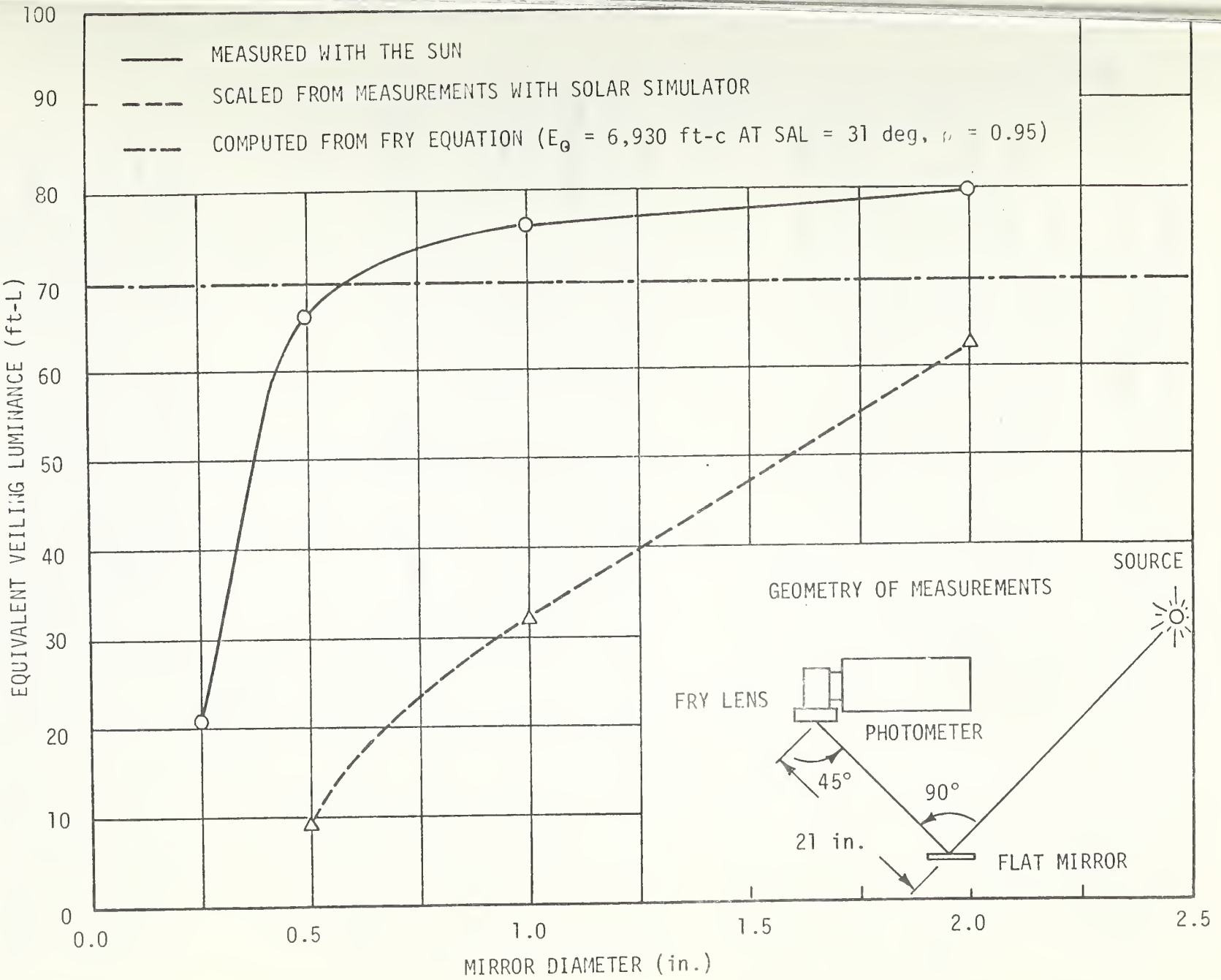

FIGURE 38. COMPARISION OF EQUIVALENT VEILING LUMINANCE MEASUREMENT ON SPOT SOURCE (SOURCE REFLECTED IN FLAT MIRROR)

diameter and are represented by the solid curve. The values decrease for mirror diameters below about 0.5 inch; this is probably a result of the Fry lens shape.

Readings with the solar simulator were taken on January 3. The measurements were taken in an otherwise darkened room to minimize the background illumination. Measurements were taken at two radial positions of the dish for each aperture size. Since illumination produced by the dish is a function of radius, each measurement was separately scaled to natural sunlight and those for the corresponding aperture sizes were averaged. Readings for aperture sizes smaller than 0.5 inch could not be made because of the weak signal. Readings with the simulator were scaled to natural sunlight with the equation

$$L = R\ K\ C_{AS}\ T_S \quad ,$$

where L is the scaled equivalent veiling luminance, R is this luminance obtained with the simulator, and K is the scaling factor [the maximum solar illuminance, 9,000 foot-candles, divided by the simulator illuminance E(r)]. The factor $C_{AS}\ T_S$ is previously defined. The resulting scaled readings are also plotted in Figure 38 and are represented by the dotted curve. These values fall off more rapidly with decreasing aperture size than the values recorded in natural sunlight; this is probably caused by the lack of collimation of the simulator. Agreement is good at the 2-inch aperture diameter.

The Fry equation,

$$L_v = \frac{33.4\ E \cos\theta}{\theta\ (1.5 + \theta)} \quad ,$$

which expresses the equivalent veiling luminance, L_v, due to a point glare source as a function of illuminance, E, at the observer and angle θ off the line of sight, was used for computing the veiling luminance expected under the natural measurement conditions. On January 2, at 16^h50^m U.T. the solar elevation at Huntsville was 31 degrees, which

corresponds to a solar illuminance of 6,930 foot-candles (Figure 11). Since θ = 45 degrees, then the Fry equation gives L_v = 73.5 foot-lamberts and for a mirror reflectivity of 95 percent, L_v = 69.8 foot-lamberts. This value is also plotted in Figure 38 as the horizontal dot-dash line.

Figure 38 indicates good agreement between all three curves at the larger mirror sizes. For an actual vehicle this corresponds to specular reflection from large, relatively flat hood areas. Such specular reflection of sunlight from the hood is probably the largest single contribution of specularly reflected light. This test indicates that the solar simulator should give results of satisfactory accuracy in this case.

MOTOR VEHICLE TEST RESULTS

Scans of veiling luminance of the 1974 Mercury Capri recorded with the solar simulator are shown in Figures 13 through 23. This set of scans is typical of that recorded for each of the 20 vehicles routinely measured in the program. In these scans the ordinate is the veiling luminance in foot-lamberts and the abscissa is the frame elevation, Φ, in degrees. As may be seen in the figures, four curves were recorded at each dish position, Ψ: one for the vehicle completely uncovered (H + D + B), one for the dash covered (H + B), one for the hood covered (D + B), and one for both hood and dash covered (B). At low frame elevations and for dish positions near zero, the photometer views the dish directly at small angles to the line of sight (the Fry lens axis) and the curves run off scale. During data acquisition an effort was made to reduce this effect as much as possible with the sun visor. However, the sun visor cannot be brought too low lest obscuration of the hood or dash occur. Placing carefully constructed baffles inside the vehicles would probably help this problem, but this was not done. Baffles could probably not be placed outside the vehicle, as shadowing of the hood or dash would very likely result. All curves show a gradual fall-off toward high frame elevation except for occasional peaks due to spot glare sources. At large positive and negative values of dish position, Ψ,

the curves become more horizontal. Here the photometer views the dish directly but at very large angles to the line of sight through the sides of the windshield and windows, and the linear distance traversed by the dish in any sweep is small.

Upon completion of the measurements, the data set for each vehicle was scanned for the maximum vehicle (hood and dash) veiling luminance with the solar simulator. This total vehicle (hood and dash) veiling luminance is the difference between the curves labeled H + D + B (vehicle uncovered) and B (hood and dash covered with nonreflecting cloth). For all vehicles the dish position for the maximum vehicle veiling luminance lay at Ψ = 0 degree or -10 degrees. For each vehicle the frame elevation corresponding to the maximum vehicle veiling luminance was read from the data, and numbers of vehicles were plotted as a distribution function of this frame elevation. Figure 39 shows the number of vehicles having their maximum vehicle veiling luminance frame elevation lying in each 10-degree interval. Note that this distribution curve has two peaks. The left-hand peak at about 45 degrees is actually a false peak; vehicles having maximum veiling luminance in this part of the curve have veiling luminances which increase with decreasing frame elevation and the curves run off the page at about Φ = 45 degrees. The right-hand peak in the distribution curve at about 75 degrees is a true peak; a number of vehicles show a maximum veiling luminance near this elevation. In a comparative study involving also the tolerable veiling luminance, the problem is simplified if a single point source position may be chosen. This is because the tolerable veiling luminance is a function of background luminance which is a function of solar position relative to the vehicle. Consequently a point source azimuth of 0 degrees and elevation of 75 degrees was chosen for the following study. For many vehicles, Figure 39 shows that it is a high glare point source position, although it is not necessarily the highest glare position.

For all the vehicles the veiling luminances measured with the solar simulator for the hood and the dash were measured at Ψ = 0 degrees and Φ = 75 degrees. These data were scaled to outside conditions at this solar position and are shown in Table 9. Measurements with the

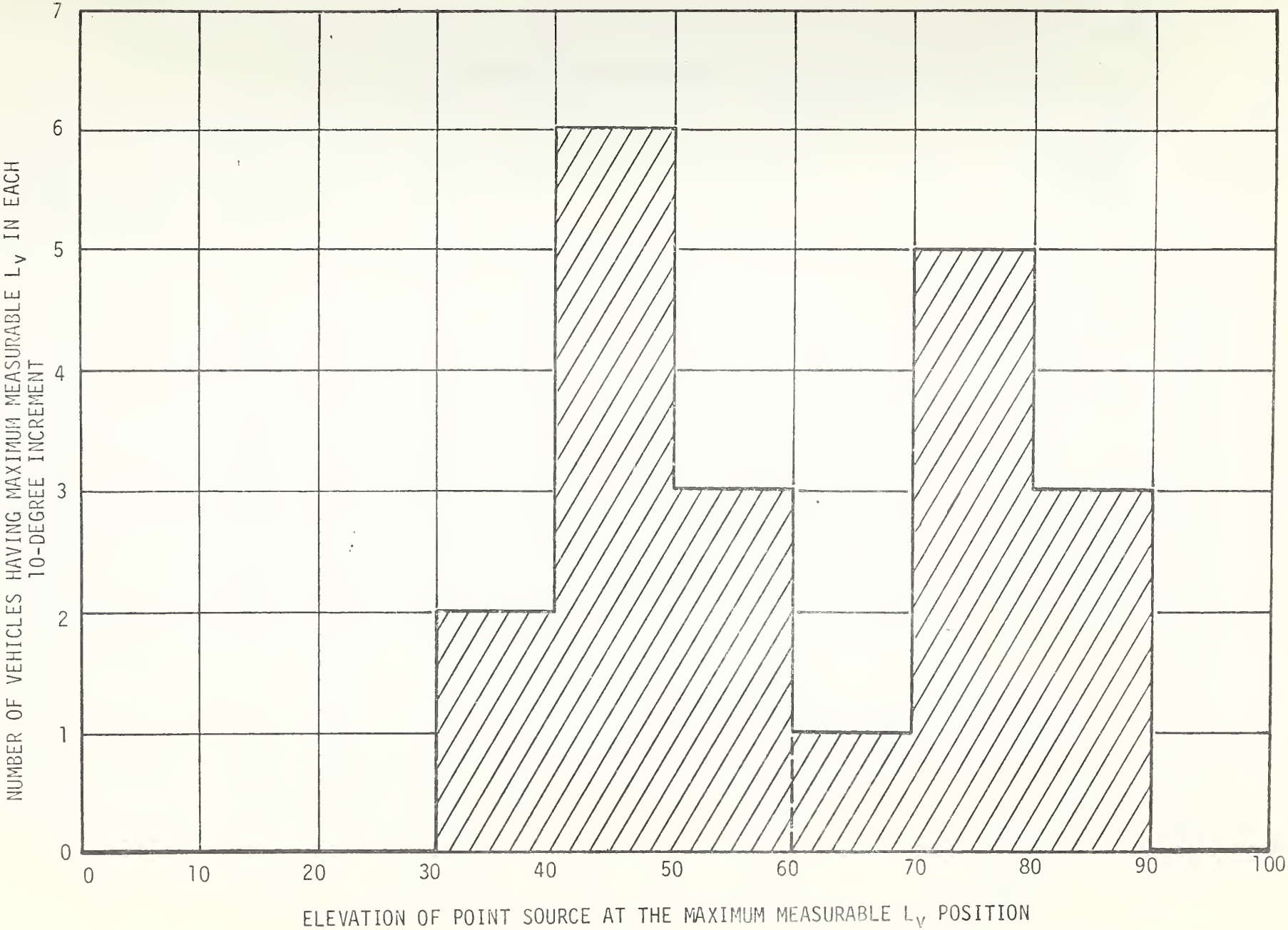

FIGURE 39. DISTRIBUTION OF VEHICLES ACCORDING TO POINT SOURCE ELEVATION AT THE MAXIMUM MEASURABLE TOTAL VEILING LUMINANCE POSITION (POINT SOURCE AZIMUTH NEAR ZERO)

TABLE 9. POINT AND DIFFUSE SOURCE VEILING LUMINANCES AT SOLAR AZIMUTH = 0 DEGREE AND ELEVATION = 75 DEGREES

VEHICLE		POINT SOURCE SCALED VEILING LUMINANCE			DIFFUSE SOURCE SCALED VEILING LUMINANCE			DASH-WINDSHIELD RELFECTED DIRECT LUMINANCE SCALED (ft-L)
MANUFACTURER	MODEL	HOOD (ft-L)	DASH (ft-L)	TOTAL (ft-L)	HOOD (ft-L)	DASH (ft-L)	TOTAL (ft-L)	
AUTOMOBILES								
Ford	Lincoln Continental	9.4	43.5	52.9	6.2	3.0	9.2	
	Maverick	7.6	14.1	21.7	13.7	5.5	19.2	2.9
	Mustang II	10.0	34.1	44.1	4.9	3.1	8.0	19.0
	Gran Torino	12.9	25.9	38.8	5.5	2.8	8.6	
	Olds Cutlass	4.1	16.5	20.6	2.2	2.9	5.1	
	Chevrolet Vega	2.9	22.3	25.2	5.6	2.3	7.9	
General Motors	Chevrolet Malibu	5.9	10.0	15.9	4.5	1.7	6.2	
	Chevrolet Nova	4.1	14.1	18.2	3.1	0.7	3.8	4.8
	Buick Regal	7.1	18.8	25.9	8.9	2.0	10.9	12.5
Chrysler	Plymouth Valiant	11.2	14.1	25.3	10.3	0.6	10.9	3.8
	Dodge Charger	5.3	19.4	24.7	1.7	0.8	2.5	9.6
American Motors	Gremlin	11.8	13.5	25.3	9.0	0.7	9.7	5.0
Volvo	242	6.5	9.4	15.9	9.5	0.9	10.4	2.6
Triumph	TR6	0.6	17.1	17.7	0.5	0.8	1.3	0
	Capri	4.1	28.8	32.9	2.9	1.0	3.9	0
TRUCKS								
Ford	F-600	18.2	7.6	25.8	94.8?	0.6?	95.4?	0.8?
Inter-national	100	8.2	24.7	32.9	7.7	1.4	9.1	5.5
	1600	9.4	7.1	16.5	12.1?	2.5?	14.6?	1.3?
GM	Chevrolet-Fleetside Pickup C10	13.5	8.8	22.3	10.4	0.8	11.2	0.2
BUS								
Ford	B-700	20.6	0.6	21.2	8.2?	0.0?	8.2?	0.0?

diffuse illumination apparatus were also scaled to these conditions with the aid of data from the IES Handbook (Ref. 19). These data are also shown in Table 9. The data have been summed for the point (sun) and diffuse (sky) sources, and these values are shown in Table 10. The direct luminance values reflected by the windshield from the dash into the driver's field of view as measured with the diffuse illumination apparatus are also listed in Table 9.

During the course of data acquisition a number of spot glare sources were recorded as peaks in the curves taken with the solar simulator. Typical spot glare sources are chrome strips (Figures 40 through 42), windshield wiper arms (Figure 43), and chrome mirror mounts (Figure 44). The direct luminances for all such sources were measured at their maximum luminance solar simulator position and were scaled to outside conditions. These scaled luminances are shown in Table 11. Since these spot glare sources approximate point sources, and the brightness of a point source is specified by the illuminance of the source, the table also gives sufficient information for calculating solid angles so that the luminances may be corrected to illuminances. The Fry equation is also usually written in terms of an illuminance. The columns of Table 11 list the vehicle, spot source, maximum luminance (or illuminance for two vehicles), the size and shape of the source, aperture diameter used for observation, distance from eyellipse centroid, solar simulator coordinates at the maximum luminance position, and coordinates of the spot source as seen at the eyellipse centroid.

During the glare reduction study with a Ford Mustang II (a different vehicle from that listed in Table 11), some spot glare sources could be seen visually from the driver's eye position, but were not recorded as peaks on the traces. These were not studied.

Specular reflection by the hoods of five vehicles was observed using the solar simulator, and the results are given in Table 12. A view of the type of reflection for the AMC Gremlin is shown in Figure 45. The table gives the maximum frame elevation at which the specular reflection could be seen for the complete range of dish positions.

TABLE 10. SUMMARY OF VEILING LUMINANCE DATA AT 0 DEGREE AZIMUTH, 75 DEGREES ELEVATION. AT THIS POINT SOURCE LOCATION THE ILLUMINANCE ON A VERTICAL IS APPROXIMATELY 400 ft-c (IES HANDBOOK). FOR REFLECTIVITY = 25% (REF. 1), BACKGROUND LUMINANCE IS 100 ft-L, TOLERABLE L_V = 18 ft-L.

MANUFACTURER	MODEL	HOOD COLOR	DASH COLOR	TOTAL SCALED VEILING LUMINANCE			SCALED L_V/ TOLERANCE L_V		
				HOOD (ft-L)	DASH (ft-L)	TOTAL (ft-L)	HOOD	DASH	TOTAL
AUTOMOBILES									
Ford	Lincoln Continental	White	Gold	15.6	46.5	62.1	0.86	2.58	3.44
	Maverick	White	Blue	21.3	19.6	40.9	1.18	1.08	2.26
	Mustang II	Yellow	Black	14.9	37.2	52.1	0.83	2.07	2.89
	Gran Torino	Pastel Blue	Dark Blue	18.7	28.7	47.4	1.04	1.60	2.64
	Olds Cutlass	Sage Green	Green	6.3	19.4	25.7	0.35	1.08	1.43
General Motors	Chevrolet Vega	Antique White	Sandstone	8.5	24.6	33.1	0.47	1.36	1.83
	Chevrolet Malibu	Light Grey	Black Vinyl	10.4	11.7	22.1	0.58	0.65	1.22
	Chevrolet Nova	Light Blue	Medium Blue	7.2	14.8	22.0	0.39	0.82	1.22
	Buick Regal	Antique White	Maroon	16.0	20.8	36.8	0.89	1.15	2.02
Chrysler	Plymouth Valiant	Spinn. White	Medium Blue	21.5	14.7	36.2	1.20	0.82	2.02
	Dodge Charger	Lt. Met. Green	Flat Black	7.0	20.2	27.2	0.25	1.13	1.51
American Motors	Gremlin	Alpine White	Medium Blue	20.8	14.2	35.0	1.15	0.79	1.94
Volvo	242	White	Flat Blue	16.0	10.3	26.3	0.89	0.57	1.46
Triumph	TR6	Orange-Red	Flat Black	1.1	17.9	19.0	0.06	1.00	1.06
Ford	Capri	Met. Grey	Vinyl Black	7.0	29.8	36.8	0.39	1.65	2.04
TRUCKS									
Ford	F-600	White	Flat Black	113.0?	8.2?	121.2?	6.28?	0.46?	6.74?
International	100	Grenoble Green	Light Brown	15.9	26.1	42.0	0.89	1.44	2.34
	1600	White	Black	21.5?	9.6?	31.1?	1.20?	0.53?	1.73?
GM	Chevrolet Fleetside Pickup C10	Willoway Green	Dark Green	23.9	9.6	33.5	1.34	0.53	1.86
BUS									
Ford	B-700	Yellow	Tan	28.8?	0.6?	29.4?	1.60?	0.03?	1.64?

TABLE 11. SUMMARY OF SPOT SOURCE MEASUREMENTS

VEHICLE	SOURCE	LUMINANCE	SIZE AND SHAPE OF SOURCE (in.)	APERTURE (deg)	DISTANCE (in.)	DISH POSITION		SOURCE POSITION	
						ϕ	θ	SAZ	SAL
AMC Gremlin	Floor Console	1.4×10^5	8 × 1/8	1/2	46	-10	93	-10	-60
	Windshield Wiper	7.0×10^4	4 × 1/8	1/2	40	-10	105	+10	-10
	Windshield Wiper	4.6×10^4	6 × 1/2	1/2	40	+23	111	0	-10
Capri	Dash-Windshield	1.7×10^3	12 × 5	2	45	- 3	63	0	- 2
	Hood bump, back surface	7.5×10^4	8 × 1.5	1/2	55	-10	64	-10	-10
Plymouth Valiant	Windshield Wiper	5.8×10^4	5 × 3/8	1/2	36	+26	107	0	-10
Ford Maverick	Windshield Wiper	10^5	8 × 1/2	1/2	40	24	103	0	-10
Chevrolet Malibu	Chrome Strip, Face of Windshield	1.2×10^4	8 × 1/2 ?	2 ?	40	-6	91	0	-10
	Outside Rear View Mirror Mount	5.1×10^4	4 × 1/2 ?	2 ?	30	-20	35	40	-10
Chevrolet Nova	Outside Rear View Mirror Mount	10^6	3 × 1/2 ?	1/2	30	-27	48	45	-15
Buick Regal	Chrome Strip, Bottom of Windshield	10^4	8 × 1/2 ?	1/2	45 ?	-10	94	0	-10
Olds Cutlass	Chrome Strip, Steering Wheel	E = 220 ft-c	6 × 3/16 ?		30 ?	+5	109	-5	-5
Ford Mustang II	Chrome Strip, Bottom of Windshield	E = 240 ft-c	8 × 1/2 ?		40 ?	-10	99	0	-10
	Dash Face	E = 290 ft-c	10 × 4 ?		30	0	116	0	-30
	Chrome Strip	E = 750 ft-c	6 × 1/2 ?		25	+20	+35	+30	-20

FIGURE 40. CHROME STRIP AND INSTRUMENT PANEL, FORD MUSTANG

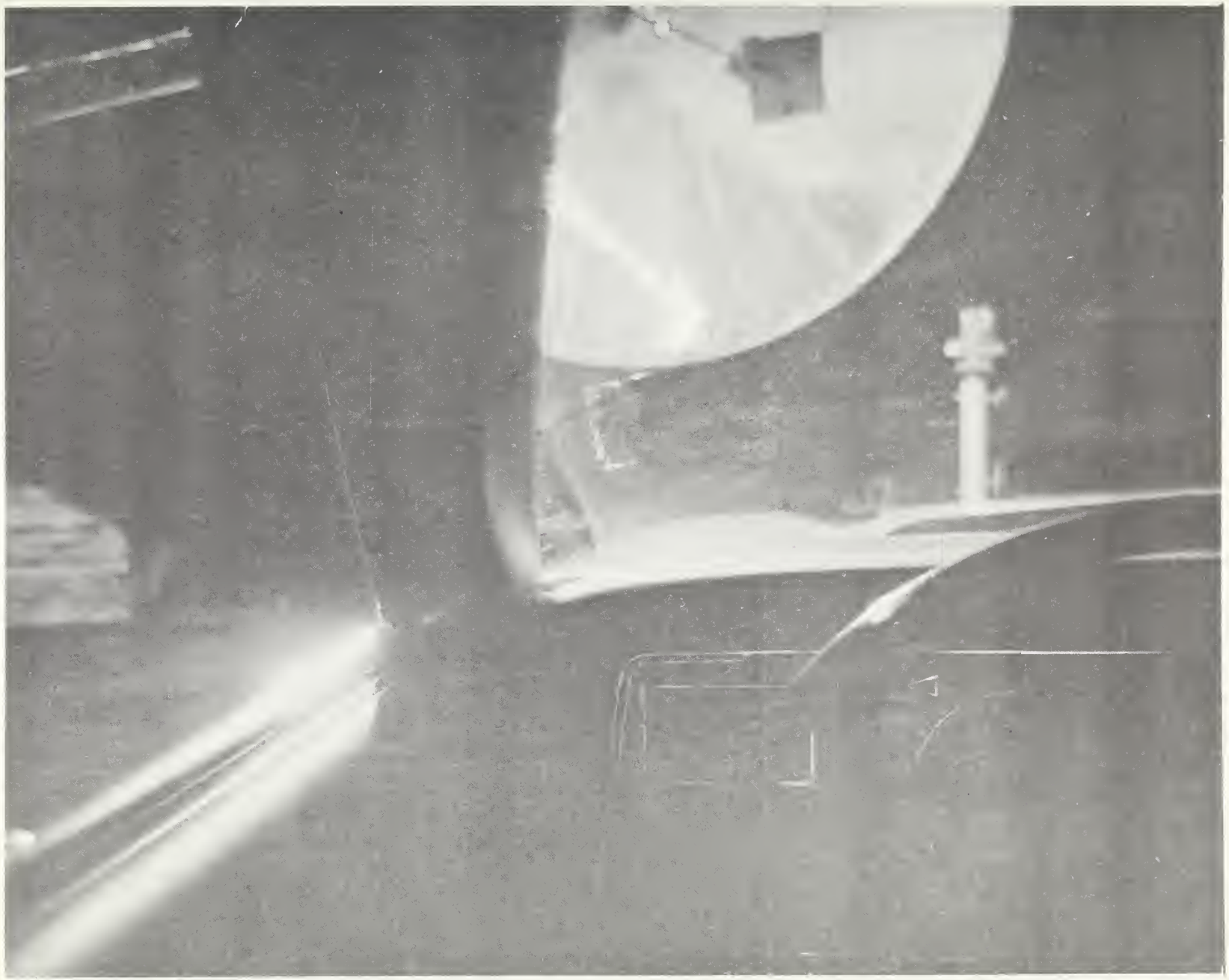

FIGURE 41. CHROME STRIP AND DRIVER'S WINDOW, FORD MUSTANG

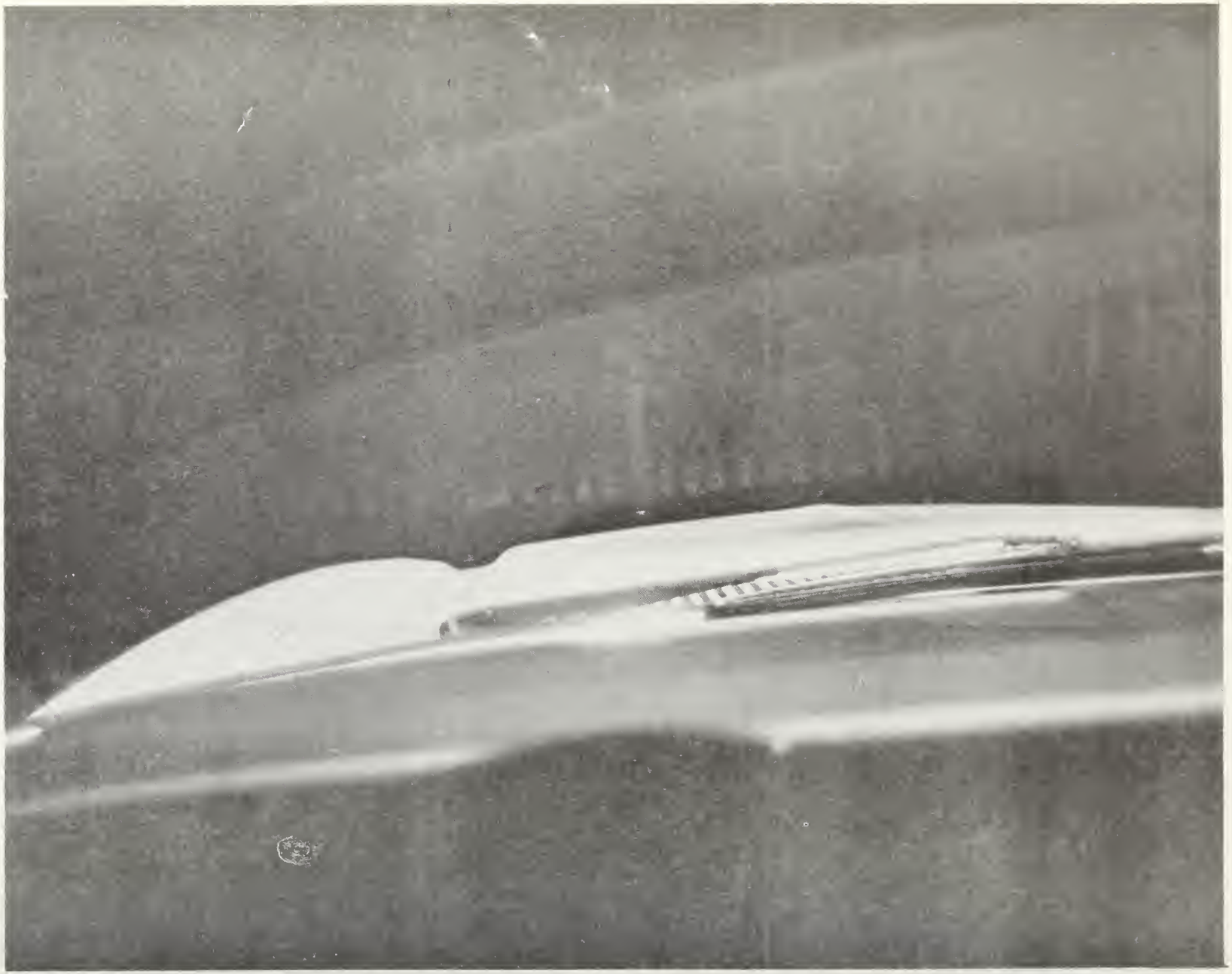

FIGURE 42. CHROME STRIP AND BASE OF WINDSHIELD, FORD MUSTANG

FIGURE 43. WINDSHIELD WIPER, AMC GREMLIN

FIGURE 44. CHROME STRIP, DRIVER'S WINDOW, AND REAR-VIEW MIRROR MOUNT, FORD MUSTANG

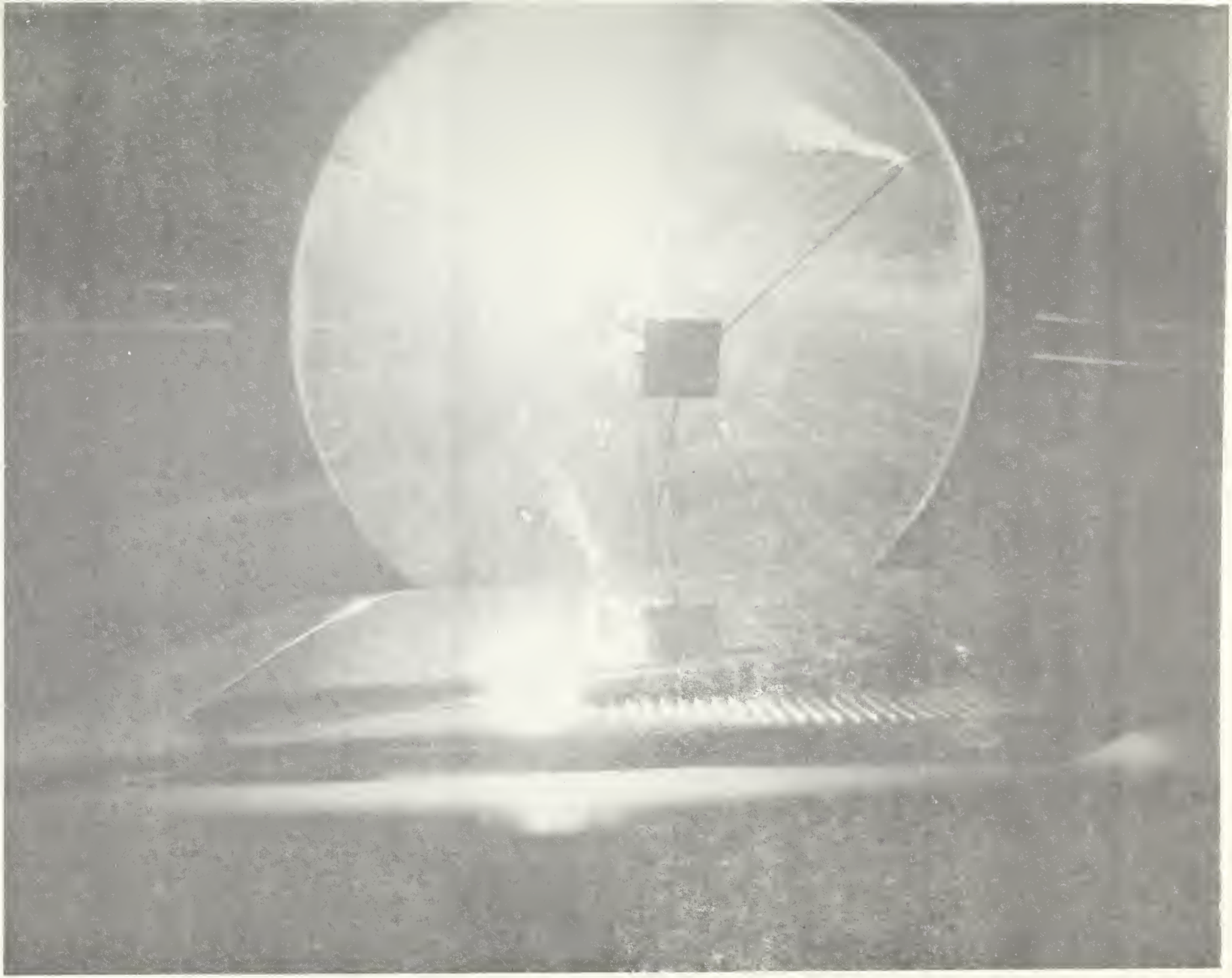

FIGURE 45. SPECULAR REFLECTION OF SOLAR SIMULATOR IN HOOD OF AMC GREMLIN

TABLE 12. MAXIMUM ELEVATION AT WHICH SPECULAR REFLECTION OF A POINT SOURCE MAY BE SEEN [FROM ELEVATION Φ (deg)]

VEHICLE	DISH AZIMUTH Ψ (deg)									
	+30	+20	+10	0	-10	-20	-30	-40	-50	-60
Plymouth Valiant	NS	23	23	17	16	13	26	16	NS	
Ford Mustang	NS	20	20	20	20	20	20	NS		
AMC Gremlin		NS	19	21	20	20	18	15	NS	
Ford Maverick	NS	20	20	23	18	17	17	15	NS	
Chevrolet Nova	NS	21	20	20	18	15	15	14	16	NS

NS - Not seen

GLARE REDUCTION RESULTS

The veiling luminance measurements recorded with the solar simulator at Ψ = 0 during the glare reduction study are shown in Figures 28, 33, and 46. Figure 46 shows this luminance with the glare reduced by covering the dash of the Gremlin with nonreflecting material. The height of the curve is the reduction in veiling luminance to be expected if the flat black cloth is used. Figure 28 shows the veiling luminance reduction achieved by tilting the dash top of the Ford Mustang. The solid curve was measured before modification, and the dashed curve was measured afterwards. Figure 33 shows the veiling luminance reduction achieved by tilting the hood of the Gremlin. This figure shows the hood veiling luminance only. The effect of shadowing of the dash is not present since the curves represent the difference between the measurements with the hood uncovered and covered.

The traces of direct luminance reflected by the vehicle in the driver's line of sight recorded with the solar simulator were used for additional verification of the veiling luminance measurements. For a single glare source the veiling luminance is given by the Fry equation as

$$B_v = \frac{33.4\,E\,\cos\,0}{\theta\,(1.5 + 0)}$$

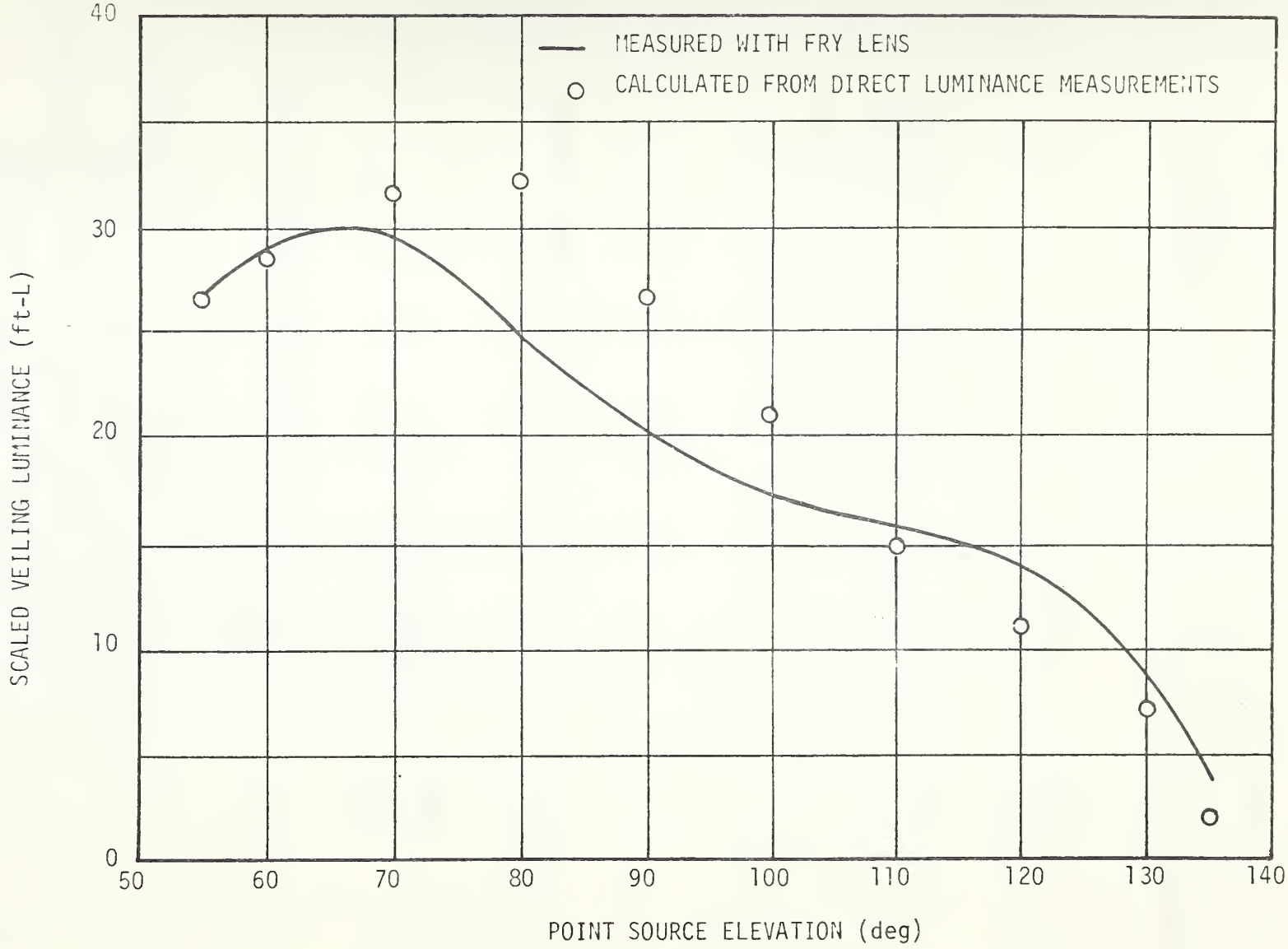

FIGURE 46. VEILING LUMINANCE OF DASH OF 1975 AMC GREMLIN, EXTERIOR MEDIUM BLUE, AZIMUTH = 0 deg

where E is the illuminance of the source at the eye in the plane of incidence of light from the source, and θ is the angle, in degrees, of the source off the line of sight. For N sources the veiling luminance is

$$B_v = \sum_{i=1}^{N} \frac{33.4\, E_i \cos \theta_i}{\theta_i\, (1.5 + \theta_i)}$$

where E_i is the illuminance due to the ith source and θ_i is the angle of this source off the line of sight. For computation of the veiling luminance due to the entire field of view, the field is divided into small solid-angle segments. If B_i is the luminance of the ith segment in foot-lamberts and Ω_i is its solid angle, then the illuminance in foot-candles due to the segment is

$$E_i = \frac{\Omega_i}{\pi} B_i$$

by the definition of the units. If this is substituted into the summation for B_v we obtain

$$B_v = \sum_{i=1}^{N} \frac{33.4 \Omega_i B_i \cos \theta_i}{\pi \theta_i\, (1.5 + \theta_i)} \quad . \tag{20}$$

This equation was used for computation of the veiling luminance values from the observed direct luminances B_i.

A problem occurs for the line-of-sight segment since $B_v \to \infty$ as $\theta \to 0$. When a reflecting dash is present the veiling luminance from this segment is due to light reflected by the windshield from the dash top directly into the driver's field of view. We found this veiling luminance to be far larger than that contribution to the veiling luminance by the rest of the field of view. When that contribution was

computed from the measured direct luminances by Equation 20, it was found to be only a small fraction of the veiling luminance measured with the Fry lens. Because of the uncertainty of the angle θ_c for the line-of-sight segment this parameter was left as an unknown, to be determined by fitting to the measurements made with the Fry lens. This was done by first calculating the contribution to the veiling luminance by the entire field of view minus the line-of-sight segment, and subtracting this contribution from the value measured with the Fry lens. This difference is the veiling luminance B_{vc} for the central segment and was computed for a sequence of frame elevations. These difference values were divided by the corresponding values of direct luminance, and the resulting quotients averaged. By substitution into

$$\left(\frac{\overline{B_{vc}}}{B_c}\right) = \frac{33.4\,\Omega_c \cos\theta_c}{\pi\theta_c\,(1.5+\theta_c)}$$

the effective off-the-line-of-sight angle θ_c for the central segment was calculated.

For the studies made of glare reduction for the dash these angles were found to be small, 3.3 degrees for the Mustang dash study and 8.1 degrees for the Gremlin dash study, as approximately expected. For the glare reduction study on the hood of the Gremlin, the segment having the greatest contribution to the veiling luminance was the portion of hood directly in front of the driver. A small amount of light is reflected by the hood and scattered by the windshield. The effective off-the-axis angle for the line-of-sight segment of the windshield was taken from the Gremlin dash study. In the Gremlin hood study, the off-the-axis angle for the hood portion in front of the driver was found by fitting to the Fry lens measurements. This was found to be 14.5 degrees, which is a reasonable value for this angle. With all parameters on the right side of Equation 20 determined, the veiling luminance values B_v were computed.

The calculated points are shown in Figures 28, 33, and 46. The circled points correspond to the unmodified surface and the triangles correspond to the modified surface. The reasonable values found for the effective off-the-axis angles by fitting, and the similarity of shape of the loci of the computed points with the observed curves, provide verification of these curves. The total scaled veiling luminances at Ψ = 0 degrees, Φ = 75 degrees for a point and diffuse source (sun and sky) before and after glare reduction modification are listed in Table 13.

Preceding photographs illustrate the glare reduction achieved by tilting the hood of the Gremlin. The driver's view of the Gremlin before modification is shown in Figure 24. Figure 32 shows this view after modification.

Early in the glare reduction study a calculation of the veiling luminance reduction based upon point-source illuminance and the reflectivities of the pertinent surfaces was contemplated. The surface reflectivities are a function of the angles of incidence and observation, and direct luminance traces taken with the solar simulator are probably the most accurate and convenient way to obtain them. Since determination of the direct luminance is an intermediate step in going from point-source illuminance and surface reflectivity to veiling luminance, there is no real need to work backward to surface reflectivities. Consequently, computing directly from luminances to veiling luminance only was decided upon.

TABLE 13. SUMMARY OF VEILING LUMINANCE AT 0 DEGREE AZIMUTH, 75 DEGREES ELEVATION

At this position: Illuminance on a vertical surface = 400 ft-c (Ref. 19)
For typical reflectivity = 25 percent (Ref. 1)
Typical background luminance = 100 ft-L
Tolerance veiling luminance = 18 ft-L.

VEHICLE, MODIFICATION	COLOR		TOTAL SCALED VEILING LUMINANCE (POINT AND DIFFUSE)			SCALED L_V/ TOLERABLE L_V		
	HOOD ORIG/MOD	DASH ORIG/MOD	HOOD ORIG/MOD (ft-L)	DASH ORIG/MOD (ft-L)	TOTAL ORIG/MOD (ft-L)	HOOD ORIG/MOD (ft-L)	DASH ORIG/MOD (ft-L)	TOTAL ORIG/MOD (ft-L)
AMC Gremlin Flat Black Dash	White/White	Blue/Black	18.9/18.9	26.5/0	45.4/18.9	1.06/1.06	1.47/0	2.53/1.06
Ford Mustang II Modified Dash	White/White	Blue/Blue	12.4/12.4	31.7/23.7	44.1/36.1	0.69/0.69	1.76/1.32	2.44/2.00
AMC Gremlin Modified Hood	White/White	Blue/Blue	18.9/12.9	26.5/26.5	45.4/39.4	1.06/0.72	1.47/1.47	2.53/2.20

ANALYSIS AND INTERPRETATION OF EXPERIMENTAL AND TEST RESULTS

DISABILITY GLARE IN CURRENT MODEL AUTOMOBILES

To determine if veiling glare reflected by a driver's vehicle is detrimental in an actual driving situation it is necessary to compare the scaled veiling luminance reflected by the vehicle into the driver's field of view, obtained from the laboratory veiling luminance data for the vehicle, with the acceptable veiling luminance for the situation. To determine if veiling glare due to the vehicle is detrimental in any driving situation, one must choose the worst case for that vehicle. Presumably this is the case having the highest veiling luminance with the least background luminance.

For the comparison studied here, the worst case situation was chosen as a clear sky with the sun at azimuth 0 degrees (relative to the vehicle) and elevation 75 degrees with the vehicle level. Here the illuminance of the target is assumed to be that on a vertical surface facing away from the sun, and is approximately 400 foot-candles (Ref. 19). For a typical background reflectivity of 25 percent (Ref. 1), the background luminance is 100 foot-lamberts. From the results given in Section 2.1, the tolerable veiling luminance is 18 foot-lamberts. The scaled veiling luminance values of Table 10 have been divided by this value.

The result of this division is shown as the last three columns in Table 10. It is seen that all vehicles measured do not meet this tolerance in the worst case. The Ford Motor Company vehicles measured were found to be among the worst of all those measured as shown in Table 10.

The question marks are for those vehicles having unusually high hoods. For these models a problem was encountered in covering the hood with the diffuse source; consequently, the diffuse source readings are probably erroneous.

Data recorded on spot glare sources such as chrome strips and outside mirror mounts indicate that these may only occasionally contribute significantly to veiling luminance. They are not considered to be a major problem. However, a driver may occasionally be "dazzled" by looking at such a source.

REDUCING DISABILITY GLARE

The results of the glare reduction study are summarized in Table 13 for a clear sky with solar azimuth 0 degree and solar elevation 75 degrees. The table shows the values before and after vehicle modification for the three methods studied.

The most promising glare reduction method appears to be use of a very near flat black covering upon the dash top, or elimination of this surface. Table 10 shows that in more cases than not, the dash top reflects a larger veiling luminance than the hood. The table also shows that some present "flat" black finishes used on vehicle dash tops are not truly nonreflecting (note especially the Dodge Charger).

Table 13 shows that changing the hood or dash shape does not so significantly reduce veiling glare. The component of light reflected by the hood and then scattered by the windshield is not reduced. Neither is that component which is reflected by the windshield from the dash top. Indeed, this study shows that this dash-windshield reflection is the greatest contributor to veiling glare, with the possible exception of specular reflection of sunlight by the hood. This is especially true since the Fry equation accounts only for scattered light in the eye and not for directly imaged veiling luminance.

CONCLUSIONS AND RECOMMENDATIONS

A systematic laboratory procedure to measure glare produced by a motor vehicle and a criterion with which to evaluate these measurements have been developed. Measurement results demonstrate that both a collimated and diffuse source must be used to evaluate a vehicle's characteristics with respect to glare production; the relative contributions associated with each source are not correlatable between vehicles. The criterion by which comparisons are made is based on a firm foundation of human response data accounting for both age factors and a logical choice of allowable degradation.

Major conclusions resulting from this study are:

- Most motor vehicles produce an unsatisfactorily high glare into the driver's eye under daylight driving conditions.

- By proper design procedures, glare levels can be held to tolerable levels (tolerable meaning at the levels established in this report).

- "Spot" glare sources on the vehicle do not contribute directly in a substantial manner to the degradation of visual capability. This is predicated on the driver not looking directly at the sources such that their contribution is always through luminance glare.

- The predominant glare source is the dash of the motor vehicle reflecting into the windshield and then into the driver's eye when the dash is illuminated with collimated light. A portion of this energy is directed along the driver's line of sight and hence the measurement procedures used here underestimate this contribution. A measurement of this contribution was performed for some of the vehicles, and on the basis of these measurements it can be concluded that the underestimation of the contribution does not effect the results as they apply to a pass/fail criterion.

- Light from the sun reflected from the hood represents the brightest glare source visible produced from the vehicle. This source exceeds the criterion in all cases, but it is unclear what solution might be applied. This must be treated as a special case.

Recommendations are:

- A standard for the glare produced by the driver's own vehicle should be developed on the basis of the criterion established in this report.

- A compliance procedure should be established whereby the vehicle glare is measured. A collimated source which illuminates the complete forward portion of the vehicle and which is positioned at an elevation angle of 75 degrees and azimuth angle of 0 degree (straight ahead of the vehicle) should be used in conjunction with a diffuse source with characteristics generally following the characteristics reported here. The elevation angle is measured about an axis about level with the hood at its midpoint front to rear. The glare should be measured with a photometer equipped with a Fry lens and positioned at the centroid of the eyellipse as specified by the vehicle manufacturer. The axis of measurement should be along the direct forward line-of-sight. Results should be scaled to daylight conditions in a manner similar to the method used in this report. Maximum allowable glare should be 18 foot-lamberts under these conditions.

- Motor Vehicle Safety Standard 107, which specifies a specular glare limit on certain vehicle components in the driver's field of view, should be strengthened and enforced. While "spot" glare sources do not demonstrate themselves to be a problem within the context of this study, they should not be disregarded. At this point, we do not see any way to quantitatively define the relationship to degradations of visual capabilities.

- Attention should be given to developing a specification for the angular limits at which the sun's rays specularly reflect into the driver's eye from the hood. The hood can, in the limit, be removed from the line of sight, as was done in this study.

RESEARCH PERSONNEL

The major participants in this research program were Dr. Neil E. Chatterton, Program Manager; Dr. Anne Dunn, Theoretical Analysis; and Mr. William Raine, Experimental Research. Brief resumes of these individuals follow.

Dr. Neil Chatterton obtained his Ph.D. in physics from the University of Florida. He served as a physicist and operations analyst working with several elements of the Air Force at Eglin Air Force Base, Florida. During this time, he was project manager for the optical measurement of boost-phase measurement of the exhaust plume of ICBMs, he participated in analyses of tactical mission concepts, and he served as the head of the terminal ballistics branch of the organization whose mission is development of conventional munitions. At Teledyne Brown Engineering, Dr. Chatterton is Manager of the Research Department. He has conducted programs in the development of optical equipment such as laser anemometers, laser calibration devices, and photometric devices. He has actively participated in DOT programs to define nighttime seeing ability through clear and tinted windshields and the program to define requirements for measuring glare.

Dr. Anne Dunn received her Ph.D. in astronomy from Rensselaer Polytechnic Institute. Before she joined TBE, while as a graduate student, she performed consulting work on calibration of photometers. All her work at TBE has been associated with development of methods of analysis of optical data. Dr. Dunn was Principal Investigator for the DOT study performed at TBE on determination of the detectability of objects through windshields at night. She has also developed models for the effects of internal scattering on the detection capability of the Large Space Telescope, a major orbiting astronomical system planned for the 1980s. She has had primary responsibility for developing calibration techniques for a NASA-owned solar magnetrograph.

Mr. William Raine received his B.S. in physics from Southwestern College and his A.M. in astronomy from Harvard University. Mr. Raine served on the faculty of Southwestern College prior to his joining TBE. He has been engaged in various programs of optical instrument development, test, and analysis while with the Company. This experience includes the optical and mechanical design work for a UBV stellar photometer, and the design of a cryogenically cooled infrared radiometer. Using the radiometer, he generated the most extensive set of thermal maps of the Moon produced from the Earth's surface. He has recently been performing analyses of the instrument requirements for the Large Space Telescope.

REFERENCES

1. "Equipment and Procedures for Measuring Glare for Motor Vehicles" Teledyne Brown Engineering, Final Report DOT-SE-1576, June 1972

2. J. H. Peterson and E. Simonson, American Journal of Ophthalmology, Vol. 34, pg. 1088 (1951)

3. L. L. Holladay, Journal of the Optical Society of America, Vol. 12, pg. 271 (1926)

4. G. A. Fry, Illuminating Engineering, Vol. 49, pg. 98 (1954)

5. A. J. Fisher and A. W. Christie, Vision Research, Vol. 5, pg. 565 (1965)

6. G. A. Fry and M. Alpern, Journal of the Optical Society of America, Vol. 43, pg. 189 (1953)

7. B. H. Crawford, Proceedings of the Physical Society of London, Vol. 48, pg. 35 (1936)

8. P. J. Bouma, Philips Technical Review, Vol. 1, pg. 225 (1936)

9. Glare and Driver Vision, University of California, PB 182 082, November 1968

10. O. W. Richards, American Journal of Optometry and Archives of the American Academy of Optometry, Vol. 35, pg. 565 (1958)

11. H. R. Blackwell and S. W. Smith, Illuminating Engineering, Vol. 65, pg. 389 (1970)

12. O. M. Blackwell and H. R. Blackwell, Journal of the IES, Vol. 1, pg. 3 (1971)

13. H. L. Snyder, "Dynamic Visual Search Patterns", in Visual Search, Committee on Vision, National Research Council. Published by the National Academy of Sciences, Washington, D.C., 1971

14. J. W. Senders, "Visual Scanning Behavior", in Visual Search, Committee on Vision, National Research Council. Published by the National Academy of Sciences, Washington, D.C., 1971

15. L. L. Holladay, Journal of the Optical Society of America, Vol. 14, pg. 1 (1927)

16. G. A. Fry, B. S. Prichard, and H. R. Blackwell, Illumination Engineering, Vol. 58, pg. 120 (1963)

17. Society of Automotive Engineers Data Sheet J941c

18. American Ephemeris and Nautical Almanac

19. IES Lighting Handbook, Fourth Edition, Illuminating Engineering Society, New York (1966)


TL
TEL
EVA
R
BORROWE
Form DOT F 1720.2
FORMERLY FORM DOT F